Mathematical Modeling of Biochemical Signal Transduction Pathways in Mammalian Cells – A Domain-Oriented Approach to Reduce Combinatorial Complexity

Von der Fakultät Konstruktions-, Produktions- und Fahrzeugtechnik
der Universität Stuttgart zur Erlangung der
Würde eines Doktor–Ingenieurs (Dr.–Ing.) genehmigte Abhandlung

Vorgelegt von

Holger Conzelmann
geboren in Albstadt

Hauptberichter:	Prof. Dr.–Ing. Dr. h.c. mult. E. D. Gilles
Mitberichter:	Prof. Dr. rer. nat. H. G. Holzhütter
Tag der mündlichen Prüfung:	19. Dezember 2008

Institut für Systemdynamik der Universität Stuttgart

2008

Vorwort

Die vorliegende Arbeit entstand in den Jahren 2003 bis 2008 während meiner Tätigkeit als wissenschaftlicher Mitarbeiter am Institut für Systemdynamik (ehemals Institut für Systemdynamik und Regelungstechnik) der Universität Stuttgart sowie am Max-Planck-Institut für Dynamik komplexer technischer Systeme in Magdeburg. Sie wurde von der Deutschen Forschungsgemeinschaft und vom Bundesministerium für Bildung und Forschung finanziell unterstützt.

Mein besonderer Dank gilt Herrn Prof. Dr.-Ing. Dr. h.c. mult. E.D. Gilles für seine Betreuung und die Unterstützung bei der Durchführung der Arbeit. Die zahlreichen Diskussionen und wertvollen Anregungen sowie die eingeräumten fachlichen Freiräume und Gestaltungsmöglichkeiten haben wesentlich zum Gelingen dieser Arbeit beigetragen. Ebenfalls herzlich bedanken möchte ich mich für seine Unterstützung bei der Planung meines an die Dissertation anschließenden Auslandsaufenthaltes an der Harvard Medical School in Boston.

Des Weiteren gilt mein Dank Herrn Prof. Dr. H.G. Holzhütter von der Berliner Charité, der freundlicherweise den Mitbericht übernommen hat.

Meinen Kolleginnen und Kollegen danke ich sehr für das gute Arbeitsklima und die stets vorhandene Diskussions- und Hilfsbereitschaft. Insbesondere möchte ich Michael Ederer und Markus Koschorreck danken, mit denen ich sehr viele und auch sehr fruchtbare Diskussionen über meine Arbeit führen konnte.

Ein großes Dankeschön gilt auch allen unseren stets hilfsbereiten Sekretariatsmitarbeiterinnen, sowohl in Magdeburg als auch in Stuttgart.

Schließlich wäre diese Arbeit nicht denkbar gewesen ohne die Unterstützung meiner Familie und meines Freundes Roland, die mir immer viel Kraft gegeben haben. Ihnen möchte ich an dieser Stellen ganz besonders herzlich danken.

Ich möchte diese Arbeit meinem verstorbenen Bruder Jochen widmen, der uns allen sehr fehlt und dessen Andenken wir immer bewahren werden.

Boston, 8. Januar 2009

Zum Gedenken an meinen Bruder Jochen

(* 12. April 1981, † 4. März 2008)

Contents

Abstract

Mathematical models of biological processes are becoming more and more important in biology. The goal of mathematical modeling is a holistic understanding of how biological processes like cellular communication, cell division, apoptosis, homeostasis, and adaptation work, how they are regulated and how they react to perturbations. The complexity of the underlying cellular reaction networks barely facilitates an intuitive understanding of how genes, proteins, metabolites and other cellular substances work together. This high complexity of most cellular processes necessitates the generation of mathematical models in order to access the aforementioned processes. In this thesis the focus is set on quantitative and dynamic modeling using ordinary differential equations (ODEs), which allow the transient system behavior to be described. Cellular signal transduction pathways and regulatory networks, in particular, exhibit a very pronounced dynamic behavior and are the main subject of this work.

The possibilities made available through quantitative dynamic modeling of biological networks are enormous. All kinds of *in silico* experiments are feasible, which in reality would be time consuming, expensive or even impossible to accomplish. Such experiments include deletion or addition of components and interactions and the changing of kinetic properties. Additionally, systems theory provides a broad spectrum of mathematical analysis tools, which may provide many suggestions for experimental design or drug target identification. However, a requirement for high quality contributions from theory is the existence of well-founded mathematical models. In modeling cellular signal transduction or regulatory reaction networks one has to face certain problems. Receptors and scaffold proteins, which participate in most of these networks, usually possess a high number of distinct binding domains inducing the formation of large multiprotein signaling complexes. Due to combinatorial reasons the number of distinguishable species grows exponentially with the number of binding domains and can easily reach several millions or even billions. These huge sets of molecular species form highly interconnected reaction networks whose dynamics are restricted by thermodynamic constraints following from the principle of detailed balance.

Most models published in literature account neither for combinatorial variety, nor for thermodynamic restrictions. The majority of available ODE models focus on small subsets of reactions and complexes. The main difficulty with these heuristically reduced model structures is their capability of giving an adequate image of the real system's dynamics especially in the case of varying environmental conditions. A recently introduced and more systematic approach is the translation of a rule-based model formulation into a complete ODE model, accounting for all

feasible reactions and species. Due to their completeness the simulation results of these models are much more reliable. However, even by including only a fairly limited number of components and binding domains the resulting models are already very large and hardly manageable. Furthermore, the problem of incorporating the previously mentioned thermodynamic constraints remains unsolved. For these reasons, new and systematic model reduction or modeling techniques are required that facilitate the generation of highly reduced but accurate models which additionally do not contradict the fundamental laws of thermodynamics.

Using common modeling strategies the resulting ODE models are only in compliance with thermodynamic constraints if the kinetic model parameters fulfill certain mathematical restrictions given by the Wegscheider condition. Systematic analysis reveals that these constraints have a descriptive interpretation when considering receptors and scaffold proteins in signaling cascades. They restrict possible interactions between binding and modification processes. Certain scenarios exist where these interactions may be free of retroactive effects, i.e. unidirectional, and others, where interactions between domains have to be bidirectional. Unidirectionality is an important feature of combinatorial reaction networks, forming the basis for model reduction and modularization methods which will be introduced after the discussion of thermodynamic constraints.

The first step in the development of new modeling or model reduction techniques is the determination of relevant quantities of signal transduction networks. The goal will be finding mathematical models which describe the dynamics of these quantities with sufficient accuracy. Probably, the most popular quantities to describe the current state of receptors or scaffold proteins are occupancy levels of binding domains. Pawson and Nash stated that domains are the fundamental elements of signal transduction, rather than individual molecules. According to this consideration, the conventional mechanistic description of all feasible multiprotein complexes can be replaced by a macroscopic one. Occupancy levels and other characteristics of individual domains like the phosphorylation states of these sites are chosen as new variables. A model using these macroscopic quantities also accounts for limitations in current experimental techniques to measure concentrations of individual multiprotein species. The results of common biological measurements often correspond to cumulative quantities like levels of occupancy or degrees of phoshorylation. Thus, the introduction of these and similar quantities into modeling simplifies the comparison of model variables and experimental readouts. Besides these considerations, this macroscopic description also provides a number of mathematical benefits, such as facilitating the elimination of unobservable and uncontrollable system dynamics which, in most cases, leads to significant model reductions. The elimination of unobservable states is often referred to as exact model reduction. Note, that the term *exact* may be misleading since the elimination of model equations is always linked with loss of information. The reduction is only exact in terms of the input/output behavior which is exactly preserved in the reduced model. In this thesis, we introduce methods that facilitate the elimination of unobservable and uncontrollable system states and also discuss new modeling approaches that allow the direct generation of these reduced model structures. Furthermore, a new approximate reduction method, which is especially suited for large models of combinatorial reaction networks, is developed on the basis

of existing techniques for general nonlinear systems. In combination these methods facilitate the reduction of vast combinatorial reaction network models to a manageable size. Finally, the developed methods are used to generate a model of ErbB and insulin receptor crosstalk.

Kurzfassung

In der Biologie spielen mathematische Modelle eine immer wichtigere Rolle. Das Ziel der mathematischen Modellierung ist hierbei die Entwicklung eines ganzheitlichen Verständnisses biologischer Prozesse wie Zellkommunikation, Zellteilung, Apoptose, Homeostase oder Adaptation. Dabei soll untersucht werden, wie diese Prozesse auf molekularer Ebene ablaufen, wie sie reguliert werden und wie sie auf Störungen reagieren. Die Entwicklung mathematischer Modelle ist zur Beantwortung der aufgezeigten Fragestellungen erforderlich, da die Komplexität der zugrunde liegenden zellulären Reaktionsnetzwerke nur in den seltensten Fällen ein intuitives Verständnis des Zusammenwirkens von Genen, Proteinen, Metaboliten und anderen zellulären Komponenten erlaubt.
In dieser Arbeit geht es um die Erstellung quantitativer dynamischer Modelle auf der Basis gewöhnlicher Differentialgleichungen (DGLn). Vor allem zelluläre Signaltransduktions- und Regulationsnetzwerke zeigen häufig ein sehr ausgeprägt dynamisches Verhalten, weswegen ausschließlich die Modellierung solcher Systeme betrachtet werden soll.

Die durch quantitative dynamische Modellierung eröffneten Möglichkeiten sind enorm. Beispielsweise lassen sich *in silico* Experimente realisieren, deren Durchführung an lebenden Zellen zeitintensiv, teuer oder schlicht unmöglich wäre. Hierzu zählen unter anderem die Deletion oder Addition einzelner Komponenten und Interaktionen sowie die Modifikation kinetischer Eigenschaften. Darüber hinaus stellt die Systemtheorie ein breites Spektrum mathematischer Analysewerkzeuge zur Verfügung, die einen großen Beitrag zum Entwurf zielgerichteter Experimente oder auch zur Identifikation neuer Arzneimittelwirkstoffe liefern können. Eine Voraussetzung dafür ist jedoch das Vorhandensein fundierter mathematischer Modelle, bei deren Erstellung sich eine Reihe von Problemen ergibt. An nahezu allen Signaltransduktions- und Regulationsnetzwerken sind Rezeptoren oder sogenannte Adaptorproteine beteiligt. Diese weisen meist eine hohe Anzahl von Bindestellen auf, wodurch die Bildung sehr großer Multiproteinkomplexe ermöglicht wird. Die Zahl der unterscheidbaren Molekülspezies wächst dabei exponentiell mit der Anzahl der Bindedomänen und kann auf mehrere Millionen oder gar Milliarden ansteigen. Die daraus resultierenden hochvernetzten Reaktionsnetzwerke sind unüberschaubar groß und komplex. Ihre Dynamik wird zudem durch thermodynamisch begründete Zwangsbedingungen eingeschränkt, die sich aus dem Prinzip der mikroskopischen Reversibilität ergeben.

Die überwiegende Anzahl der in der Literatur veröffentlichten Modelle berücksichtigt weder die kombinatorische Komplexität dieser Systeme noch die erwähnten thermodynamischen Beschränkungen. Stattdessen werden die Betrachtungen auf eine kleine Teilmenge von Reaktionen

und Proteinkomplexen begrenzt. Ob die daraus resultierenden, heuristisch reduzierten Modellstrukturen eine zutreffende Vorhersage der wirklichen Systemdynamik zulassen, insbesondere unter variierenden Umweltbedingungen, ist schwierig festzustellen. Ein neuer, sehr viel systematischerer Modellbildungsansatz ist die automatische Generierung vollständiger mechanistischer Modelle auf der Grundlage einer regelbasierten Modellbeschreibung. Aufgrund der Berücksichtigung und Abbildung der kompletten realen Netzwerkstruktur sind die aus diesen Modellen resultierenden Simulationsergebnisse weitaus verlässlicher als diejenigen heuristisch reduzierter Modelle. Allerdings wachsen die Modelle bei Verwendung dieser Methode in vielen Fällen zu einer nicht mehr handhabbaren Größe heran. Selbst die Betrachtung einer sehr beschränkten Menge von Komponenten und Bindestellen führt zu Modellen, die aus mehreren hundert bis mehreren tausend DGLn aufgebaut sind. Darüber hinaus ermöglicht die Methode keine einfache oder gar automatische Integration der angesprochenen thermodynamischen Zwangsbeziehungen. Aus den genannten Gründen ist es notwendig, zum einen neue systematische Verfahren zur Modellreduktion und zur reduzierten Modellierung zu entwickeln und zum anderen Werkzeuge zur Verfügung zu stellen, die eine einfache Einbeziehung thermodynamischer Beschränkungen ermöglichen.

Bei der Verwendung üblicher kinetischer Modellierungsansätze wie beispielsweise dem Massenwirkungsansatz müssen die Modellparameter die sogenannte Wegscheiderbedingung erfüllen, damit das erstellte Modell dem thermodynamischen Grundprinzip der mikroskopischen Reversibilität nicht widerspricht. Systematische Analysen dieser Zwangsbedingungen bei großen kombinatorischen Reaktionsnetzwerken liefern eine anschauliche Interpretationsmöglichkeit dieser Restriktionen. Letztere schränken die Interaktionsmöglichkeiten unterschiedlicher molekularer Binde- oder Modifikationsprozesse ein. So gibt es Netzwerkstrukturen, in denen rückwirkungsfreie, d.h. unidirektionale, Interaktionen realisierbar sind, wohingegen andere Strukturen nur wechselseitige Interaktionen zulassen. Rückwirkungsfreiheit ist ein wichtiges Charakteristikum kombinatorischer Netzwerke, da sie die Grundlage für die ebenfalls im Rahmen dieser Arbeit vorgestellten Modellreduktions- und Modularisierungsmethoden darstellt.

Der erste Schritt in der Entwicklung neuer Modellierungs- und Modellreduktionsmethoden ist die Bestimmung charakteristischer Kenngrößen zur Beschreibung von Signaltransduktionssystemen. Anschließend folgt die Erstellung eines mathematischen Modells, das die Dynamik dieser Kenngrößen hinreichend genau wiedergeben kann. Die gebräuchlichsten Größen, die zur Zustandsbeschreibung eines Rezeptors oder Adaptorproteins verwendet werden, sind Belegungs- und Phosphorylierungsgrade einzelner Bindestellen. Laut Pawson und Nash stellen nicht einzelne Proteinkomplexe, sondern Bindedomänen die wesentlichen Grundelemente der Signaltransduktion dar. In Anlehnung an diese Betrachtung wird in dieser Arbeit die konventionelle, mechanistische Beschreibung kombinatorischer Reaktionsnetzwerke auf Molekülebene durch eine makroskopische Sichtweise auf Bindestellenebene ersetzt. Die so modifizierten Modelle, deren Zustandsvariablen nicht mehr einzelne Molekülkonzentrationen sondern Belegungsgrade sind, werden auch eher den gegenwärtigen Restriktionen bei experimentellen Messungen gerecht. Die gängigen Messmethoden liefern Daten über aggregierte Größen wie Belegungs- oder Phosphorylierungsgrade und nicht über die Konzentrationen einzelner Proteinkomplexe. Somit ermöglicht

die Einführung neuer makroskopischer Zustandsvariablen auch eine einfachere Vergleichbarkeit von Simulation und Messung. Darüber hinaus bringt die Einführung neuer Zustandsvariablen auch eine Reihe mathematischer Vorteile mit sich. Die in dieser Arbeit vorgeschlagene Wahl der Systemkoordinanten ermöglicht die Elimination nicht beobachtbarer und nicht steuerbarer Systemzustände, woraus ein nicht unerhebliches Potential für Modellreduktionen entsteht. Die Elimination nicht beobachtbarer Zustände wird in der Literatur häufig auch als exakte Modellreduktion bezeichnet. Dabei kann das Wort *exakt* missverstanden werden. Jede Modellreduktion ist untrennbar mit einem Informationsverlust verbunden. Exakte Modellreduktionen eines Systems sind nur bezüglich dessen Ein-/Ausgangsverhaltens exakt. Im Rahmen dieser Arbeit werden Methoden zur Durchführung exakter Modellreduktionen vorgestellt. Außerdem werden neue Modellierungsansätze diskutiert, die eine direkte Generierung der sich ergebenden reduzierten Modellstrukturen erlauben. Zur weiteren approximativen Reduktion dieser Modelle werden ebenfalls neue Verfahren vorgestellt, die auf bereits existierenden Methoden für allgemeine nichtlineare Systeme basieren und speziell an die Anforderungen kombinatorischer Reaktionsnetzwerke angepasst sind. Die Kombination all dieser neuen Methoden ermöglicht schließlich die signifikante Reduktion sehr großer Signaltransduktionsmodelle. Die abschließende Anwendung dieser Modellierungs- und Modellreduktionsmethoden bei der Erstellung eines Crosstalk-Modells von EGF- und Insulinrezeptor zeigt beispielhaft, welchen großen praktischen Nutzen die hier entwickelten Verfahren bieten.

Chapter 1

Introduction

The cell is the structural and functional unit of all living organisms. The variety of existing cell types adapted to most different environmental conditions is enormous. Despite this great variety, cells share a lot of fundamental design principles and elementary cellular functions such as cell division, metabolism or response to stimuli. Our current knowledge about these processes is fragmentary, and we are far away from a holistic understanding of entire cells. The recent development of new and improved measurement techniques in molecular biology has given rise to substantial progress in this field. Knowledge about cellular processes has highly increased and revealed a nearly unmanageable complexity of molecular detail. The tremendous number of molecular species and processes occurring within a cell, form strongly interconnected biochemical reaction networks. One main focus of recent research is on different eucaryotic signal transduction pathways like insulin, epidermal growth factor (EGF) or tumor necrosis factor (TNF) signaling. These and other signaling pathways control cellular processes like proliferation, differentiation and apoptosis. Malfunctions within these networks cause maladies like cancer, diabetes mellitus or neurodegenerative disorders [92]. An intuitive understanding of these complex networks and especially of their transient behavior is in most cases unfeasible. The immense complexity necessitates a systematic approach using mathematical models to describe and analyze cellular processes.

Mathematical models facilitate all kinds of virtual experiments, which in reality would be time consuming, expensive or even impossible to accomplish. Such experiments include deletion or addition of components and interactions, and the changing of kinetic properties. Another advantage is the possibility to test new hypotheses for consistency with available data and knowledge about physical laws. Systems theory additionally provides a broad spectrum of mathematical analysis tools which may provide a number of ideas for experimental design or drug target identification.

However, mathematical modeling of biological systems is a quite new and unexplored field. Many of the available modeling and analysis techniques are either not, or only conditionally applicable to such complex systems. Hence, new approaches are required. One big problem occurring in nearly all signaling networks is combinatorial complexity. In this thesis it is shown how this problem can be circumvented using a new approach, which allows for the creation

of reduced dynamic models of combinatorial systems providing an excellent approximation accuracy.

1.1 Signal Transduction Pathways

Cells are equipped with highly developed signaling systems which allow them to sense their environment, receive and process signals and react accordingly. Depending on the environmental conditions, the cell has to take decisions about cell division, differentiation, apoptosis and metabolic control [33]. Despite the great diversity of signaling networks and their functions, most of them share some common principles. Cells most often sense their environment using transmembrane receptors which transfer extracellular signals across the plasma membrane. Activation of these receptors usually results in conformational changes of the receptor protein, initiating a chain of intracellular reactions [2]. In the case of receptor tyrosine kinases (RTKs), binding of extracelluar signaling proteins or growth factors trigger conformational changes that allow for receptor dimerization and subsequent autophosphorylation of numerous cytoplasmic domains [120]. However, receptors can also be activated by small water soluble molecules such as nutrients [33] or by non-chemical signals such as light in the case of rhodopsin receptors [91]. In the cytoplasm, the signal is transduced to other molecules. In many cases, receptor activation induces the formation of large multiprotein complexes [105] that often activate a variety of effector kinases [33]. One of the most prominent examples is the mitogen activated protein kinase cascade (MAPK) [22]. Most signaling pathways finally result in the activation of transcription factors, which translocate to the nucleus and directly influence gene expression [77].

1.2 Combinatorial Complexity and Modeling of Signal Transduction Pathways

The complexity of cellular reaction networks, in most cases, does not facilitate an intuitive understanding of how genes, proteins, metabolites and other cellular components work together. In the field of systems biology, mathematical models are used to access the complexity of these networks systematically. The spectrum of conventional approaches to model signal transduction networks reaches from qualitative models solely relying on the network structure to quantitative ones, with the additional integration of kinetic information. The usage of structural approaches like logical modeling, as proposed by Klamt *et al.* [74]), is especially recommended for highly interconnected large-scale signaling networks where primarily qualitative information is available. Quantitative methods, regardless of whether they are deterministic or stochastic, do have a higher predictive capability. They are also suited to describe and to analyze transient system behavior, as well as nonlinear phenomena such as molecular switches, quantitative signal adaptation or limit cycles, which play crucial roles in biochemical networks. Signal transduction and regulatory networks are highly involved in decision making processes

associated with proliferation, cell division or apoptosis, as well as in the control of other pivotal mechanisms like the circadian rhythm or the cell cycle. Most of these processes have been shown to provide nonlinear system dynamics indicating that a broad understanding requires quantitative modeling [36, 127, 128, 72]. Hence, the focus of this work is on kinetic modeling of signal transduction networks using ordinary differential equations (ODEs), which arguably is the most common modeling methodology. However, one has to stress the greater degree of complexity in kinetic modeling when compared with qualitative methods. A major problem in modeling signal transduction and regulatory networks is the enormous combinatorial complexity of these networks. In signal transduction, receptors and scaffold proteins often possess a high number of distinct binding domains inducing the formation of large multiprotein signaling complexes. Due to combinatorial reasons the number of distinguishable species grows exponentially with the number of binding domains and can easily reach several millions or even billions [56]. Hlavacek *et al.* mention that a complete mechanistic model of EGFR signaling, including a very limited number of signaling proteins and binding domains, would consist of $1,232$ ODEs. The problem of combinatorial complexity has also been recognized earlier by other modelers. Endy and Brent mentioned that the molecules Ste5p, Ste11p, Ste7p, and Fus3p can form $25,666$ distinct multiprotein complexes [37]. Arkin pointed out that the tumor suppressor protein p53 may exist in $2^{27} = 134,217,728$ phospho-forms due to its 27 phosphorylation sites [6]. Many other receptors and scaffold proteins provide a similarly large number of phosphorylation residues. The ErbB receptor family, which will be discussed below, consists of four receptor species providing between 19 and 27 phosphorylation sites. Since these receptors can additionally form homo- and heterodimers, the number of feasible receptor species alone grows to over 10^{16}. This enormous complexity cannot be managed using conventional ODE modeling approaches which are based on mass balances for all feasible species. In the following sections, the way this problem has been tackled previously will be reviewed.

1.2.1 Heuristic Reduction Approach

Many existing models evade the problem of combinatorial variety by substituting the complete mechanistic network structure with a reduced and heuristic one focusing on a restricted number of molecular species and reactions [7, 52, 53, 54, 73, 93, 122, 124]. Common assumptions range from competitive mechanisms for effector binding to consecutive binding of effector proteins in a defined sequence. To illustrate the problems associated with such a heuristic approach, we will show that even in a simple example, seemingly reasonable simplifications may lead to wrong model predictions. The example that will be discussed is a receptor, denoted as R, with three binding domains. One of them is an extracellular domain 1 while the other two are intracellular domains 2 and 3. We assume that extracellular ligand binding induces conformational changes, which highly increase the affinity of the intracellular domains towards their binding partners. The assumed kinetic parameters are depicted in Table 1.1.

A complete mechanistic model comprises eleven different molecular species (extracellular ligand L, intracellular effectors E and F, receptor species $R(0,0,0)$, $R(L,0,0)$, $R(0,E,0)$,

Affinity of domain	$k_{\text{on}} \quad [\text{M}^{-1}\text{min}^{-1}]$	$k_{\text{off}} \quad [\text{min}^{-1}]$	Equilibrium $K_d \quad [\text{M}^{-1}]$
1 (always)	$k_1 = 3 \cdot 10^5$	$k_{-1} = 6$	$5 \cdot 10^4$
2 (domain 1 unoccupied)	$k_2 = 1$	$k_{-2} = 18$	$5.6 \cdot 10^{-2}$
2 (domain 1 occupied)	$k_3 = 5 \cdot 10^7$	$k_{-3} = 24$	$2.1 \cdot 10^6$
3 (domain 1 unoccupied)	$k_4 = 1$	$k_{-4} = 12$	$8.3 \cdot 10^{-2}$
3 (domain 1 occupied)	$k_5 = 1 \cdot 10^5$	$k_{-5} = 60$	$1.7 \cdot 10^3$

Table 1.1: Kinetic parameters of the reaction network.

$R(0,0,F)$, $R(L,E,0)$, $R(L,0,F)$, $R(0,E,F)$ and $R(L,E,F)$) and twelve binding reactions (four reactions describing L binding to $R(0,0,0)$, $R(0,E,0)$, $R(0,0,F)$ and $R(0,E,F)$, four describing E binding to $R(0,0,0)$, $R(L,0,0)$, $R(0,0,F)$ and $R(L,0,F)$, and four describing F binding to $R(0,0,0)$, $R(L,0,0)$, $R(0,E,0)$ and $R(L,E,0)$). For a reduced model some heuristic but reasonable assumptions are made. Since the affinities of the intracellular domains are extremely low for an unoccupied extracellular domain, it seems reasonable to neglect the related reactions. After an extracellular ligand has bound, the resulting affinity as well as the resulting association constant of domain 2 is several hundred-fold higher than the affinity or the association constant of the third domain. Hence, we additionally assume that the effector E, in the majority of cases, will bind before F and that the reduced model only has to include the following three reactions

$$\begin{aligned} R(0,0,0) + L &\leftrightharpoons R(L,0,0) \\ R(L,0,0) + E &\leftrightharpoons R(L,E,0) \\ R(L,E,0) + F &\leftrightharpoons R(L,E,F), \end{aligned} \tag{1.1}$$

and the seven state variables $[L]$, $[E]$, $[F]$, $[R(0,0,0)]$, $[R(L,0,0)]$, $[R(L,E,0)]$ and $[R(L,E,F)]$. Note, that the notation $[X]$ describes the molar concentration of a molecular species X. The model is parameterized with the related kinetic constants shown in Table 1.1.

This represents the assumption of consecutive ligand and effector binding. In the EGF signaling model, presented by Schoeberl *et al.* [122], the two effectors GAP and Shc also bind consecutively to the receptor after stimulation, although the EGF receptor provides two distinct binding domains for these proteins, similar to the example discussed above. In order to compare the predictions of the reduced model with a complete one accounting for all feasible molecular species and reactions, one considers the aggregated concentration of receptors with occupied domains 1, 2 and 3. These cumulated quantities correspond to the levels of occupancy of each domain. A comparison of the simulation results shows that the predictions of the reduced model are incorrect, revealing just how problematic such heuristic reduction approaches are (compare Figure 1.1). The discussed example is also consistent with the findings of Faeder *et al.* [38]. In their work they showed through simulation studies, that in combinatorial reaction networks only a relatively small part of the network might be active meaning that the concentration of many species is negligible. By eliminating these species as well as the associ-

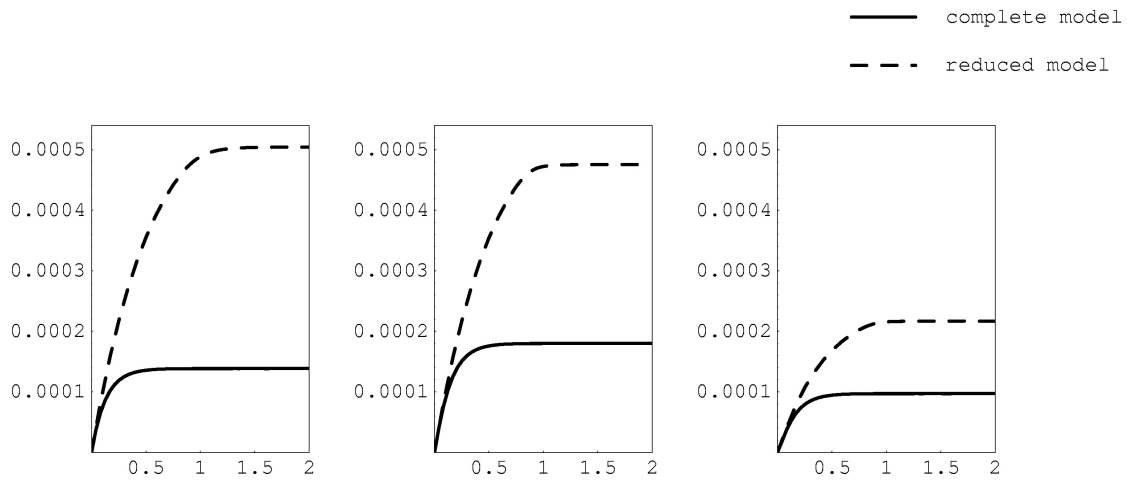

Figure 1.1: Simulation results of the reduced and complete models. The three graphs show the three levels of occupancy of the considered receptor. The left graph shows the level of occupancy of domain 1, the graph in the middle the one of domain 2 and the graph on the right the one of domain 3. Both models are simulated using the same kinetic parameters and initial conditions. The concentrations are plotted in Molar.

ated reactions a fairly reduced model can be obtained. Although predictions of this reduced model match those of the complete one for the original parameter values quite well, the reduced model is not predictive over a larger range of parameter values. Even very small perturbations in the parameters may result in large approximation errors. Consequently, one can conclude that reduced network structures might provide good approximations in a limited parameter domain, however, their derivation necessitates knowledge about the kinetic parameters of the system as well as extensive simulation studies similar to other reduction methods such as POD (see below). In the majority of cases, a heuristically derived model structure will be insufficient when making an approximation of the real system.

1.2.2 Stochastic Approaches

An alternative approach to tackle combinatorial complexity is stochastic simulation. Stochastic models do have a number of advantages. Such advantages include the concentration that stochastic models are probably more realistic representations of real systems than ODE models, since cellular processes have an inherently stochastic nature. Additionally, it can be shown that stochastic mechanisms can have significant effects on a system's dynamic behavior [36, 35, 80], which can only be analyzed using stochastic models. Examples of tools which allow for the creation of stochastic models of combinatorial networks are StochSim and Moleculizer 1.0. StochSim was developed in 1998 to circumvent the problem of combinatorial complexity in

modeling bacterial chemotaxis [94, 125]. MOLECULIZER 1.0 is a novel modeling tool, which allows for the automatic generation of cellular reaction networks [88]. Similar to other tools that are designed for combinatorial reaction networks, MOLECULIZER allows model specification using reaction rules which will be discussed in more detail below. The enormous complexity of the stochastic model is reduced by a new approach which incorporates complexes and reactions only when they are needed as the simulation proceeds. MOLECULIZER as well as STOCHSIM facilitate non-spatial stochastic simulations and are based on the famous work of Gillespie [48, 49].
However, the computational cost for stochastic simulations is in most cases extremely high, since it increases disproportionately with the number of molecules. Additionally, it is much harder to analyze the dynamic behavior of a stochastic model or to identify the model parameters from measurements [15].

1.2.3 Complete Mechanistic Representations

A novel approach that is based on ODE models has been introduced by Blinov *et al.* [13]. The modeling tool BIONETGEN allows a rule-based model specification, which is automatically expanded to a complete mechanistic ODE model that can be simulated and analyzed. BIONETGEN has been used to create a number of signaling models including EGF receptor signaling and FcεRI signaling [40, 14]. Blinov *et al.* call their approach *generate-first* modeling [15] in contrast to *on-the-fly* modeling such as that proposed by Lok and Brent [88]. The expression *generate-first* refers to the fact that BIONETGEN initially generates all species, reactions and equations out of the specified reaction rules before a simulation can be performed. MOLECULIZER on the other hand incorporates complexes and reactions only when they are required as the simulation proceeds [88]. Note, that the *generate-first* method can also be applied when generating stochastic models [15]. However, if one keeps in mind that combinatorial reaction networks can easily comprise 10^{16} or even more feasible multiprotein complexes as shown for the ErbB signaling cascade, it becomes clear that both methods cannot cope with this complexity. The mechanistic models of EGF and FcεRI signaling generated by BIONETGEN include only a very limited number of components and binding domains.

1.2.4 Domain-Oriented Approach

An alternative approach has been proposed by Borisov *et al.* [16, 17]. The approach adopts the point of view that the fundamental elements of signal transduction are domains instead of molecular species [106]. Accordingly, Borisov *et al.* has suggested the substitution of the common mechanistic network description which includes all individual molecular species with a macrodescription. In this context, the term *micro-state* is used to describe individual multiprotein complexes, whereas the term *macro-state* refers to large sets of micro-states sharing a certain characteristic, for example, the phosphorylation of a defined binding domain. These macro-states correspond to descriptive biological quantities, such as phosphorylation degrees or

levels of occupancy. Macro-states describe the evolution of an isolated binding or phosphorylation process at a defined domain. A model using these macroscopic quantities also accounts for limitations in current experimental techniques to measure concentrations of individual multi-protein species. The results of common biological measurements (such as immunoprecipitation followed by western blotting) correspond to cumulative quantities, such as levels of occupancy or degrees of phoshorylation.
Hence, the goal of this approach is the generation of a dynamic ODE model describing the concentrations of these macro-states. Borisov *et al.* show, for two important special cases, that a reduced number of ODEs is sufficient to describe the dynamics of these macro-states accurately. One of the discussed examples is a scaffold protein with a large number of independent binding domains. The other special case discussed by Borisov *et al.* is a scaffold protein with one controlling domain, for which the kinetic properties of all other domains change if and only if the controlling domain is occupied or phosphorylated. This approach is very promising although it still lacks a systematic procedural method applicable to all kinds of signaling networks.

1.3 Goals and Outline of the Thesis

Most models published in literature do not account for the combinatorial variety of signal transduction networks. Software tools like Moleculizer or BioNetGen facilitate the translation of a rule-based model formulation into more detailed and realistic models. However, even by limiting the considerations to a relatively small number of components and binding domains the resulting models tend to be unmanageably large. A novel approach is required to reduce combinatorial complexity in a systematic manner.

The goal of this thesis is the development of new reduction techniques for ODE models of combinatorial networks based on the work of Borisov *et al.* [16, 17]. In terms of model reduction this includes systematization and extension of the exact reduction approach described by Borisov *et al.* [16] and the development of new approximate methods. In this context simple criteria are required which allow one to determine whether or not an exact reduction of a model can be produced. For approximate methods on the other hand the approximation error should be assessable by some simple characteristics. In addition to model reduction, which allows the *reduction* of a large model, we also discuss reduced order modeling, providing for the possibility of immediate derivation of reduced model equations. Most real signaling networks are only accessible by reduced order modeling, since the generation of a complete mechanistic model and its subsequent reduction is not practical due to its enormous complexity. Another requirement is compatibility with the widely-used rule-based modeling approach for combinatorial networks which will also be included in the forthcoming version of the Systems Biology Markup Language (SBML Level 3) [57, 45].

The detailed discussion of these issues requires preliminary work and definitions which are given in the following chapter. We introduce the ErbB and the insulin signaling networks, which will serve as representative examples for highly complex signal transduction networks throughout

the thesis. Like most other model reduction techniques that are described in literature, the methods developed here are either based on time-scale separation or on the elimination of unobservable and uncontrollable system dynamics. Hence, we review some fundamental principles of model reduction in the mathematical background section. This section also serves the purpose to draw the readers attention to the advantages and drawbacks of already available methods. Additionally, Chapter 2 gives a detailed discussion of rule-based modeling and clarifies the notation used in this thesis.

The results of Borisov *et al.* [16], as discussed above, indicate that the reduced model structures highly depend on interactions between distinct binding and modification processes. Such interactions, which are also introduced in Chapter 2, correspond to certain relations between kinetic parameters. However, the kinetic properties of a combinatorial reaction system are highly restricted by thermodynamic constraints. In Chapter 3 we analyze the implications of thermodynamic constraints on the feasibility of process interactions in combinatorial networks and on model reduction.

Chapters 4 and 5 focus on the development of new domain-oriented reduction techniques. Chapter 4 deals with the systematization and extension of the exact reduction approach introduced by Borisov *et al.* [16, 17] in order to provide procedures applicable to all kinds of combinatorial networks. Approaches for both model reduction and reduced order modeling are provided. In Chapter 5, we also present a new approximate reduction technique and discuss its advantages and drawbacks. Important aspects of this work have already been published [29, 30, 31, 32, 78], and will be reviewed and extended here.

Finally, the developed methods are used to generate a model of ErbB and insulin receptor crosstalk. The exact reduction of this model is presented in Chapter 4 while the approximately reduced model version is discussed in Chapter 5. In order to evaluate its approximation quality, the approximately reduced model will be compared to one reduced with another common nonlinear model reduction method.

Chapter 2

Preliminaries and Background

2.1 Biological Background - Receptor Tyrosine Kinases

In this thesis, receptor tyrosine kinases (RTKs) are used to exemplify the developed model reduction and reduced modeling techniques. In many cases, greatly simplified models of real RTKs will be used in order to illustrate the main principles of the discussed methods. However, we will also provide a more detailed model of receptor crosstalk.
RTKs form a family of high affinity cell surface receptors with a large number of ligands including growth factors, cytokines and hormones. In the human genome one has identified about ninety genes that represent protein tyrosine kinases of which 58 encode receptor tyrosine kinase proteins [114, 3]. The RTKs are divided into several classes [2]. Two of the most prominent and best studied RTK subfamilies are the ErbB receptor and the insulin receptor families. All of the following examples will be based on these two signaling networks. Hence, the basic knowledge about these receptor families shall be reviewed below.

2.1.1 The ErbB Receptor Family

The ErbB/HER family of RTKs plays a crucial role in proliferation, differentiation, migration and survival of mammalian cells [120, 68], where dysfunction of the ErbB signaling network can cause cell transformation and cancer [146, 64]. The ErbB receptor family contains four cell surface receptors, namely ErbB1-4, and can bind at least 13 different ligands such as EGF, TGFα, NRG and Amphiregulin. Note, that the ErbB1 receptor is also known as EGFR (Epidermal Growth Factor Receptor), while ErbB2-4 are also often referred to as HER2-4. All ligands of these receptors share an epidermal growth factor (EGF) domain [108, 27]. After stimulation, the monomeric receptors form receptor dimers resulting in autophosphorylation of their cytoplasmic domains [83, 66, 120].

A lot of insights into ErbB signaling are based on the molecular structure of these receptors. The extracellular domain of ErbB receptors consists of four subdomains (I, II, III and IV).

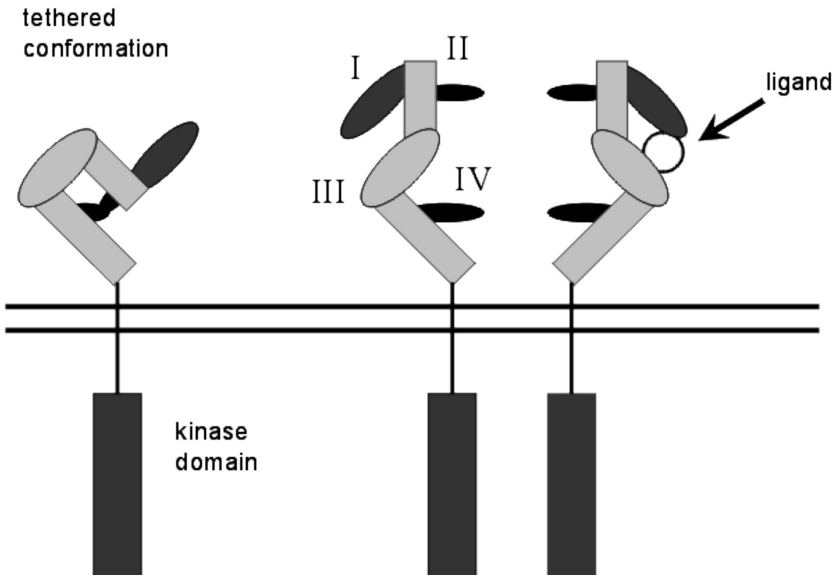

Figure 2.1: Schematic depiction of the ErbB receptor structure with its four subdomains adapted from Klein et al. [76]. The receptor is shown in both its tethered and its extended form. In the extended form the dimerization arms are exposed and dimerization can occur.

Subdomains I and III contain leucine-rich sequences that can bind to the ligands, whereas subdomains II and IV consist mainly of cysteine-rich sequences that comprise two dimerization arms [81, 18]. Intramolecular forces between domains II and IV stabilize the protein in an autoinhibited or tethered conformation and prevent access to the dimerization arms [26, 44, 76]. The intramolecular tether is, however, not very strong and receptors can undergo a conformational change to uncouple domains II from IV, which is preferably what will happen if a ligand binds to the receptor [104]. A schematic structure of the extracellular receptor domain is shown in Figure 2.1. The extended state exposes both dimerization arms and brings domains I and III closer together which increases ligand binding affinity. In their untethered form domains I and II are free to pivot about a hinge-like region connecting them to domains III and IV. Receptors in this extended conformation can form homo- or heterodimers that are stabilized by the exposed dimerization arms [18, 100, 46]. Another interesting feature of the ErbB receptor family is that ErbB2 and ErbB3 cannot autonomously relay extracellular signals to the cytoplasm. For ErbB2 no ligand has been identified which might be explained by the fact that ErbB2 is permanently in its untethered state due to a strong interaction between its domains I and III. This prevents ligand access to these binding domains [27, 51]. However, ErbB2 serves as the preferred partner for heterodimerization with other ErbB receptors. ErbB3 on the other hand possesses a defective kinase domain [75], but also signals through ErbB heterodimers.
Dimerization induces receptor kinase activity resulting in autophosphorylation of various cytoplasmic residues. After phosphorylation of the cytoplasmic domains the ErbB receptors can recruit numerous effector proteins such as Gab1, Shc, Grb2 and PLCγ which have very different downstream targets. These effector proteins can also be phosphorylated by the receptor

	ErbB1	ErbB2	ErbB3	ErbB4
Total number of cytosolic tyrosines	20	19	23	27
No binding partner	8	11	14	16
One binding partner	6	7	8	7
More than one interaction partner	6	1	1	4
Number of different binding partners	8	4	4	7
Binding domains for Grb2	6	1	2	6
Binding domains for Shc	6	5	1	4
Binding domains for PI3K	0	0	6	1
Binding domains for Cbl	1	0	0	0
Binding domains for STAT5	2	0	0	1
Binding domains for PTP-2c	3	1	0	1
Binding domains for Crk	1	0	0	1
Binding domains for Nck	0	0	0	1
Binding domains for Src	1	0	1	0
Binding domains for SH3BGRL	1	1	0	0

Table 2.1: Overview of phosphorylated tyrosine residues of the ErbB receptor family. The data is taken from Alory et al. and Schulze et al. [4, 123].

kinase after binding [41, 58, 107, 20]. Altogether, 89 potential tyrosine phosphorylation sites on the four ErbB receptors are known [123, 136]. For 28 of them, one single binding partner has been identified. For 12 phosphorylation sites, more than one binding partner has been found, and 49 tyrosine residues do not seem to have any binding partner. Most of the residues that lack a binding partner are located near the kinase domain, while the others were found at the C-terminal regions of the receptor. Table 2.1 gives an overview of the phosphorylated tyrosine residues for the ErbB receptors and their potential binding partners. These adaptor proteins themselves can recruit further signaling proteins and/or activate downstream signaling cascades such as the MAP kinase cascade [22]. The effector protein Shc, for example, is known to possess both a phosphotyrosine binding domain (PTB) and a Src homology 2 domain (SH2). With its PTB domain Shc primarily interacts with the ErbB and other RTK receptors, whereas the phosphorylated SH2 domain predominantly interacts with Grb2 [115]. Grb2 possess two additional domains which recruit the adaptor protein SOS. SOS is a guanine exchange factor (GEF) which can activate the membrane bound small G-protein Ras, by effecting the exchange of GDP to GTP [86, 24]. Active RasGTP in turn initiates the MAP kinase cascade. Phosphorylated ERK which is a component of the MAP kinase cascade stimulates a serine/threonine phosphorylation of SOS, resulting in dissociation of the Grb2-SOS complex [137, 24].

A further very important process in signal transduction is receptor internalization. Thereby the ErbB receptors cluster over clathrin-coated regions of the cell surface and are subsequently invaginated by the plasma membrane forming endocytic vesicles [147]. The main purpose of

ligand induced internalization and endocytosis is assumed to be the downregulation of growth factor signaling. However, there is growing evidence suggesting that internalized receptors activate signaling pathways other than just receptors at the plasma membrane [147, 95, 97]. Most data about internalization of ErbB receptors is available for EGFR/ErbB1. In literature there is a controversial discussion about how internalization is induced [25, 43, 142, 121]. More recent experimental data suggests that ErbB1 kinase activity and autophosphorylation only play a minor role in receptor internalization, while dimerization seems to be essential [135]. Additionally, the effector molecule Grb2 is also reported to play a crucial role in the initial steps of receptor internalization [67].

Internalized and phosphorylated ErbB1 receptors might bind the E3 ubiquitin ligase Cbl which induces ubiquitination. Receptors that are marked by ubiquitin are targeted to the lysosome for degradation [27]. Receptors that are not ubiquitinated, as well as those that are deubiquitinated by so-called DUBs (deubiquitinating enzymes), are more likely recycled to the cell surface [27]. The other three ErbB receptors are endocytosis impaired and are mostly recycled to the plasma membrane [147, 109, 8]. ErbB1 receptors are reported to be predominantly targeted to the lysosome, while ErbB3 is recycled more often. Heterodimerization with the ErbB2 receptor decreases the degradation rate and increases recycling of its partners [147, 143, 84].

2.1.2 The Insulin Receptor Family

The insulin receptor signaling system is of high medical interest and therefore well studied [71, 116, 117, 129]. Insulin regulates cellular glucose uptake [23, 71] and has a major impact on metabolism [110, 117]. It promotes synthesis and storage of glycogen, proteins and lipids and negatively regulates their degradation. Furthermore, it negatively regulates secretion of sugars, amino acids and fatty acids [116]. It is involved in gene expression [96], cell survival and differentiation. Defects in the insulin signaling system give rise to wide spread maladies like insulin resistance and obesity [85, 21, 89].

The insulin receptor family consists of three distinct receptors: the insulin receptor (IR), the insulin-like growth factor receptor (IGFR) and the IR related receptor (IRR) [136]. The insulin receptor (IR) plays a crucial role in regulation of protein, carbohydrate and lipid metabolism of higher organisms. The closely related insulin-like growth factor receptor (IGFR) is involved in normal growth and development [1, 136]. Only very limited information is available about the IR related receptor IRR. Until now no ligand has been identified for this receptor. It is known, however, that IRR can mediate male sexual differentiation in mice, which indicates that a yet unknown IRR ligand may exist [98]. Another discussed possibility is that IRR has a similar function such as ErbB2 [69, 126]. All three members of the insulin receptor family are constitutively dimerized. Each monomeric receptor consists of two disulfide-linked protein subunits (α, β). The α subunit is completely extracellular. The β subunit comprises an extracellular, a transmembrane and an intracellular part. In contrast to most other receptor tyronsine kinases the constitutively dimerized insulin receptors are activated exclusively by

ligand binding without further oligomerization [103]. Consequently, ligand binding alone has to induce conformational changes which increase the kinase activity of the receptors and lead to autophosphorylation of the intracellular binding domains [103].

The available data about binding domains and binding partners of insulin receptors is not as detailed as that for the ErbB signaling system. However, it is known that, similar to the ErbB system, phosphorylation of the receptors directly or indirectly activates a number of common downstream signaling proteins, such as Grb2, Shc, PLCγ and PI3K. Additionally, most signaling events are mediated through the family of insulin receptor substrates (IRS). IRS is a family of scaffold proteins providing 20-22 potential binding domains which recruit various other downstream proteins [103].
The insulin receptor IR has binding sites for IRS and Shc. Both sites become phosphorylated before effector binding [116]. Similar to the processes in the ErbB signaling network, Shc then becomes phosphorylated and binds to Grb2. Grb2 can bind with SOS, which in turn can be phosphorylated. IRS has four binding sites for PI3K (in fact, it has at least nine binding sites for PI3K, with each PI3K occupying two binding sites), one for Grb2 and one for SHP2 [140].

Although we only discuss two RTK receptor families and restrict our further considerations to a very limited number of adaptor proteins, these systems highlight the enormous complexity of eukaryotic signal transduction networks. Complete mechanistic descriptions of these complex networks are unfeasible. Model reduction techniques are required in order to generate practically manageable ODE models. In the following section, we give an introduction and overview to common modeling and model reduction techniques.

2.2 Modeling Background - Kinetic ODE Models

Modeling is an ambiguous term which comprises a wide spectrum of model types and modeling methods. Firstly, one has to specify what kind of models will be generated. In the following sections and chapters, we will always consider ordinary differential equation (ODE) models given in state space representation

$$\begin{aligned} \dot{\vec{x}}(t) &= \vec{f}\left(\vec{x}(t), \vec{u}(t), \vec{p}\right) \qquad \vec{x}(t_0) = \vec{x}_0 \\ \vec{y}(t) &= \vec{h}\left(\vec{x}(t)\right), \end{aligned} \tag{2.1}$$

where $\vec{x}(t)$ denotes the n-dimensional vector of all dynamic states or variables, $\vec{u}(t)$ represents the m-dimensional vector of all external input signals and $\vec{p}$ is the q-dimensional vector of all model parameters. The vector $\vec{y}(t)$ comprises all ρ output variables of the system, which either correspond to measured quantities or more generally to all quantities of interest. The vector field $\vec{f}$ and the vector valued function $\vec{h}$ do have appropriate dimensions.

2.2.1 Kinetic Modeling of Reaction Networks

An ODE model of a biological reaction network is usually deduced on the basis of mass or mole balances. The first modeling step is the translation of all feasible reactions $A + B \leftrightharpoons C$ into reaction rates. In this thesis, we will always assume that reaction rates are formulated using mass action kinetics such as $r = k_{\text{on}}[A]\,[B] - k_{\text{off}}[C]$, where k_{on} and k_{off} denote the association and dissociation constants, while $[A]$, $[B]$ and $[C]$ refer to the mole concentrations or molarities of the corresponding species. The second step is the derivation of the mass or mole balances. The mole balances for all feasible species have the form

$$\frac{dn_i}{dt} = \left(\sum r_{\text{production}} - \sum r_{\text{consumption}}\right) \cdot V. \tag{2.2}$$

V is the volume of the cellular compartment in which the reactions occur. These mole balances can be translated into ODEs for the concentrations $[X_i]$ using the relation $n_i = [X_i]\,V$. For constant volume V, which we will assume in this thesis, the ODEs have the form

$$\frac{d[X_i]}{dt} = \sum r_{\text{production}} - \sum r_{\text{consumption}}. \tag{2.3}$$

In vector notation this can also be written using the stoichiometric matrix N

$$\dot{\vec{x}} = N\vec{r}(\vec{x}, \vec{u}, \vec{p}) = \vec{f}(\vec{x}, \vec{u}, \vec{p}), \tag{2.4}$$

which will be explained below. In this equation, $\vec{x}$ is the vector of all concentrations $[X_i]$, and $\vec{r}$ is the vector of all reaction rates which are functions of the state variables and the inputs. The kinetic reaction constants k_{on} and k_{off} correspond to the model parameters $\vec{p}$.

As a simple example, we consider a receptor R which provides two binding domains for the two ligands L and E. In this case the reaction system consists of four reversible reactions (two describing L binding to $R(0,0)$ and $R(0,E)$, and two describing E binding to $R(0,0)$ and $R(L,0)$), for which the following reaction rates can be constructed

$$\begin{aligned}
r_1 &= k_1[R(0,0)] \cdot [L] - k_{-1}[R(L,0)] \\
r_2 &= k_2[R(0,E)] \cdot [L] - k_{-2}[R(L,E)] \\
r_3 &= k_3[R(0,0)] \cdot [E] - k_{-3}[R(0,E)] \\
r_4 &= k_4[R(L,0)] \cdot [E] - k_{-4}[R(L,E)].
\end{aligned} \tag{2.5}$$

We assume that the concentration $[L]$ can be considered as input function. For the remaining five concentrations, one can construct the ODEs

$$\frac{d}{dt}\begin{bmatrix} [R(0,0)] \\ [R(L,0)] \\ [R(0,E)] \\ [R(L,E)] \\ [E] \end{bmatrix} = \underbrace{\begin{bmatrix} -1 & 0 & -1 & 0 \\ 1 & 0 & 0 & -1 \\ 0 & -1 & 1 & 0 \\ 0 & 1 & 0 & 1 \\ 0 & 0 & -1 & -1 \end{bmatrix}}_{N} \begin{bmatrix} r_1 \\ r_2 \\ r_3 \\ r_4 \end{bmatrix}, \tag{2.6}$$

which, however, are linearly dependent due to conservation relations. In this simple example it can be easily seen that

$$\begin{aligned} \frac{d}{dt}\left([R(0,0)] + [R(L,0)] + [R(0,E)] + [R(L,E)]\right) &= 0 \\ \frac{d}{dt}\left([E] + [R(0,E)] + [R(L,E)]\right) &= 0. \end{aligned} \tag{2.7}$$

These two equations correspond to conservation relations for R and E. Since the model does not comprise production or degradation of any species, it is obvious that the overall concentrations $[R_{tot}]$ and $[E_{tot}]$ remain constant. In this thesis, such a conserved quantity is referred to as a thermodynamic component or a conserved moiety.

2.2.2 Combinatorial Reaction Networks

Cellular signal transduction networks as well as regulatory networks are characterized by an enormous complexity. This complexity results from combinatorial effects which are due to the relatively high number of binding domains of receptors or scaffold proteins. Within the last few years a number of new approaches have been explored in order to model, analyze and structure these networks and to cope with their complexity. New representation formalisms peculiar to combinatorial reaction networks emerged within the last few years. The notation for combinatorial reaction networks used in this thesis follows these new formalisms, which are reviewed below.

Multiprotein Complexes in Signaling. The formation of multiprotein complexes is a characteristic feature of numerous signaling cascades. The reason for this complex formation is that many receptors and scaffold proteins participating in signaling networks provide a high number of binding domains. Even most effector proteins possess more than one binding domain. This can result in large and branched multiprotein complexes. From a mathematical point of view these complexes can be depicted as undirected graphs [12]. In a simplified representation, which will be sufficient for our purpose, each protein corresponds to a node and each active binding represents an edge. These graphs can be divided into two main categories, namely trees and other more general graphs. A tree is defined as a graph in which any two nodes are connected by exactly one path. Trees can also be characterized as connected graphs without cycles. The mentioned classification is also reasonable from a biological point of view since cycles in a graph structure indicate that the corresponding multiprotein complex can theoretically get infinitely large. This can be further exemplified when considering two proteins A and B, both of which have two binding domains. Let us assume that the two domains of A can bind B and both domains of B can bind A. This constellation theoretically facilitates an infinitely long chain of alternating A and B proteins or closed protein chains of arbitrary size. Receptor clustering phenomena such as that observed in TNF signaling may result from such or similar

mechanisms [148]. The multiprotein complexes occurring in ErbB and insulin signaling can both be represented by trees. In this thesis, we will only consider such systems. Systems including clustering phenomena, like the TNF receptor system, have to be treated differently. One possible approach to handle such systems could be the concept of population balances as used in modeling crystallization processes in chemical engineering.
Trees can either be represented graphically or textually. A graphical representation of the resulting trees is used in BioNetGen [13]. In this thesis, multiprotein complexes will be represented by a simplified textual representation similar to that introduced by Faeder *et al.* [39]. Since undirected trees do not possess a uniquely determined root node, their schematic textual representation is not unique either. However, it appears reasonable to choose the receptor or scaffold providing the largest number of domains as the root node.

Receptors with Single Protein Ligands. Let us consider a receptor R with a number of binding domains, where each domain j can bind an effector E^j. If this effector E^j cannot recruit further signaling proteins it will be called a *single protein ligand*. One possible molecular species could be $R(E^1, 0, E^3, ..., E^n)$. The introduced identifiers describe the status of the binding domain. The identifier 0 depicts an unoccupied domain while E^j indicates that the j-th domain is occupied. Alternatively, the molecular species $R(E^1, 0, E^3, ..., E^n)$ can also be represented by $R(1, 0, 1, ..., 1)$ if each domain can only be occupied by one specific effector. In this case the identifier 1 represents an occupied domain. This representation also allows the definition of macro-states as introduced by Borisov *et al.* [16]. The definition of macro-states requires an additional identifier, like an asterisk, which has the meaning of a replacement character. $R(1, *, ..., *)$ describes the set of all micro-states that have bound E^1 no matter if other domains are occupied or not. Macro-states such as those can be interpreted as levels of occupancy of the considered domains. The usage of the asterisk label allows the additional characterization of other sets of micro-states such as $R(1, *, *, 1, *, ..., *)$ which is a subset of the earlier definied occupancy level. These states can be considered as some generalized macro-states or mesoscopic states. Concentrations of macro-states depicted as $[R(1, *, ..., *)]$ correspond to the sum of all related micro-state concentrations.

Receptors with Multiprotein Ligands. Many multiprotein complexes include chains of associated proteins. Let us assume that the receptor R can bind the effector E_1, which in turn can bind E_2 and so on, until the effector E_{n-1} finally binds E_n. Generally, an adequate representation of such a complex would be $R(E_1(E_2(....)))$ which is difficult to handle due to the high number of nested parentheses. Hence, we will restrict our considerations on multiprotein complexes in which the sequence of proteins within the chain is unique. This assumption facilitates an alternative simplified representation $R(E_i)$ which indicates that the chain of proteins includes all effectors from R to E_i. Additionally, a new type of macro-state has to be introduced, namely $R(E_i(*))$ which corresponds to the set of all complexes that at least comprise the protein chain from R to E_i.

Branched Systems. Branched systems usually consist of a receptor and a number of further scaffold proteins associating to the receptor in the process of signaling. One example is the binding of the scaffold IRS to the insulin receptor. A receptor R that can bind the effectors E^1 to E^n as well as a scaffold S which in turn can bind numerous further effector proteins shall be represented by $R(E^1, ..., S(E^{S1}, ..., E^{Sn}), ..., E^n)$. By using the asterisk label one can characterize any type of generalized macro-state.

Receptor Dimers. We will study one special case of branched systems in more detail; namely receptor dimers such as those occurring in ErbB signaling. In contrast to the already introduced representation for branched systems, an alternative one will be used for dimeric species for the purpose of clarity. Let us assume that the receptor R can bind several effector proteins and additionally forms homodimers. The resulting multiprotein species shall be represented by $R(E^1, ..., E^n).R(E^1, ..., E^n)$. Note that we will not distinguish between symmetric dimers. Hence, the two species $R(E^1, 0, E^3).R(0, 0, E^3)$ and $R(0, 0, E^3).R(E^1, 0, E^3)$ will be considered as equivalent. In terms of macro-states, we will distinguish between $R(E^1, *, ..., *).R(*, ..., *)$ and $R(E^1, *, ..., *).*$. The first expression describes all dimers of which at least one receptor has bound E^1, whereas the latter expression characterizes all receptors that have bound E^1 no matter if they are part of a monomeric species or a dimeric one. All these agreements also apply for heterodimers.

The post-translational modification of binding domains through phosphorylation or ubiquitination will be depicted by the labels P and Ub. In order to distinguish between receptor phosphorylation and phosphorylation of an effector protein we write $R(P)$ and $R(E^1(P))$ respectively.

2.2.3 Reaction Rules

As discussed above, combinatorial reaction networks may consist of billions of species and reactions. An interesting question is that of how the essence of these networks can be captured without specifying all species and reactions manually. Within the last few years, several research groups have suggested the use of reaction rules as a form of generalized reaction, to characterize combinatorial networks. Rules serve as patterns which allow for the automatic generation of all reactions and species [57, 39, 12]. A rule comprises patterns for reactants and products, a mapping from reactants to products and a rate law. Patterns for reactants or products can be depicted by macro-states. The most commonly used approach to quantify rate laws in signaling networks is probably the mass action kinetic. Unless otherwise noted we assume mass action kinetics for all reactions considered in this thesis. A rule like

$$R(0, *, ..., *) + L \leftrightharpoons R(L, *, ..., *) \tag{2.8}$$

is used to identify, through pattern matching, the species that have specific features required to undergo the specified transformation. By convention, the rate laws for all implied elementary

reactions are parameterized by the same kinetic parameters, indicating that the described binding or modification is independent of all features not explicitly included [57]. Hence, reaction rules imply interactions between distinct domains or binding processes. Let us assume that binding of L increases the phosphorylation degree at another domain. This interaction can be depicted by formulating two reaction rules for the considered phosphorylation

$$\begin{aligned} R(0,0,*,...,*) &\leftrightharpoons R(0,P,*,...,*) \\ R(L,0,*,...,*) &\leftrightharpoons R(L,P,*,...,*) \end{aligned} \tag{2.9}$$

where each rule is parameterized with different kinetic parameters. In general, the exact number of reactions generated by rules like these depends on the entire set of rules in which the considered rule is embedded.
Reaction rules have proven to be a representation offering all required degrees of freedom in order to specify models of combinatorial networks. Hence, the concept of reaction rules is a new feature that will be included in SBML Level 3 (Systems Biology Markup Language). SBML is the standard exchange format for computational models of biochemical networks [45, 63]. However, one drawback of a rule-based representation is that interactions between distinct binding and modification processes, which will play a major role in the following subsection, are hard to extract for complex systems. An ideal modeling tool should probably provide a visualization of the process interactions realized by the specified reaction rules. A more detailed introduction to the concept of process interactions is given below.

2.2.4 Process Interactions

A common problem in modeling large reaction networks is the enormous number of unknown kinetic parameters. This especially holds true for combinatorial networks, which describe multiprotein complex formation. In accordance with thermodynamics, we assume in this thesis that all reactions are reversible. In conjunction with the law of mass action this yields two kinetic parameters per reaction. Considering different models [73, 122, 40, 12] and modeling techniques [13, 16, 32, 78] for signal transduction networks, it becomes apparent that the large number of occurring reactions must be parameterized by a relatively small number of different kinetic parameters. However, the assumptions which determine those reactions that are parameterized by the same parameter values and those determined by different parameter values vary. The most accurate suggestion is probably to determine this qualitative parameterization on the basis of process interactions.
In this context, we adapt the point of view that domains instead of molecular species are the fundamental elements in signal transduction [106]. Binding domains can be either occupied by other proteins or can undergo post-translational modifications such as phosphorylation. We define a binding process as the sum of all reactions that change the occupancy level of the considered domain. Analogously, we define a modification process as the sum of all reactions changing the degree of modification of a domain. Two arbitrary processes, no matter whether they are

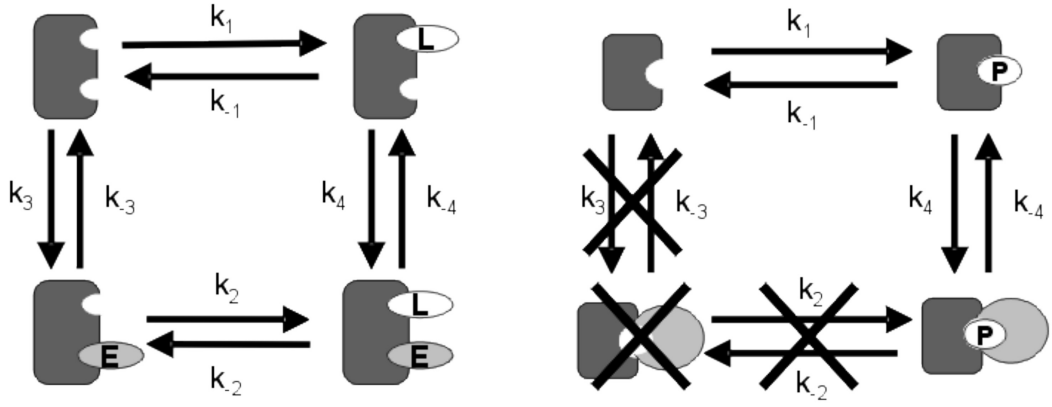

Figure 2.2: A reaction cycle such as that depicted on the left can describe non-interacting processes, unidirectionally or mutually interacting processes. A reaction chain as shown on the right realizes a special mutual interaction, called an *all-or-none* interaction [78].

binding or modification processes, may be either completely independent, interact unidirectionally or interact mutually. Koschorreck *et al.* [78] additionally discuss so-called all-or-none interactions which represent an important border case of mutually interacting processes. These different types of interactions will be further explained by considering a very simple example. In this simple example, one considers a receptor R which provides two binding domains for the two ligands L and E. Hence, the system comprises two binding processes, namely L binding and E binding. In this case the reaction system consists of four reversible reactions depicted in Equation 2.5 (two describing L binding to $R(0,0)$ and $R(0,E)$, and two describing E binding to $R(0,0)$ and $R(L,0)$). The following process interaction types can be distinguished

- **non-interacting processes**
  Complete independence implies that the kinetic association and dissociation constants of one domain do not change upon ligand binding on the other domain. Hence, it follows for the parameters $k_2 = k_1$, $k_{-2} = k_{-1}$, $k_4 = k_3$ and $k_{-4} = k_{-3}$.

- **unidirectionally interacting processes**
  The binding of one ligand, for example ligand L, is not influenced by the binding of the other one. However, L binding does change the kinetic properties of the other domain. In this case, only the conditions $k_2 = k_1$ and $k_{-2} = k_{-1}$ have to be fulfilled.

- **mutually interacting processes**
  This is the most general case. Binding of a ligand has an influence on the binding of the other ligand and vice versa. In this case, all parameters can have different values.

Koschorreck *et al.* [78] introduce another type of interaction in addition to the aforementioned interactions:

- **all-or-none interactions**
  All-or-none interactions are a special case of mutual interactions. A mutual interaction between two processes is called an all-or-none interaction, if the reaction cycle given by the four reactions of our example degenerates to a reaction chain (compare Figure 2.2). In real biochemical networks, such interactions are usually given by domain phosphorylation and subsequent ligand binding. Phosphorylation can generally be considered as a necessary precondition for ligand binding. On the other side ligand binding prevents dephosphorylation of the domain for steric reasons. To realize an all-or-none interaction in our example, one has to choose $k_2 = k_{-2} = k_3 = k_{-3} = 0$. In this case the species $R(0, E)$ will not occur and the remaining reactions r_1 and r_4 form a reaction chain.

Note, that these are theoretic considerations. The question of whether a certain type of interaction is feasible from a thermodynamic point of view will be discussed in Chapter 3.

2.3 Mathematical Background - Model Analysis and Reduction Techniques

The main focus of this thesis is on the development of new model reduction techniques for combinatorial reaction networks. In literature, one can already find plenty of different reduction techniques. Thus, it is essential to give an overview of existing methods, the possibilities offered by them as well as their limitations. Furthermore, these methods will serve as a basis for the development of new techniques that are adapted to the special requirements of combinatorial reaction networks. Note, however that the literature regarding approximation of dynamical systems is very extensive and as such, the consecutively given overview can only provide a rough picture. A more detailed discussion of available approximation techniques is given in the textbook from A. C. Antoulas [5].

Although the number of different reduction techniques is relatively high, all of these methods can be divided into two categories; namely methods based on time-scale separation and methods based on observability and controllability measures. Time-scale separation techniques are applicable if the model comprises processes that evolve at different time-scales. The fast dynamics of the system can be approximated by setting all slow variables to a constant value. On the other hand, the slow dynamics of the system can be described by taking the steady state assumption for all fast variables. Methods based on observability and controllability measures eliminate states whose influence on the considered input/output behavior is negligible. In many cases both approaches are combined. In this section, the underlying system-theoretic concepts and analysis tools will be introduced and defined. Afterwards we will review some of the available reduction methods.

2.3.1 Preliminaries

All considerations will be restricted to models consisting of ordinary differential equations given in state space representation. One basically distinguishes between linear

$$\begin{aligned} \dot{\vec{x}}(t) &= A\vec{x}(t) + B\vec{u}(t) \qquad \vec{x}(0) = \vec{x}_0 \\ \vec{y}(t) &= C\vec{x}(t) \end{aligned} \tag{2.10}$$

and nonlinear systems

$$\begin{aligned} \dot{\vec{x}}(t) &= \vec{f}\left(\vec{x}(t), \vec{u}(t)\right) \qquad \vec{x}(t_0) = \vec{x}_0 \\ \vec{y}(t) &= \vec{h}\left(\vec{x}(t)\right). \end{aligned} \tag{2.11}$$

In both cases, $\vec{x}(t)$ denotes the n-dimensional vector of all dynamic states or variables, while $\vec{u}(t)$ represents the m-dimensional vector of all external input signals. The vector $\vec{y}(t)$ comprises all ρ output variables of the system. The matrices A, B and C as well as the vector field $\vec{f}$ and the vector valued function $\vec{h}$ do have appropriate dimensions. Systems are termed *autonomous* for vanishing input signals ($\vec{u}(t) \equiv 0$).

2.3.1.1 State Space Transformations

The first step in model reduction of a large class of techniques is a state space transformation. The goal of these transformations is in general, the separation of fast state variables from slow ones or of observable from unobservable ones. Again one distinguishes between linear and nonlinear transformations

$$\vec{z} = T\vec{x} \qquad \text{and} \qquad \vec{z} = \vec{\phi}(\vec{x}). \tag{2.12}$$

In this thesis, it is assumed that each transformation is a diffeomorphism, which in the case of linear transformations requires that the matrix T is invertible, and in the case of nonlinear transformations that $\vec{\phi}(0) = 0$, $\vec{\phi}$ is invertible and both $\vec{\phi}$ and $\vec{\phi}^{-1}$ are differentiable. The transformed model equations can be deduced from Equation 2.12 by differentiation as shown below

$$\vec{z} = T\vec{x} \quad |\frac{d}{dt} \qquad \Rightarrow \qquad \dot{\vec{z}} = T\dot{\vec{x}} = T\vec{f}(\vec{x}, \vec{u}). \tag{2.13}$$

Finally, the old variables $\vec{x}$ have to be replaced by the new ones using the inverse transformation $\vec{x} = T^{-1}\vec{z}$ resulting in

$$\begin{aligned} \dot{\vec{z}}(t) &= T\vec{f}\left(T^{-1}\vec{z}(t), \vec{u}(t)\right) \qquad \vec{z}(t_0) = \vec{z}_0 = T\vec{x}_0 \\ \vec{y}(t) &= \vec{h}\left(T^{-1}\vec{z}(t)\right). \end{aligned} \tag{2.14}$$

In the case of nonlinear transformations, the transformed model equations can be deduced following the same procedure. However, note that the inversion of a nonlinear transformation can be extremely difficult.

2.3.1.2 Analysis Tools from Matrix Theory

Two fundamental analysis tools from matrix theory which play a crucial role in the field of model reduction, especially in the reduction of linear systems, are the *Eigenvalue Decomposition (EVD)* and the *Singular Value Decomposition (SVD)*. In the subsequent paragraphs we consider the mathematical background from matrix theory adapted from the textbook of A. C. Antoulas [5]. The application of the EVD as well as the SVD in terms of model reduction is discussed afterwards.

Eigenvalue Decompostion (EVD). Given a square matrix $A \in \mathbb{R}^{n\times n}$ the eigenvalue problem consists of finding the complex eigenvalues λ_i and the corresponding nonzero eigenvectors $\vec{v} \in \mathbb{R}^n$ satisfying the equation

$$A\vec{v} = \lambda\vec{v} \qquad \text{or} \qquad (A - \lambda I)\,\vec{v} = 0. \tag{2.15}$$

The defined problem has a solution if and only if $A - \lambda I$ has a nontrivial kernel. For finite dimensional matrices A, this leads to the nonlinear equation for the eigenvalues

$$\det(A - \lambda I) = 0, \tag{2.16}$$

which is called characteristic polynomial of A. For each root of the characteristic polynomial λ_i, one can calculate the corresponding eigenvectors by determining the kernel of $A - \lambda_i I$. Two square matrices A and B do have the same eigenvalues λ_i if there exists a similarity transformation given be the invertible matrix T, such that $B = T^{-1}AT$. If $\vec{v}_A$ are the eigenvectors of A and $\vec{v}_B$ the eigenvectors of B it holds $\vec{v}_B = T\vec{v}_A$. If the algebraic multiplicity of each eigenvalue is equal to its geometric multiplicity, there also exists another invertible matrix $\tilde{T}$ that yields $\Lambda = \mathrm{diag}(\lambda_i) = \tilde{T}^{-1}A\tilde{T}$. The algebraic multiplicity of an eigenvalue λ_i of the characteristic polynomial $p(\lambda) = (\lambda - \lambda_i)^k\, s(\lambda)$ is given by k. The geometric multiplicity is defined as the dimension of the nullspace $\ker(A - \lambda_i I)$. The transformation matrix $\tilde{T}$ that diagonalizes the matrix A is given by the n eigenvectors $\tilde{T} = [\vec{v}_1, ..., \vec{v}_n]$. If the matrix A is not diagonalizable it can be transformed to Jordan canonical form with nontrivial Jordan blocks. However, an EVD of A requires that A is diagonalizable and is given by the decomposition $A = \tilde{T}\Lambda\tilde{T}^{-1}$. More details about the EVD as well as the Jordan canonical form can be found in the textbook of A. C. Antoulas [5].

Singular Value Decomposition (SVD). Given a rectangular matrix $A \in \mathbb{R}^{n\times m}$, with $n \leq m$ and rank n, a matrix decomposition always exists, such that

$$A = U\Sigma V^T \tag{2.17}$$

where $U \in \mathbb{R}^{n\times n}$ with $UU^T = I$ and $V \in \mathbb{R}^{m\times m}$ with $VV^T = I$. The matrix Σ is a $n \times m$ matrix with $\Sigma_{ii} = \sigma_i$, $i = 1, ..., n$ and zero elsewhere. σ_i are non-negative numbers and furthermore it holds that $\sigma_1 \geq \sigma_2 \geq ... \geq \sigma_n \geq 0$. The matrix decomposition 2.17 is called *singular value*

decomposition of A, and σ_i are the *singular values*. The columns of the two matrices U and V are referred to as *left* and *right singular vectors*. The matrix A can also be depicted using these left and right singular vectors as

$$A = \sum_{i=1}^{n} \sigma_i \vec{u}_i \vec{v}_i^T. \tag{2.18}$$

If the singular values σ_i for $i > r$ are much smaller than σ_1 to σ_r the matrix A can be approximated by

$$A^* = \sum_{i=1}^{r} \sigma_i \vec{u}_i \vec{v}_i^T. \tag{2.19}$$

The 2-induced norm of the error matrix $E = A - A^*$, defined as

$$\|E\|_{\text{2-ind}} = \sup_{\vec{x} \neq 0} \frac{\|E\vec{x}\|_2}{\|\vec{x}\|_2}, \tag{2.20}$$

is given by σ_{r+1}. SVD and EVD are closely related since the singular values σ_i of A correspond to the positive square roots of the eigenvalues of AA^T. Analogously, the left singular vectors $\vec{u}_i$ correspond to the eigenvectors of AA^T while the right singular vectors $\vec{v}_i$ are the eigenvectors of A^TA.

2.3.1.3 Concepts from Systems Theory

In systems theory, models are usually classified in terms of stability, controllability and observability. These fundamental system characteristics also play crucial roles in model reduction. Stability, for example, is required in order to guarantee that the approximation error is finite. If a system is unobservable, it comprises internal dynamics that do not have any influence on the system output. Hence, the unobservable system states can simply be neglected. Below we will introduce and define these characteristics regarding linear systems. However, note that these fundamental properties find analogues in the theory of nonlinear systems.

Stability. The linear system 2.10 is called stable if, for vanishing inputs $\vec{u} \equiv 0$, all solution trajectories are bounded. The system is called asymptotically stable if the trajectories go to zero for $t \to \infty$. For linear systems asymptotic stability is given if and only if the real parts of all eigenvalues of the dynamic matrix A are negative. A system is stable if and only if all eigenvalues of A have nonpositive real parts, and furthermore all eigenvalues with vanishing real parts have multiplicity one. The stability of the nonlinear system 2.11 can be checked by calculating the eigenvalues of its Jacobian matrix J. However, note that if the Jacobian has eigenvalues with vanishing real parts this does not allow us to decide whether the system is stable or not. In this case, one has to use the Lyapunov criterion to analyze the stability of the system [5].

Observability. Let us consider the linear ODE system

$$\begin{bmatrix}\dot{\vec{x}}_1\\ \dot{\vec{x}}_2\end{bmatrix} = \begin{bmatrix}A_{1,1} & 0\\ A_{2,1} & A_{2,2}\end{bmatrix}\begin{bmatrix}\vec{x}_1\\ \vec{x}_2\end{bmatrix} + \begin{bmatrix}B_1\\ B_2\end{bmatrix}\vec{u} \qquad \begin{bmatrix}\vec{x}_1(0)\\ \vec{x}_2(0)\end{bmatrix} = \begin{bmatrix}\vec{x}_{1,0}\\ \vec{x}_{2,0}\end{bmatrix}$$
$$\vec{y} = C_1\vec{x}_1. \tag{2.21}$$

Obviously, the variables denoted as $\vec{x}_2$ do not have any influence on the output variables $\vec{y}$. Hence, any initial states whose values for $\vec{x}_{1,0}$ coincide result in identical outputs for arbitrary initial conditions $\vec{x}_{2,0}$. The differences in the states $\vec{x}_2$ cannot be observed considering these outputs. From this, the definition of observability follows.

Definition: A system is called *observable*, if and only if for each pair of distinct initial conditions $\vec{x}_{0,1}$ and $\vec{x}_{0,2}$ with $\vec{x}_{0,1} \neq \vec{x}_{0,2}$ the produced output of the autonomous system is distinguishable [65, 119].

Apparently, the question of whether a system is observable or not, as well as, how many and which state variables can be observed, is closely related to the choice of the output variables. The dimension d of the so-called observability space can be determined for linear systems by

$$d = \operatorname{rank}(Q) \qquad \text{with} \qquad Q = \begin{bmatrix} C\\ C\,A\\ \vdots\\ C\,A^{n-1}\end{bmatrix}. \tag{2.22}$$

The first d linearly independent rows of Q build a basis $(\vec{e}_i)$ for the observability space $\mathcal{O}$ [65]. For $d = n$ the system is called observable.

These considerations imply that an unobservable system can always be reduced without affecting the dynamics of the output variables. In Example 2.21, a reduced system would exclusively comprise the ODEs for the state variables $\vec{x}_1$. Such reductions are exact with respect to the output. Hence, methods that are based on the elimination of unobservable states are often referred to as *exact reduction techniques*.

Controllability. Now let us consider a differently structured linear system of the form

$$\begin{bmatrix}\dot{\vec{x}}_1\\ \dot{\vec{x}}_2\end{bmatrix} = \begin{bmatrix}A_{1,1} & A_{1,2}\\ 0 & A_{2,2}\end{bmatrix}\begin{bmatrix}\vec{x}_1\\ \vec{x}_2\end{bmatrix} + \begin{bmatrix}B_1\\ 0\end{bmatrix}\vec{u} \qquad \vec{x}(0) = \vec{x}_0$$
$$\vec{y} = C\vec{x}. \tag{2.23}$$

In this case the state variables $\vec{x}_2$ cannot be influenced by the inputs. Hence, the chosen input does not allow for the control of the system in any desired way, which explains why the system is said to be *uncontrollable*.

Definition: A system is called controllable, if it can be directed from an arbitrary initial state to any desired final state within a finite time frame by choosing a convenient input signal [65].

In analogy to the considerations regarding observability, there also exists a controllability space $\mathcal{C}$ whose dimension and basis can be deduced from the matrix

$$P = \begin{bmatrix} B & A\,B & \dots & A^{n-1}\,B \end{bmatrix}. \tag{2.24}$$

Uncontrollable systems can also be reduced without affecting the dynamics of the output, if an additional assumption is fulfilled. If the dynamics of the uncontrollable subsystem ($\vec{x}_2$ in Example 2.23) is already decayed, $\vec{x}_2$ can be replaced by its steady state value which, in the example previously discussed, corresponds to zero. Note, that controllability of nonlinear systems can be defined in numerous ways. In this thesis, a nonlinear system which is defined on a manifold $\mathbb{M}^n$ shall be called controllable if it can be directed from an arbitrary initial state $\vec{x}_0 \in \mathbb{M}^n$ to any final state $\vec{x}_e \in \mathbb{M}^n$ in a finite time frame.

2.3.2 Reduction Methods Based on Time-Scale Separations

A few time-scale based model reduction methods will be reviewed in this section. In this section, we distinguish between methods for linear and nonlinear ODE models. It is worth noting that all reduction techniques discussed for nonlinear systems are also applicable to linear ones.

2.3.2.1 Linear Systems

In the linear case, the system's time-scales can be characterized by its eigenvalues λ_i. If the real and the imaginary parts of all eigenvalues vary over some orders of magnitude, the system comprises processes that evolve at very different time-scales. As described above, the linear system can be diagonalized under certain conditions using a state space transformation $\vec{z} = T^{-1}\vec{x}$. The special property of the transformed system is the complete separation of the different time-scales

$$\begin{aligned} \dot{\vec{z}} &= \underbrace{T^{-1}A\,T}_{A^*}\,\vec{z} + \underbrace{T^{-1}B}_{B^*}\,\vec{u} \qquad A^* = \mathrm{diag}(\lambda_i) \\ \vec{y} &= \underbrace{C\,T}_{C^*}\,\vec{z}. \end{aligned} \tag{2.25}$$

The slow dynamics of the output variables can be approximated by taking the steady state assumption for all fast variables z_i. Let us assume that the states are divided into slow states $\vec{z}_1$ and fast states $\vec{z}_2$

$$\begin{aligned} \begin{bmatrix} \dot{\vec{z}}_1 \\ \dot{\vec{z}}_2 \end{bmatrix} &= \begin{bmatrix} \mathrm{diag}(\lambda_{1,i}) & 0 \\ 0 & \mathrm{diag}(\lambda_{2,i}) \end{bmatrix} \vec{z} + \begin{bmatrix} B_1^* \\ B_2^* \end{bmatrix} \vec{u} \\ \vec{y} &= \begin{bmatrix} C_1^* & C_2^* \end{bmatrix} \vec{z}. \end{aligned} \tag{2.26}$$

Taking the quasi steady state assumption for $\vec{z}_2$ results in a reduced model of the following form

$$\begin{aligned} \dot{\vec{z}}_1 &= \text{diag}(\lambda_{1,i})\vec{z}_1 + B_1^*\vec{u} \\ \vec{y} &= C_1^*\vec{z}_1 - C_2^*\text{diag}\left(\frac{1}{\lambda_{2,i}}\right)B_2^*\vec{u}. \end{aligned} \tag{2.27}$$

This approach is also known as singular perturbation method, which can be generalized for nonlinear systems, as shown below. The advantage of this model representation is not only the reduced number of ODEs, but also the fact that the ODEs are completely decoupled. One necessary requirement for the applicability of this method, besides the linearity of the model, is that all parameters are numerically determined.

2.3.2.2 Nonlinear Systems

As already mentioned, the singular perturbation approach is also applicable to nonlinear systems, but it requires some modifications. Another very important approach applicable to nonlinear systems is the rapid equilibrium assumption. Both approaches will be outlined in the following paragraphs.

Singular Perturbations. Singular perturbation theory has been extensively studied in mathematical literature [130, 131, 133, 61, 62]. The nonlinear model equations have to be converted to the form

$$\begin{aligned} \begin{bmatrix} \dot{\vec{z}}_1 \\ \epsilon\dot{\vec{z}}_2 \end{bmatrix} &= \begin{bmatrix} \vec{f}_1(\vec{z}_1, \vec{z}_2, \vec{u}, \epsilon) \\ \vec{f}_2(\vec{z}_1, \vec{z}_2, \vec{u}, \epsilon) \end{bmatrix} \qquad \begin{matrix} \vec{z}_1 \in \mathbb{R}^{n-d} \\ \vec{z}_2 \in \mathbb{R}^d \end{matrix} \\ \vec{y} &= \vec{h}(\vec{z}_1, \vec{z}_2). \end{aligned} \tag{2.28}$$

The scalar ϵ represents all parameters that are small enough to be neglected. The model can be reduced by a singular parameter perturbation setting $\epsilon = 0$. This corresponds to the assumption that the states $\vec{z}_2$ are very fast compared to $\vec{z}_1$ and hence are assumed to be in quasi steady state. The resulting model consists of $n-d$ ODEs and d algebraic equations. By solving these algebraic equations for $\vec{z}_2$ and subsequent insertion in the remaining ODEs, one obtains the reduced model. However, note that one has to face different problems when following this procedure. The d nonlinear coupled algebraic equations may not be resolvable analytically, or numerous different real roots may exist. Another aspect one has to keep in mind is that complex dynamic behaviors of the unreduced system, such as limit cycles or chaotic behavior, might get lost using this approach. The conditions under which the singular perturbation method can be applied were formulated by Tikhonov [130, 131].

Rapid Equilibrium Assumption. In contrast to the approach described above, the rapid equilibrium assumption does not focus on the question of which states quickly reach their

steady state but rather which processes are fast in comparison to others. In terms of reaction networks this corresponds to the question of which reactions quickly converge to equilibrium. In this context the term equilibrium corresponds to the thermodynamic equilibrium which, in the case of reactions, is characterized by vanishing reaction rates. Consider a reaction $A \leftrightharpoons B$ with the reaction rate $r = k_{\text{on}}[A] - k_{\text{off}}[B]$, thermodynamic equilibrium is characterized by

$$k_{\text{on}}[A] - k_{\text{off}}[B] = 0 \quad \Rightarrow \quad K_{eq} = \frac{k_{\text{on}}}{k_{\text{off}}} = \frac{[B]}{[A]}. \tag{2.29}$$

The parameter K_{eq} is the equilibrium constant. A more detailed introduction to thermodynamics of reactions and reaction networks is given in Chapter 3.

In order to describe the reduction method based on the rapid equilibrium assumption we choose a model representation using the stoichiometric matrix N and the vector of reaction rates $\vec{r}$

$$\begin{aligned} &\dot{\vec{x}} = N\vec{r} \qquad \vec{x} = \begin{bmatrix} \vec{x}_1 \\ \vec{x}_2 \end{bmatrix}, \quad \vec{r} = \begin{bmatrix} \vec{r}_1 \\ \vec{r}_2 \end{bmatrix} = \begin{bmatrix} \vec{g}_1(\vec{x}_1, \vec{x}_2) \\ \vec{g}_2(\vec{x}_1, \vec{x}_2) \end{bmatrix} \\ &\vec{y} = \vec{h}(\vec{x}). \end{aligned} \tag{2.30}$$

Now, we assume that all reactions described by $\vec{r}_2$ are fast in comparison to the other reactions. The mathematical formulation of this assumption yields $\vec{g}_2(\vec{x}) = 0$. Observe, that this assumption is not equivalent to $\vec{r}_2 = 0$. The reaction rates only vanish if the whole reaction network is in thermodynamic equilibrium. In fact we presume that $\vec{r}_2$ is chosen such that all species involved in the corresponding reactions are equilibrated in zero time. These so defined reaction rates $\tilde{\vec{r}}_2$ are not explicitly given through our assumption, but they are required to evaluate the ODEs as defined above. In order to determine these rates we take the time derivative of the algebraic equations

$$\underbrace{\left(\frac{\partial \vec{g}_2}{\partial \vec{x}}\right)}_{=J} \dot{\vec{x}} = 0 \qquad \Leftrightarrow \qquad J \begin{bmatrix} N_1 & N_2 \end{bmatrix} \begin{bmatrix} \vec{r}_1 \\ \tilde{\vec{r}}_2 \end{bmatrix} = 0, \tag{2.31}$$

where J is the Jacobian matrix. Equation 2.31 is linear in the unknown reaction rates $\tilde{\vec{r}}_2$, and the solution is given by

$$\tilde{\vec{r}}_2 = -\left(JN_2\right)^{-1} JN_1\vec{r}_1 = \tilde{\vec{g}}_2(\vec{x}, \vec{r}_1). \tag{2.32}$$

Insertion of this result into the model equations still does not yield a reduced number of ODEs. One additionally has to include the algebraic equations $\vec{g}_2(\vec{x}_1, \vec{x}_2) = 0$, which can be solved for $\vec{x}_2$. The reduced model, hence, only comprises the $n - d$ states $\vec{x}_1$.

2.3.3 Reduction Methods Based on Observability Measures

We have already mentioned above that observability, as well as controllability, are important properties of dynamic systems and can be used as indicators for possible model reductions.

If a system comprises unobservable states, they can be eliminated without affecting the input/output behavior. This reduction principle can be extended by eliminating states that are difficult to observe, i.e., those that yield small amounts of observation energy. More detailed information about the aforementioned, as well as further reduction methods can be found in [5].

2.3.3.1 Linear Systems

States of linear systems that are difficult to observe or control can be directly determined from the observability and controllability gramians $\mathcal{Q}$ and $\mathcal{P}$. They are given by the eigenvectors of these gramians corresponding to small eigenvalues. The observability and controllability gramians are defined as

$$\mathcal{Q} = \int_0^\infty e^{A^T t} C^T C e^{At} dt \tag{2.33}$$

$$\mathcal{P} = \int_0^\infty e^{At} B B^T e^{A^T t} dt \tag{2.34}$$

and therefore satisfy the following Lyapunov equations

$$A^T \mathcal{Q} + \mathcal{Q} A + C^T C = 0 \tag{2.35}$$

$$A\mathcal{P} + \mathcal{P} A^T + B B^T = 0. \tag{2.36}$$

In order to eliminate states that are difficult to observe and at the same time difficult to control, the system is transformed to a so-called balanced representation. A system is said to be balanced if

$$\mathcal{Q} = \mathcal{P} = \Sigma = \mathrm{diag}(\sigma_i), \tag{2.37}$$

with $\sigma_i \geq \sigma_{i+1}$ for all $i = 1, 2, ..., n-1$. In the balanced system

$$\begin{bmatrix} \dot{\vec{z}}_1 \\ \dot{\vec{z}}_2 \end{bmatrix} = \begin{bmatrix} A^*_{1,1} & A^*_{1,2} \\ A^*_{2,1} & A^*_{2,2} \end{bmatrix} \vec{z} + \begin{bmatrix} B^*_1 \\ B^*_2 \end{bmatrix} \vec{u} \qquad \Sigma = \begin{bmatrix} \Sigma_1 & 0 \\ 0 & \Sigma_2 \end{bmatrix}$$
$$\vec{y} = \begin{bmatrix} C^*_1 & C^*_2 \end{bmatrix} \vec{z} \tag{2.38}$$

the concurrent controllability and observability measure σ_i can be directly assigned to the state z_i. Hence, all d states corresponding to the d smallest values σ_i can be eliminated without strongly affecting the input/output behavior of the system if $\sigma_{n-d} \gg \sigma_{n-d+1}$. Since the states $\vec{z}_2$ only rarely influence the input/output behavior of the system, they can simply be set to zero as one possible approximation. Another possibility is taking the steady state assumption for $\vec{z}_2$, which guarantees a vanishing steady state error.

2.3.3.2 Nonlinear Systems

In the case of nonlinear systems, balanced truncation is practically unfeasible. An alternative approach is given by the proper orthogonal decomposition (POD) method. For a fixed input

$\vec{u}$, the trajectory of the systems can be determined by simulation and evaluated at certain instances of time t_k. These snapshots of the state trajectory can be accommodated in a matrix

$$\mathcal{X} = \left[\vec{x}(t_1) \quad \vec{x}(t_2) \quad \dots \quad \vec{x}(t_N)\right] \in \mathbb{R}^{n \times N}, \tag{2.39}$$

with $N \gg n$. In a second step, the singular value decomposition of $\mathcal{X}$ is computed. If the singular values fall off rapidly, $\mathcal{X}$ can be approximated by

$$\mathcal{X} = U\Sigma V^T \approx U_k \Sigma_k V_k^T, \quad k < n. \tag{2.40}$$

The matrix U_k can be used as transformation matrix $\vec{z} = U_k^T \vec{x}$ with $\vec{z} \in \mathbb{R}^k$, which implies the reduced order state equation

$$\begin{aligned} \dot{\vec{z}} &= U_k^T \vec{f}(U_k \vec{z}, \vec{u}) \\ \vec{y} &= \vec{h}(\vec{z}). \end{aligned} \tag{2.41}$$

However, it should be noted that small approximation errors of this reduced model can only be guaranteed if the system is stimulated by the input $\vec{u}$ chosen to create the matrix $\mathcal{X}$.

2.3.4 Conclusions

The application of common model reduction techniques to combinatorial models of signal transduction networks is problematic for various reasons. The first problem is that these models are nonlinear, whereas many model reduction techniques are restricted to linear systems. Methods available for nonlinear systems have strong limitations. For instance they pose the problem of resolving a large set of nonlinear algebraic equations in the case of the quasi steady state assumption. The problem of POD is that the reduced model only provides very good approximation accuracy for fixed input signals. Furthermore, many of the available techniques necessitate a state space transformation resulting in a model representation in which the state variables generally do not correspond to biological characteristics. Another problem is that the majority of methods require the numerical determination of all parameter values, which in systems biology are mostly unknown. In fact, one central aspect of model reduction in systems biology is to provide simpler model structures, more suitable for common parameter identification methods.

The methods discussed in this thesis can overcome these problems for a large class of biological signal transduction models. The methods are applicable to nonlinear systems, the required transformations preserve biological interpretability of the state variables, and one only requires qualitative information about the parameters values. However, these advantages can only be achieved at the expense of generality. Thus, the methods are only designed for the reduction of combinatorial complexity of reaction networks including receptors or scaffold proteins that provide a large number of binding domains. Additionally, there are some further restrictions on the reaction kinetics that might be used, which will be discussed later in detail. However, it has already been stated that the methods always work for mass action kinetics.

Chapter 3

Thermodynamics of Signal Transduction

An important aspect in kinetic modeling of complex biochemical reaction networks is the analysis of thermodynamic constraints following from the well known principle of microscopic reversibility or detailed balance. In 1902 Wegscheider discussed restrictions for reaction networks and showed that the kinetic parameters of reactions forming a reaction cycle have to fulfill certain constraints [138]. In 1931 Onsager showed that microscopic reversibility restricts the parameter values for all thermodynamic systems near equilibrium [101, 102]. The fundamentals of this theory are nicely reviewed by Heinrich and Schuster [55]. More recent discussions focus on the restrictions for stationary far-from-equilibrium flux distributions [113, 112, 144, 111, 10, 9, 11, 60]. Another subject of recent research in this field is the question of how to create thermodynamically feasible models of complex reaction networks. The proposed methods vary from systematic identification of stoichiometric cycles [28], to finding alternative parameterizations of the model [145, 34].

In this chapter we discuss the implications of detailed balance constraints on signal transduction networks. We show that thermodynamics highly restricts possible process interactions between domains of receptors and scaffold proteins. Stoichiometric information is sufficient to derive some interesting statements about these interactions. Thus, it is possible to decide whether an interaction, for example between two bindings, might be unidirectional, or whether the two processes have to interact mutually. It turns out that unidirectionality, which is an important feature for reduction and modularization, may only occur in special scenarios. The comparison of simulations and experimental data suggests that the cell actually realizes such unidirectional interactions. Our analyses also give a new interpretation of the kinetic degrees of freedom in reaction networks including receptors and scaffold proteins and provide a new intuitive method to impose detailed balance on these networks.

3.1 Basic Principles of Thermodynamics

Thermodynamics can be divided into the branches of classical and irreversible thermodynamics [19]. Classical thermodynamics only considers equilibrium states of thermodynamic systems, while irreversible thermodynamics deals with the processes that try to balance existing disequilibria. Thermodynamic equilibria can be characterized by a small number of macroscopic state variables such as temperature, pressure and chemical potentials [19]. Another basic feature of thermodynamic equilibrium is the absence of all driving forces such as temperature gradients or free energies of reactions. These driving forces are the cause of irreversible balance processes. Hence, a system can only reach thermodynamic equilibrium if no external forces are impressed on the system, for example, if the considered system is completely isolated. The second law of thermodynamics implies that, if no external forces exist, all systems finally have to end up in thermodynamic equilibrium. The principle of microscopic reversibility or detailed balance [101, 102] additionally postulates that for vanishing driving forces the conjugated balance flows also vanish. This can be exemplified considering a simple mono-molecular reaction $A \leftrightharpoons B$. In thermodynamic equilibrium, transitions $A \to B$ as well as reverse transitions $B \to A$ still occur at a microscopic scale. However, detailed balance postulates that the frequency of both transitions is equal, and hence the overall flow is zero. From this one can deduce constraints for kinetic parameters of reaction networks including reaction cycles, which can be further explained by considering a scaffold protein with two binding domains such as that in Example 2.5 from the last chapter. The corresponding reaction network

$$\begin{aligned} r_1 &= k_1[R(0,0)] \cdot [L] - k_{-1}[R(L,0)] \\ r_2 &= k_2[R(0,E)] \cdot [L] - k_{-2}[R(L,E)] \\ r_3 &= k_3[R(0,0)] \cdot [E] - k_{-3}[R(0,E)] \\ r_4 &= k_4[R(L,0)] \cdot [E] - k_{-4}[R(L,E)]. \end{aligned} \tag{3.1}$$

obviously forms a cycle (see Figure 3.1). If the system is isolated from its environment it has to end up in thermodynamic equilibrium and all reaction rates have to vanish ($r_i = 0$). This leads to the condition that the product of the equilibrium constants along the reaction cycle has to be

$$\frac{[R(0,0)]\,[L]}{[R(L,0)]} \frac{[R(L,E)]}{[R(0,E)]\,[L]} \frac{[R(0,E)]}{[R(0,0)]\,[E]} \frac{[R(L,0)]\,[E]}{[R(L,E)]} = \frac{k_{-1}}{k_1} \frac{k_2}{k_{-2}} \frac{k_3}{k_{-3}} \frac{k_{-4}}{k_4} = \frac{K_{eq,1}K_{eq,4}}{K_{eq,2}K_{eq,3}} = 1. \tag{3.2}$$

This relation is also known as Wegscheider condition [138]. Similar conditions exist for all independent reaction cycles within a reaction network. Due to combinatorial complexity, the number of these constraints on the kinetic parameters is very high for signal transduction networks. This can be further explained by considering a scaffold protein with ten distinct binding domains. A complete deterministic model of the system, which could be automatically generated using BioNetGen [13], would comprise 1,034 ODEs and 5,120 reactions. However, it also comprises 4,097 reaction cycles, which highly restricts the choice of parameters (example taken from Ederer *et al.* [34]). If one does not account for these 4,097 restrictions, the chance

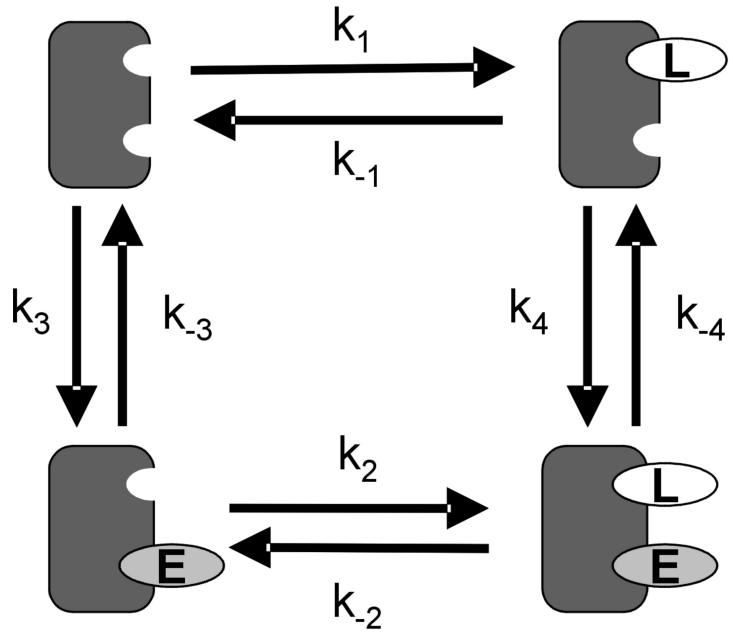

Figure 3.1: A scaffold with two binding domains can exist in four different states. The feasible reactions in such a system form a reaction cycle.

of creating a model that contradicts the laws of thermodynamics will be very high.
Before the effects of these parameter restrictions are discussed in detail, one very essential question remains that shall be addressed here. A quite common objection against the usage of Wegscheider conditions in modeling biological systems is that these parameter restrictions are deduced from laws characterizing thermodynamic equilibrium, whereas living cells usually operate far from thermodynamic equilibrium. This rationale seems to be reasonable. However, it does not bear a more detailed analysis. If we take the assumption that the kinetic parameters do not change during the evolution of a reaction, the parameter restrictions that are valid for thermodynamic equilibrium also have to hold for non-equilibrium states. The reason why living cells do not reach thermodynamic equilibrium is not that the kinetic parameters of the underlying reaction networks do not fulfill the Wegscheider condition, but that these reaction networks are constantly stimulated by external forces (e.g. energy from nutrition). As soon as a cell is isolated from its environment it will die and finally reach thermodynamic equilibrium. A virtual cell that is modeled without taking the Wegscheider conditions into account will not provide the same behavior. Only the kinetic parameters of reactions forming a futile cycle do not have to fulfill Wegscheider conditions. A futile cycle is defined as a set of opposing, non-equilibrium reactions catalyzed by different enzymes which act simultaneously. At least one of the reactions in a futile cycle has to be driven by consumption of an energy rich compound such as ATP. However, the existence of futile cycles within a reaction network does not imply

that none of the Wegscheider conditions have to be considered. The Wegscheider conditions for all true stoichiometric cycles within the network still have to hold in that case.

3.2 Chemical Potentials, Equilibrium Constants and the Wegscheider Condition

In this section, we give a brief introduction to the elementary relations between chemical potentials, equilibrium constants of reactions and Wegscheider conditions, which build the basis for further considerations. The chemical potential of a chemical reactant i is defined as the partial derivative of the Gibbs free energy

$$\mu_i = \left(\frac{\partial G}{\partial n_i}\right)_{T,p,n_{j\neq i}}. \tag{3.3}$$

Using the ideal gas law one can deduce the following formula for the chemical potential

$$\mu_i = \mu_{i,0}(T,p) + RT \ln x_i \tag{3.4}$$

of ideal mixtures. Therein, $\mu_{i,0}$ is the standard potential of the chemically pure substance which is only a function of temperature T and pressure p, R is the ideal gas constant and x_i is the mole fraction of component i. Note that kinetic modeling usually is based on the assumption that the mixture in which the reaction takes place behaves ideally. Taking the assumption that we consider strongly diluted aqueous solutions in which the total molarity c_{tot} remains nearly constant, which is generally assumed for cells, the chemical potential can also be written as

$$\mu_i = \mu^*_{i,0} + RT \ln c_i, \tag{3.5}$$

wherein $\mu^*_{i,0} = \mu_{i,0}(T,p) - RT \ln c_{tot}$, and c_i is the dimensionless molarity of substance i. Observe, that $\mu^*_{i,0}$ does not describe the chemical potential of the pure substance i but the chemical potential of an one molar aqueous solution. We will only consider the chemical potential of one molar aqueous solutions, and therefore remove the asterisk in order to simplify the notation.

From the second law of thermodynamics it follows that any reaction

$$\sum_{\text{reactants}} |\nu_i| E_i \leftrightharpoons \sum_{\text{products}} |\nu_i| P_i \tag{3.6}$$

is in thermodynamic equilibrium if the free energy of reaction is

$$\Delta g_R = \sum_i \nu_i \mu_i = 0. \tag{3.7}$$

Herein, ν_i are the stoichiometric coefficients, which are defined to be negative for reactants and positive for products. The free energy of a reaction can be interpreted as a chemical force which drives the corresponding reaction flow. From the stated equilibrium condition,

$$\prod_i c_i^{\nu_i} = \exp\left(-\frac{\sum \nu_i \mu_{i,0}}{RT}\right) := K_{eq} \tag{3.8}$$

follows directly, which is defined as the equilibrium constant of the considered reaction. This relation is also an explanation for the possible restrictions on the choice of equilibrium constants in a reaction network. An equilibrium constant can be determined from a sum of $\mu_{i,0}$. If one considers a reaction network comprising i_0 substances, it is obvious that at most i_0 linearly independent sums of chemical standard potentials might exist.

Considering a complete reaction network with a high number of reactions, the condition for thermodynamic equilibrium (Equation 3.7) can be written as

$$N^T \vec{\mu} = 0 \qquad \Leftrightarrow \qquad N^T \left(\vec{\mu}_0 + RT \ln \vec{c}\right) = N^T \vec{\mu}_0 + RT \ln \vec{K}_{eq} = 0, \tag{3.9}$$

in which N^T is the transposed stoichiometric matrix of the reaction network and $\vec{K}_{eq}$ the vector of all equilibrium constants. In the next step this equation is multiplied by a kernel matrix B, which has the property such that $B \cdot N^T = 0$. From this, it follows that

$$B \ln \vec{K}_{eq} = 0 \tag{3.10}$$

must hold for any reaction system. This is the so-called generalized Wegscheider condition, which should be accounted for in modeling reaction networks [55].

From these considerations one can see that each representation of a reaction network using chemical potentials can be directly translated into equilibrium constants $\vec{K}_{eq}$. Observe that equilibrium constants that are determined in that way will automatically fulfill the Wegscheider conditions. On the other hand, it is also clear that a parameterization of a reaction network that does not fulfill the Wegscheider conditions cannot have any equivalent representation in terms of chemical potentials. By determining the chemical potentials one directly obtains equilibrium constants fulfilling the Wegscheider conditions. This is a big advantage and will help us to find a descriptive way to parameterize and analyze signal transduction networks comprising scaffold proteins and receptors.

3.3 The Chemical Potential of Scaffold Proteins

As we have seen, one can assign a chemical potential to each substance within a cell. However, much more important than the absolute values of the chemical potentials are the sums and differences of chemical potentials that are defined by the equilibrium conditions. Hence, we will introduce a parameterization of the chemical potentials that will allow us to characterize the important sums and differences in a simple and structured way.

3.3.1 Example

The idea can be further explained by considering the example introduced above (Equation 3.1, Figure 3.1). The complete reaction system comprises six chemical substances L, E, $R(0,0)$, $R(L,0)$, $R(0,E)$ and $R(L,E)$. Interestingly, the three species $R(L,0)$, $R(0,E)$ and $R(L,E)$

are composed by the other three components. Hence, we first define three different chemical potentials for the three basic components or monomers L, E and $R(0,0)$, namely $\mu_{L,0}$, $\mu_{E,0}$ and $\mu_{R00,0}$. Observe, that here we consider the chemical potential of one molar aqueous solutions, since these are required to formulate the equilibrium constants. For the sake of simplicity, we will omit the index 0 in the following discussion. If we now assume that the binding of the two proteins L and $R(0,0)$ has no effect on the chemical potential, the chemical potential of $R(L,0)$ is the sum of μ_L and μ_{R00}. Under this assumption ($\mu_{RL0} = \mu_{R00} + \mu_L$), it follows for the equilibrium constant

$$K_{eq} = \exp\left(-\frac{-\mu_L - \mu_{R00} + \mu_{RL0}}{RT}\right) = 1. \tag{3.11}$$

It is clear that this assumption is not suitable in most cases. However, we use this assumption as a basis for some further considerations and introduce an additional term $\Delta\mu_L$ describing the deviation of the real chemical potential from the ideal assumption. The chemical potentials of the complexes $R(L,0)$ and $R(0,E)$ are given by

$$\begin{aligned} \mu_{RL0} &= \mu_{R00} + \mu_L + \Delta\mu_L \\ \mu_{R0E} &= \mu_{R00} + \mu_E + \Delta\mu_E. \end{aligned} \tag{3.12}$$

One can see that the equilibrium constants of the reactions r_1 and r_3 are defined as

$$K_{eq,1} = \exp\left(-\frac{\Delta\mu_L}{RT}\right) \qquad K_{eq,3} = \exp\left(-\frac{\Delta\mu_E}{RT}\right). \tag{3.13}$$

The two terms $\Delta\mu_L$ and $\Delta\mu_E$ correspond to the Gibbs free binding energies of the two considered reactions. Analogously, we can define the chemical potential of the substance μ_{RLE}, as

$$\mu_{RLE} = \mu_{R00} + \mu_L + \mu_E + \Delta\mu. \tag{3.14}$$

In contrast to the previous definitions $\Delta\mu$ does not describe one single binding effect. Hence, the term $\Delta\mu$ can be divided into the already known binding effects $\Delta\mu_L$ and $\Delta\mu_E$. If one assumes that $\Delta\mu = \Delta\mu_L + \Delta\mu_E$, the resulting equilibrium constants of the reactions r_2 and r_4 will be the same as these for reactions r_1 and r_3

$$K_{eq,2} = K_{eq,1} = \exp\left(-\frac{\Delta\mu_L}{RT}\right) \quad K_{eq,4} = K_{eq,3} = \exp\left(-\frac{\Delta\mu_E}{RT}\right). \tag{3.15}$$

However, $\Delta\mu$ cannot, in general, be characterized simply as the sum of these two effects. Generally, one has to assume that the simultaneous binding of L and E has an additional effect on the chemical potential of $R(L,E)$. For this reason, the chemical potential of this complex can be written as

$$\mu_{RLE} = \mu_{R00} + \mu_L + \mu_E + \underbrace{\Delta\mu_L + \Delta\mu_E + \Delta\mu_{LE}}_{=\Delta\mu}. \tag{3.16}$$

With this definition one can calculate the equilibrium constants of the reactions r_2 and r_4 as

$$\begin{aligned} K_{eq,2} &= \exp\left(-\frac{\Delta\mu_L + \Delta\mu_{LE}}{RT}\right) = \exp\left(-\frac{\Delta\mu_L}{RT}\right)\exp\left(-\frac{\Delta\mu_{LE}}{RT}\right) = K_{eq,1}\, a_{LE} \\ K_{eq,4} &= \exp\left(-\frac{\Delta\mu_E + \Delta\mu_{LE}}{RT}\right) = \exp\left(-\frac{\Delta\mu_E}{RT}\right)\exp\left(-\frac{\Delta\mu_{LE}}{RT}\right) = K_{eq,3}\, a_{LE}. \end{aligned} \tag{3.17}$$

Interestingly, both equilibrium constants can be written as products of the already defined constants for the reactions r_1 and r_3 and a common factor a_{LE}. The three parameters $K_{eq,1}$, $K_{eq,3}$ and a_{LE}, which directly correspond to the quantities $\Delta\mu_L$, $\Delta\mu_E$ and $\Delta\mu_{LE}$, represent the three degrees of freedom one has in order to choose the equilibrium constants of the considered system. The values of μ_{R00}, μ_L and μ_E do not play any role in the calculation of the equilibrium constants. Hence, the chosen parameterization separates important and unimportant fractions of the chemical potential and additionally allows the simple translation into equilibrium constants.

3.3.2 Generalized Consideration

In analogy to the already discussed example, we will define a generalized pattern to describe the chemical potentials of all feasible multiprotein species which can occur in systems including scaffold proteins and receptors. We will show that the equilibrium constants in these reaction systems can always be characterized in a similar way, as demonstrated above. The equilibrium constants of all reactions describing the binding of one effector to a certain domain can always be formulated using a standard equilibrium constant and additional multiplicative factors. The multiplicative factors describe the thermodynamically feasible effects of domain or process interactions.

In order to generalize our considerations, we first introduce some definitions. We will consider a scaffold protein R which provides n distinct binding domains for n distinct effectors E^i. In order to simplify our considerations we assume that at each domain only one specific protein can bind. Note that this assumption does not restrict the generality of the results. A certain multiprotein complex can be written as $R(i_1, ..., i_n)$, where i_k is zero if the k-th domain is not occupied and one if it is occupied. Below, we will discuss how the corresponding chemical potentials $\mu(i_1, ..., i_n)$ for all these multiprotein species can be characterized. For this characterization we define different terms $\Delta\mu(i_1, ..., i_n)$ which describe the effects of certain binding constellations on the chemical potential.

Using the so defined quantities the chemical potential of each feasible multiprotein complex can be written as

$$\begin{aligned}\mu(i_1, ..., i_n) =& \mu(0, ..., 0) + i_1\mu_{E^1} + ... + i_n\mu_{E^n} \\ &+ i_1\Delta\mu(1, 0, ..., 0) + ... + i_n\Delta\mu(0, ..., 0, 1) \\ &+ i_1\, i_2\Delta\mu(1, 1, 0, ..., 0) + ... + i_{n-1}\, i_n\Delta\mu(0, ...0, 1, 1) \\ &+ i_1\, i_2\, i_3\Delta\mu(1, 1, 1, 0, ..., 0) + ... + i_{n-2}\, i_{n-1}\, i_n\Delta\mu(0, ..., 0, 1, 1, 1) \\ &... \\ &+ i_1...i_n\Delta\mu(1, ..., 1).\end{aligned} \tag{3.18}$$

Observe, that this reparameterization of the chemical potentials is unique and bijective, i.e. each chemical potential has a unique representation in the new formalism. Analogously, all new

$\Delta\mu$ terms can also be uniquely determined if the chemical potentials of all species are known. Mathematically, this can be considered as a linear transformation from one set of variables to another. This transformation is structurally equivalent to that introduced in Chapter 4. A proof that this transformation is unique and invertible is also given there.

The formula will be further explained by considering a scaffold protein with three binding domains. In this case the chemical potentials of the two complexes $R(1,0,1)$ and $R(1,1,1)$ are given by

$$\begin{aligned}\mu(1,0,1) =&\mu(0,0,0) + \mu_{E^1} + \mu_{E^3} + \Delta\mu(1,0,0) + \Delta\mu(0,0,1) + \Delta\mu(1,0,1)\\ \mu(1,1,1) =&\mu(0,0,0) + \mu_{E^1} + \mu_{E^2} + \mu_{E^3} + \Delta\mu(1,0,0) + \Delta\mu(0,1,0) + \Delta\mu(0,0,1)\\ &+ \Delta\mu(1,1,0) + \Delta\mu(1,0,1) + \Delta\mu(0,1,1) + \Delta\mu(1,1,1).\end{aligned} \tag{3.19}$$

This notation may appear cumbersome to the reader. However, it proves to be very helpful in the characterization of the dependencies of equilibrium constants in a very simple way. This becomes apparent when considering the Gibbs free reaction energy of different binding reactions. We will consider binding of an effector E^1, to the scaffold protein in different scenarios, and calculate the corresponding equilibrium constants of these reactions. The resulting equilibrium constants will automatically fulfill the Wegscheider conditions. Firstly, we assume that E^1 binds to a scaffold protein with all domains being unoccupied. The Gibbs free reaction energy for this reaction is $\Delta g_R = \Delta\mu(1,0,...,0)$. With this we can formulate

$$RT \ln K_{eq} = -\Delta\mu(1,0,...,0) \qquad K_{eq} = \exp\left(-\frac{\Delta\mu(1,0,...,0)}{RT}\right) = K_{eq,0}. \tag{3.20}$$

If we consider the same binding process with a scaffold protein that has one occupied domain, for example the second one, it follows that

$$RT \ln K_{eq} = -\left(\Delta\mu(1,0,...,0) + \Delta\mu(1,1,0...,0)\right) \qquad K_{eq} = K_{eq,0}\, a_{110...0}. \tag{3.21}$$

Hence, the original equilibrium constant is altered by the additional factor $a_{110...0}$. Importantly, the same factor also occurs if one considers the binding of E^2 to a scaffold with an occupied first binding domain. This means that each pair of binding domains can be characterized by two equilibrium constants and an additional common modification factor. The two equilibrium constants describe the binding of an effector to the related domain of the scaffold, if the latter is completely unoccupied. The modification factor illustrates how much the equilibrium constants of both domains change if the effector binds to a scaffold at which the other domain is already occupied.

Using these findings we can already partly characterize the scenario where a third effector is considered. Firstly, it is clear that for each domain one can define a basic equilibrium constant, describing effector binding to the domain of the completely unoccupied scaffold. Furthermore, in the consideration of three binding domains, there exist three distinct pairs of domains, and for each pair one can determine a modification factor. If the scaffold has already bound

two effectors E^2 and E^3, and the third effector E^1 binds, the equilibrium constant can be characterized by

$$-RT \ln K_{eq} = \Delta\mu(1,0,...,0) + \Delta\mu(1,1,0...,0) + \Delta\mu(1,0,1,0,...,0) + \Delta\mu(1,1,1,0,...,0) \quad (3.22)$$

with $K_{eq} = K_{eq,0}\, a_{110...0}\, a_{1010...0}\, a_{1110...0}$. Now, one has three different modification factors. Two of them describe the already discussed effects between pairs of domains, the third one describes additional effects which only occur if two domains are already occupied and the third domain becomes occupied. Observe that for all cases in which two of the effectors E^1, E^2 and E^3 have already bound to the scaffold and the third one binds, this new modification factor is exactly the same. The same consideration can be made for all triples of scaffold domains. One can already see a pattern in the structure of the derived equilibrium constants. The available degrees of freedom for the equilibrium constants are given by a basic equilibrium constant for each single domain, first tier modification factors for all distinct pairs of domains and second tier modification factors for all distinct triples of domains. Further analyses reveal that more tiers of modification factors for all higher tuples of domains also exist. Each modification factor characterizes the interaction of the corresponding pair, triple or higher tuple. If a factor, for example $a_{1110...0}$, equals one, this means that the effects on the tier below (here of pairs) superpose undisturbed.

Hence, one can create a thermodynamically feasible model of a scaffold protein or receptor without explicitly considering the Wegscheider conditions. It is only necessary to guarantee that the equilibrium constants fit into the described pattern. This extremely simplifies the generation of thermodynamically feasible models for reaction networks that include scaffolds or receptors.

3.4 Restrictions on Process Interactions

In the previous section, it is shown how thermodynamic constraints restrict the choice of parameters in modeling signal transduction networks or other biological systems, including scaffold proteins or receptors. The provided formalism allows one to account for all these constraints in a very simple way. Now we discuss the implications of these constraints on signal transduction. Initially, we again consider the simple example of a receptor R with two binding domains. In the background section we already discussed theoretically feasible interactions between the two domains, and we defined conditions for the kinetic parameters that have to be fulfilled in order to realize a certain type of interaction. Additionally, it has been shown that from a thermodynamic point of view, the equilibrium constants have to fulfill the following conditions

$$K_{eq,2} = K_{eq,1}\, a_{LE} \qquad K_{eq,4} = K_{eq,3}\, a_{LE}. \quad (3.23)$$

Under this restriction not all theoretically feasible interactions can occur, as shown below:

- **non-interacting binding processes**
  The relations between the kinetic parameters that are required to realize non-interacting binding domains ($k_2 = k_1$, $k_{-2} = k_{-1}$, $k_4 = k_3$ and $k_{-4} = k_{-3}$) do not contradict the Wegscheider condition. These relations only imply that $a_{LE} = 1$ ($\Delta\mu_{LE} = 0$), which is thermodynamically feasible and reflects the missing interaction between the two binding processes.

- **unidirectionally interacting binding domains**
  An unidirectional interaction can be realized if $k_2 = k_1$, $k_{-2} = k_{-1}$, which corresponds to $K_{eq,2} = K_{eq,1}$, and additionally $k_4 \neq k_3$, $k_{-4} \neq k_{-3}$, which in general implies $K_{eq,4} \neq K_{eq,3}$. Obviously, these requirements contradict the Wegscheider condition, since from $K_{eq,2} = K_{eq,1}$ it follows $a_{LE} = 1$, while $K_{eq,4} \neq K_{eq,3}$ would require $a_{LE} \neq 1$. Thus, thermodynamics does not allow unidirectional interactions between binding processes at the level of equilibrium constants, which is a very significant restriction. However, thermodynamics only makes statements about the equilibrium constants not about the reaction velocities. One special case of unidirectional interaction is allowed, namely if $k_4 = k_3\, b \neq k_3$ and $k_{-4} = k_{-3}\, b \neq k_{-3}$, where $b \in \mathbb{R}^+$. In this case, the equilibrium constants $K_{eq,4}$ and $K_{eq,3}$ are equal. The two reactions proceed with different velocities. In conjunction with the aforementioned futile cycles, this type of unidirectionality may play an important role in signal transduction. This will be discussed in more detail in the subsequent section.

- **mutually interacting processes**
  Mutually interacting processes are all processes which do not fit into the categories *non-interacting* or *unidirectionally interacting*. There are no requirements for the kinetic parameters from a theoretical point of view. However, the thermodynamic restrictions given by the Wegscheider conditions exist. From this it follows that if binding of L increases or decreases the affinity of E for the receptor R by a factor a_{LE}, the affinity of L for R will also increase or decrease by exactly the same factor if E is bound to R. Again, there are no restrictions on the reaction velocities.

- **all-or-none interactions**
  All-or-none interactions are an important special case of mutual interactions, which are characterized by vanishing kinetic parameters. A kinetic parameter which is exactly zero is not feasible from a thermodynamic point of view, which means that all pairs of binding and modification processes always form reaction cycles. Naturally, the kinetic parameters of the reactions forming these cycles have to fulfill the Wegscheider condition. However, reactions can proceed at a very slow pace, such that the assumption of vanishing kinetic parameters, meaning that the reaction does not proceed, is reasonable. A model representation of all-or-none interactions, consistent with the laws of thermodynamics, is that both k_i and k_{-i} go to zero such that $K_{eq,i}$ remains constant and fulfills the Wegscheider condition. From an applicatory point of view these reactions are too slow to play any role

for the dynamic behavior of the network and can be completely omitted. Hence, the remaining reaction network does not form a cycle anymore, and the Wegscheider condition does not give any restrictions on all-or-none interactions.

Our considerations show that non-interacting binding processes, as well as all-or-none interactions are thermodynamically feasible. However, we have found strong restrictions for mutual and especially for the theoretically very important unidirectional interactions. These principal statements also hold for scaffold proteins with higher numbers of binding domains, although these have a greater degree of freedom. Non-interacting binding processes can be always realized if the modification factors of all interaction tiers equal one. All-or-none interactions are not restricted by the Wegscheider conditions and are always feasible since they are based on the assumption of being extremely slow reactions. Unidirectionality is highly restricted and only feasible in terms of reaction velocities. In the following section, we will discuss under which conditions the assumption of unidirectional interactions provides a good approximation of the real system behavior despite its contradiction of the Wegscheider condition.

3.5 Unidirectionality in Signal Transduction

Unidirectionality is an important feature of technical signal transmission systems. Unidirectionality in this context means that the signal transmission is not influenced by the state of the receiver, but only by the emitter. The question of whether biological signal transduction networks can and do utilize unidirectional interactions is of special interest. Unidirectionality of process interactions allows the systematic and significant reduction of combinatorial complexity in mathematical signal transduction models, and it also allows to modularize them [32, 78, 16, 17]. In a first step, we will discuss theoretic possibilities that exist to realize at least approximately unidirectional signal transduction without contradicting the Wegscheider condition. Additionally, we will show that in the case of insulin signaling, unidirectionality seems to be realized.

3.5.1 Unidirectionality and Futile Cycles

We have already discussed above that a unidirectional change of reaction velocities does not contradict the Wegscheider condition. However, the acceleration or deceleration of a reaction does not seem to be sufficient to achieve functional signal transduction. Measurements show that stationary levels of occupancy before and after stimulation of a receptor differ [42, 82]. However, one has to be aware of the fact that stationarity of a reaction system does not imply that it has reached thermodynamic equilibrium. For instance if an open system is constantly perturbed by a constant impressed force, it reaches a stationary non-equilibrium state. These states are characterized by stationarity but non-vanishing driving forces. Hence, stationary levels of occupancy might vary in nature without equilibrium constants of reactions changing.

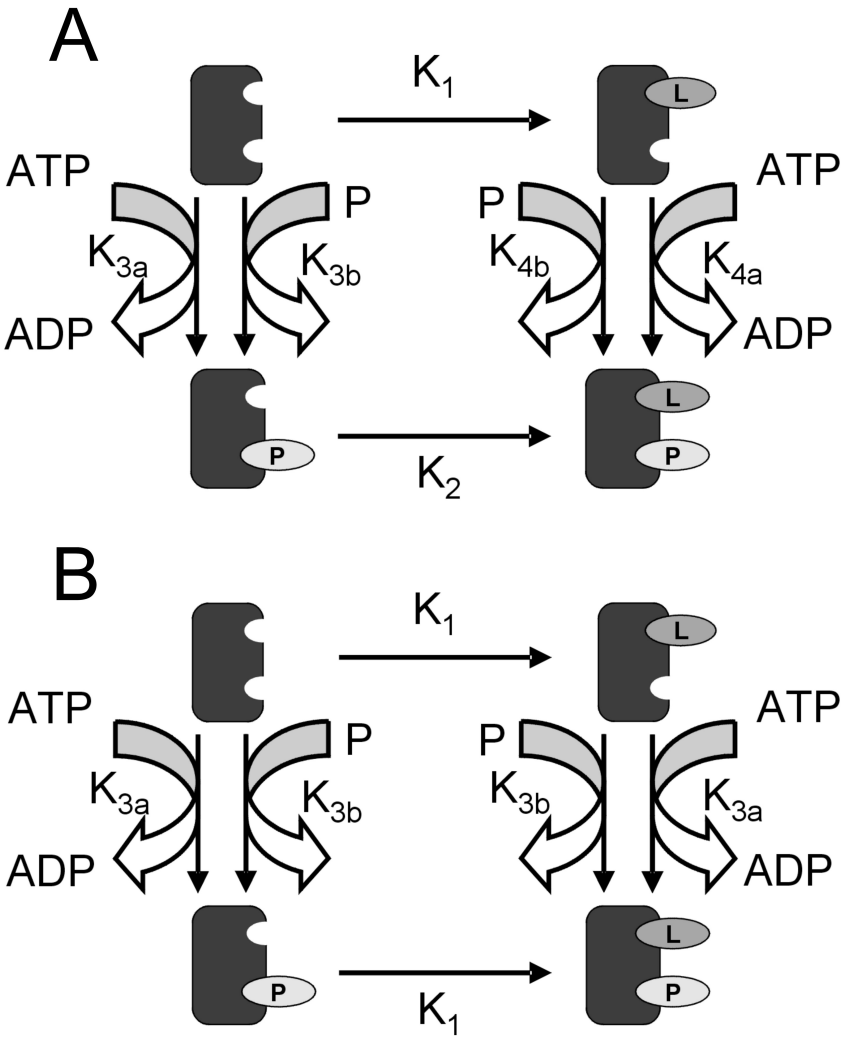

Figure 3.2: All shown reactions are reversible. The arrows only indicate which reactions are considered to be the forward reactions and which are the backward ones. In Figure 3.2 A the system is parameterized analogously to Figure 3.1. In this case the model has to fulfill two Wegscheider conditions, namely $K_1 K_{4a} K_2^{-1} K_{3a}^{-1} = 1$ and $K_1 K_{4b} K_2^{-1} K_{3b}^{-1} = 1$. The parameterization of Figure 3.2 B realizes the independence of L binding and concurrently fulfills the two Wegscheider conditions.

As discussed before, a stationary reaction system which is not in thermodynamic equilibrium is always characterized by at least one impressed driving force and non-vanishing reaction flows. A system like that has to include at least one futile cycle which is constantly consuming energy. A futile cycle is defined as a set of opposing, non-equilibrium reactions that are catalyzed by different enzymes and which act simultaneously, with at least one of the reactions being driven by energy consumption. From this, it follows that a stationary non-equilibrium is only sustainable as long as the provided reservoir of energy is not exhausted. The most important energy reservoir in living cells is given by ATP.

In order to analyze the dynamic behavior of a reaction system including futile cycles, we

consider a scaffold protein R with two binding domains (see Figure 3.2). One of the two domains can bind a ligand L and the other domain can be phosphorylated. All reactions are assumed to be reversible. The arrows in Figure 3.2 only indicate which reactions are regarded as forward and which as backward reactions. Although the considered scaffold also possesses two binding domains, the considered reaction network differs from that given by Equation 3.1. The complete mechanistic model comprises four phosphorylation reactions, two reactions in which ATP is converted to ADP, and two in which free phosphates bind to and dissociate from the domain (see Figure 3.2 A). This reaction network consists of two independent true reaction cycles meaning that it has to fulfill two Wegscheider conditions, namely $K_1 K_{4a} K_2^{-1} K_{3a}^{-1} = 1$ and $K_1 K_{4b} K_2^{-1} K_{3b}^{-1} = 1$. All cycles that are not futile cycles, according to the definition given above, are true cycles. Let us take the assumption that ligand binding is not influenced by phosphorylation. As a result the thermodynamic constraints imply that both phosphorylation reactions in which ATP is converted to ADP must have the same equilibrium constants and both reactions in which free phosphates bind must also have the same equilibrium constants (see Figure 3.2 B). However, we can assume that these reactions proceed with different velocities depending on whether the scaffold has bound L or not. For instance, one can assume that L is an enzyme which only accelerates or decelerates the reactions but does not change their equilibrium constants. Hence, the six reactions of the considered system can be written as

$$\begin{aligned}
r_1 &= k_1 [L] [R(0,0)] - k_{-1} [R(L,0)] \\
r_2 &= k_1 [L] [R(0,P)] - k_{-1} [R(L,P)] \\
r_{3a} &= k_{3a} [ATP] [R(0,0)] - k_{-3a} [ADP] [R(0,P)] \\
r_{4a} &= x \left(k_{3a} [ATP] [R(L,0)] - k_{-3a} [ADP] [R(L,P)] \right) \\
r_{3b} &= k_{3b} [P] [R(0,0)] - k_{-3b} [R(0,P)] \\
r_{4b} &= y \left(k_{3b} [P] [R(L,0)] - k_{-3b} [R(L,P)] \right),
\end{aligned} \tag{3.24}$$

in which x and y are real positive numbers describing the change of velocity for both forward and backward reactions, caused by L. If one additionally assumes that the concentrations [ATP], [ADP] and [P] in the cell are approximately constant, the reactions r_{3a} and r_{3b} as well as r_{4a} and r_{4b} can be combined to form two virtual phosphorylation reactions

$$\begin{aligned}
r_3^* &= \underbrace{(k_{3a} [ATP] + k_{3b} [P])}_{=k_3^*} [R(0,0)] - \underbrace{(k_{-3a} [ADP] + k_{-3b})}_{=k_{-3}^*} [R(0,P)] \\
r_4^* &= \underbrace{(x\, k_{3a} [ATP] + y\, k_{3b} [P])}_{=k_4^*} [R(L,0)] - \underbrace{(x\, k_{-3a} [ADP] + y\, k_{-3b})}_{=k_{-4}^*} [R(L,P)].
\end{aligned} \tag{3.25}$$

The asterisk indicates that the reaction is a virtual reaction. The resulting reduced network structure only now consists of one single cycle. Interestingly, the virtual equilibrium constants of the two reactions r_3^* and r_4^* which we define as the quotient of k_{on} and k_{off}

$$K_3^* = \frac{k_{3a} [ATP] + k_{3b} [P]}{k_{-3a} [ADP] + k_{-3b}} \qquad K_4^* = \frac{x\, k_{3a} [ATP] + y\, k_{3b} [P]}{x\, k_{-3a} [ADP] + y\, k_{-3b}} \tag{3.26}$$

are not identical. They only describe a steady state and not a thermodynamic equilibrium of the system. It is possible to unidirectionally shift a steady state but not thermodynamic equilibrium. Thus, the reduced network with its single reaction cycle does not fulfill the Wegscheider condition. This reduced model includes a unidirectional process interaction and describes a shift between non-equilibrium steady states correctly, if all assumptions made above are fulfilled. However, the reduced model cannot describe the behavior of the system near thermodynamic equilibrium.
The important message is that unidirectional interactions are possible and *may* occur. Requirements are that the modification of a scaffold protein is realized by at least two different reactions (corresponding to the existence of a so-called futile cycle), and the corresponding substrates required for the modification (like ATP, ADP and P) are approximately constant. However, if one assumes unidirectional interactions, one has to be aware of the fact that the model will probably give wrong predictions if any of the underlying assumptions is not fulfilled. Note, that if the described process includes futile cycles it is also possible to realize any mutual interaction, which does not fulfill the Wegscheider condition. Such a parameterization is only valid under the defined boundary conditions, and cannot describe a system's behavior globally in each thermodynamically feasible situation.

3.5.2 Unidirectionality in Insulin Signaling

We have shown that theoretically a cell can realize unidirectional interactions between signaling processes. An interesting question is whether such interactions can be found in real signaling networks. There is, in fact, very strong evidence to suggest that unidirectional interactions are used in signal transduction. This will be shown in the consideration of the insulin signaling pathway.
Insulin is a hormone that regulates essential physiological processes. A well know example is cellular glucose uptake [23, 117]. Insulin also has strong effects on metabolism [117, 110] and regulates gene expression [96]. Cell survival and differentiation are also subjected to regulation by insulin. Defects in the insulin signaling system may lead to obesity and insulin resistance [85, 21, 89].
The insulin receptor consists of two monomers that are constitutively dimerized [90]. Each receptor monomer can bind one insulin molecule. Additionally, several phosphorylation sites on the receptor exist. After insulin binding complex formation on the receptor is initiated by autophosphorylation of various binding sites [116].

In 1986 Gherzi *et al.* experimentally addressed the question of whether receptor phosphorylation has an effect on insulin binding or not. They used purified insulin receptors from liver cells of male Sprague-Dawley rats, and in other experiments purified insulin receptors of an human placenta. The receptors were incubated with 0.4 ng/ml radioactively labeled insulin and 2.5-1000 ng/ml unlabeled insulin. For both cell types, the experiments were performed using both completely unphosphorylated, and in a second experiment, phosphorylated insulin receptors. Gherzi *et al.* determined the amount of labeled receptor-bound hormone and employed a

Scatchard analysis [118]. The resulting plots show that phosphorylated and unphoshorylated insulin receptors have exactly the same steady state binding characteristic for insulin. They concluded from this experimental data that receptor phosphorylation does not have any effect on insulin binding [47]. On the other hand, it is well known that insulin binding induces receptor phosphorylation, which clearly suggests an unidirectional interaction between insulin binding and receptor autophosphorylation.

In order to confirm these conclusions, we created steady state models of the described scenarios. The models incorporate radioactively labeled (I_m) as well as unlabeled insulin (I_u). Additionally, we presume that the insulin receptor dimers provide two binding domains for insulin as well as two binding domains that can be phosphorylated. According to the experiments performed by Gherzi *et al.* [47], we consider two steady state scenarios. In the first scenario the insulin receptors are completely unphosphorylated, in the second they are completely phosphorylated. Since the setup for both experiments neither included phosphatases and kinases nor ATP and ADP, we can exclude the possibility of active futile cycles in these scenarios. Hence, we developed a model in which all intra-cellular domains are constantly phosphorylated. By taking the assumption that insulin binding is independent of receptor phosphorylation due to unidirectionality of the interaction, it is obvious that the steady state curves for phosphorylated and unphosphorylated receptors are equivalent. If we additionally include insulin binding affinities measured by Wanant et al. [134], the resulting steady state curve has the same shape as that measured by Gherzi *et al.* (see Figure 3.3 A). The only parameter that had to be fitted to the data is the concentration of insulin receptors in the experiment, since this cannot be extracted from the data provided by Gherzi *et al.* [47]. Hence, the measured data is consistent with the assumption of unidirectional process interactions between insulin binding and receptor phosphorylation.

In order to prove that the finding by Gherzi *et al.* [47] really implies unidirectionality, one has to answer the question of whether retroactive effects would have a noticeable effect on the measured steady state curve. We can show that in most cases, even slight retroactive effects lead to strongly varying steady state curves (see Figure 3.3 B), confirming the assumption of unidirectionality. However, it should also be mentioned that there exist special constellations of the previously introduced thermodynamic modification factors for which the steady state curves for completely unphosphorylated and completely phosphorylated receptors are also equivalent (data not shown). However, the experimental setup of Gherzi *et al.* [47] is highly unphysiological. In a physiological environment, the found parameter constellations would not noticeably distinguish the system from others with mutual interactions. Hence, it is very unlikely that these are the real system parameters. We take the opinion that the assumption of an unidirectional interaction is the much more probable hypothesis.

Thus, there is strong evidence to suggest that unidirectional interactions really occur in biological systems, which however, cannot be proved by the available data.

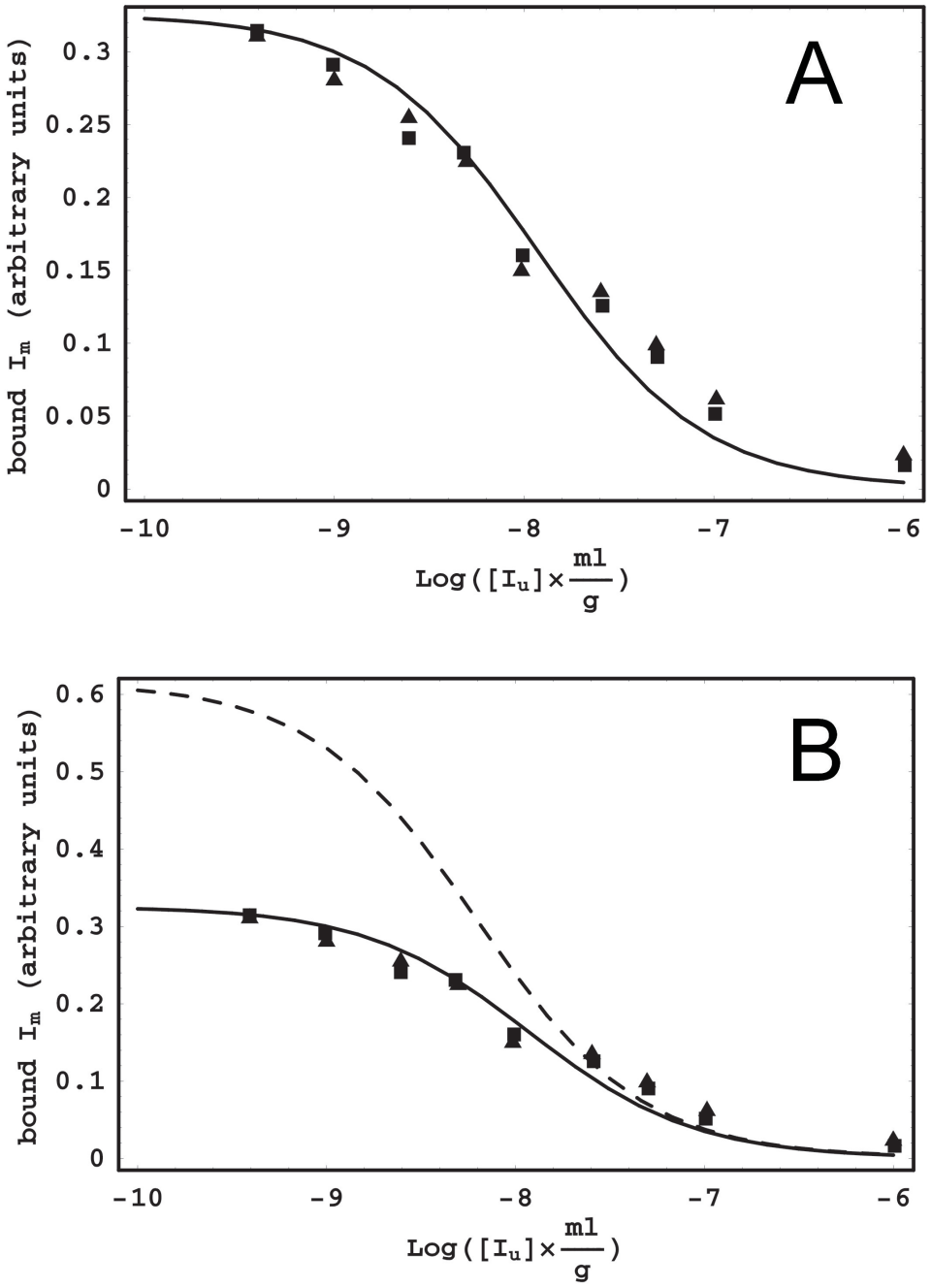

Figure 3.3: Both phosphorylated (triangles) and unphosphorylated (squares) insulin receptors purified from liver cells of male Sprague-Dawley rats were incubated with 0.4 ng/ml radioactively labeled insulin and 2.5-1000 ng/ml unlabeled insulin. In Figure A these measurements are compared with the simulation results of the developed steady state models taking the assumption that insulin binding and receptor phosphorylation interact unidirectionally. The simulation results in Figure B show the steady state behavior of the system taking the assumption that insulin binding and receptor phosphorylation interact mutually. The dashed line describes the phosphorylated receptors for relatively weak retroactive effects.

3.6 Conclusions

We have discussed the implications introduced thermodynamic constraints for complex signaling networks, including scaffold proteins and receptors. These thermodynamic constraints are given by restrictions on the kinetic parameters of reactions forming a reaction cycle, and they can be mathematically formulated using the Wegscheider condition. Due to the combinatorial complexity of many signal transduction networks and their immense number of possible reactions, these systems comprise a huge number of cycles and are therefore highly restricted by the Wegscheider conditions.

Based on consideration of the chemical potential of scaffold proteins or receptors, we introduced a new formalism which allows for the direct parameterization of models of such systems with parameters that fulfill the Wegscheider condition. Interestingly, the restrictions given by the Wegscheider condition have a descriptive interpretation in terms of domain or process interactions, which play an important role in model reduction and model modularization. According to the Wegscheider condition, processes can either interact mutually with each other or they can be independent. Additionally, it turns out that different tiers of interactions exist. It is not the case that only each pair of domains can interact with each other. Indeed, interactions between triples and higher tupels of domains or processes also exist. However, unidirectional interactions are highly restricted. Only reaction velocities can be changed unidirectionally, not equilibrium constants. This finding is highly problematic since a lot of available model reduction and modularization techniques are based on the unidirectionality of process interactions [16, 17, 32]. However, we have also been able to show that in reaction networks which include futile cycles, it is possible to realize at least approximately unidirectional interactions. Finally, we compared a steady state model of the insulin receptor with measurements made by Gherzi *et al.*, which indicates that phosphorylation of the insulin receptor is unidirectionally influenced by insulin binding.

Chapter 4

Exact Model Reduction - A Domain-Oriented Approach

Receptor-mediated signal transduction is the subject of intense research, since it plays a crucial role in the regulation of a variety of cellular functions. Within the last few years, a lot of mathematical models have been created in order to gain a deeper understanding of these processes. One problem all modelers of signal transduction networks have to face is combinatorial complexity. Due to the occurrence of receptors and scaffold proteins with high numbers of binding domains and binding partners the number of feasible molecular species is enormous. Complete mechanistic models of these extremely complex reaction networks are not practical, and model reductions are an inevitable requirement in order to get useful models. This requirement for model reductions is further emphasized by a lack of computing power, as well as a distinct lack of suitable analysis tools. In most real signaling networks the number of theoretically feasible multiprotein species by far exceeds the number of proteins within a cell. Thus, it is obvious that most of these multiprotein species will not occur in the signaling process. However, being able to predict which species will occur and play an important role in the signaling cascade is difficult and requires a profound knowledge about the kinetic parameters, as shown by Faeder *et al.* [38]. These findings indicate that common modeling strategies are insufficient, or at least very problematic, when attempting to mathematically describe signal transduction networks.

The first step in the development of new modeling or model reduction techniques is the determination of the most relevant quantities of signal transduction networks. The goal will be finding mathematical models which describe the dynamics of these quantities. Probably, the most popular quantities to describe the current state of receptors or scaffold proteins are occupancy levels of certain binding domains, or their degree of phosphorylation (compare [122, 13, 38, 16, 17, 32, 78] and others). According to Pawson and Nash [106], domains are the fundamental elements of signal transduction rather than individual molecules. In this thesis, we will use the terms *level of occupancy* or *degree of phosphorylation* to describe cumulated concentrations of all multiprotein species sharing a common feature such as phosphorylation of a certain domain. Borisov *et al.* refer to these quantities as macroscopic quantities or macro

states [16], which we will adopt here. Macro-states have a number of further advantages, such as their simple biological interpretability, or the fact that they often correspond to experimental readouts. The aim of this thesis will be to provide new and systematic methods that facilitate the generation of reduced signal transduction models which approximately describe the dynamics of these and similar macroscopic quantities.

From a system theoretical point of view the discussed occupancy levels correspond to the output variables $\vec{y}$ of the dynamic model. One usually chooses measureable quantities or states of special interest as output variables. In order to assure that their dynamics are accurately described, our starting point will be a complete mechanistic model of first order ordinary differential equations. However, since we assume that $\vec{y}$ includes all essential quantities, we are solely interested in the systems input/output behavior. The question is whether the complete mechanistic model is a so-called *minimal realization*. If a model is not a minimal realization, it comprises uncontrollable or unobservable states, which can be eliminated without changing the systems input/output behavior. The elimination of unobservable states in particular is often referred to as exact lumping or exact model reduction. Note, that the term *exact* may be misleading since the elimination of model equations is always linked with loss of information. The reduction is only exact in terms of the input/output behavior which is exactly preserved in the reduced model. In this chapter we discuss whether combinatorial reaction networks are minimal realizations under the condition that occupancy levels are chosen as output variables. We additionally provide methods to eliminate uncontrollable and unobservable states. Firstly, we consider how a previously generated combinatorial reaction network can be exactly reduced by eliminating unobservable and uncontrollable states. We refer to this approach as exact model *reduction* since the number of equations is reduced. However, it is obvious that a model reduction technique is not practical for really large combinatorial networks, comprising millions or even billions of equations. On this account we also present a closely related alternative approach which facilitates a direct generation of the reduced model equations. In this thesis, this approach is called *reduced order modeling*. A further approximate reduction of the models will be considered in the subsequent chapter.

4.1 Exact Model Reduction of Combinatorial Reaction Networks

In literature, the term exact model reduction as well as exact lumping usually refers to the elimination of unobservable states. In this thesis, the term exact model reduction will be extended and will comprise the elimination of uncontrollable states. Note, that the elimination of uncontrollable states, in contrast to that of unobservable ones, cannot be achieved by lumping but by steady state assumptions. For this reason we do not use the term exact lumping. Additionally, the elimination of uncontrollable states will only be exact if the uncontrollable system dynamics have already decayed. In the following, we take the assumption that this requirement is always fulfilled.

The elimination of unobservable and uncontrollable states can be achieved by a formal dissection of the model's state space into observable and controllable, observable but not controllable, controllable but not observable as well as neither observable nor controllable subspaces. Such a dissection is called Kalman decomposition [139]. The major challenge is the derivation of a suitable state space transformation $\vec{z} = \vec{\phi}(\vec{x})$ that realizes a Kalman decomposition. As indicated by the notation used this transformation will, in general, be nonlinear because the considered models are nonlinear, too. One also has to be aware of the fact that the transformation cannot be unique. Only the mentioned subspaces are uniquely determined but not the specific choice of their coordinates. This degree of freedom can be regarded as advantage, since it facilitates a choice of coordinates, adequate for the treated problem.

Example. In control theory one usually aims at the synthesis of a controller or observer which suggests a certain model structure such as the controllable canonical form or the observable canonical form [70, 65]. Let us focus on observability and assume that we consider a n-dimensional system with d unobservable states. The textbook by Alberto Isidori about nonlinear control systems [65], provides an algorithm to decompose a general nonlinear system into observable and unobservable states. The resulting observable submodel is given in observable canonical form. For the sake of simplicity, we consider a single output system

$$\begin{aligned} \dot{\vec{x}} &= \vec{f}(\vec{x}, \vec{u}) \qquad \vec{x}(t_0) = \vec{x}_0 \\ y &= h(\vec{x}), \end{aligned} \tag{4.1}$$

and additionally assume that the observable subsystem is *uniformly* observable. This means that the output y and its first $n - d - 1$ derivatives build a basis for the observable subspace. Note, that a similar but more complex method also exists for general nonlinear systems with multiple outputs.
According to Isidori, we use the Lie derivative of the output function $h(\vec{x})$ along the vector field $\vec{f}$ to depict the time derivatives of y. The Lie derivative is defined as

$$L_f h(\vec{x}) = \frac{\partial h}{\partial \vec{x}} \vec{f}(\vec{x}) \qquad \text{and} \qquad L_f^n h(\vec{x}) = L_f L_f^{n-1} h(\vec{x}). \tag{4.2}$$

Using the Lie operator the required transformation $\vec{\phi}(\vec{x})$ can be written as

$$\vec{\phi}(\vec{x}) = \left[\underbrace{h(\vec{x}), L_f h(\vec{x}), ..., L_f^{n-d-1} h(\vec{x})}_{\vec{\phi}_1(\vec{x})}, \underbrace{\varphi_1(\vec{x}), ..., \varphi_{n-d}(\vec{x})}_{\vec{\phi}_2(\vec{x})} \right]^T . \tag{4.3}$$

The first $n - d$ new coordinates correspond to the output and its first $n - d - 1$ derivatives. Since the system only comprises $n - d$ observable states $L_f^k h(\vec{x})$ with $k > n - d - 1$ depends algebraically on the output and its first $n - d - 1$ derivatives. The remaining d coordinates of the transformed system have to be chosen such that the transformation $\vec{\phi}$ is invertible, smooth

and fulfills $\vec{\phi}(0) = 0$ [65]. The transformed system has the following structure

$$\begin{bmatrix} \dot{z}_1 \\ \vdots \\ \dot{z}_{n-d-1} \\ \dot{z}_{n-d} \\ \dot{z}_{n-d+1} \\ \vdots \\ \dot{z}_n \end{bmatrix} = \begin{bmatrix} z_2 \\ \vdots \\ z_{n-d} \\ g_{n-d}(z_1, ..., z_{n-d}) \\ g_{n-d+1}(z_1, ..., z_n) \\ \vdots \\ g_n(z_1, ..., z_n) \end{bmatrix} \tag{4.4}$$
$$y = z_1$$

However, in spite of the quality of its properties for the synthesis of controllers as well as its generality, this method is not suited for models of large reaction networks. The computational cost to analytically calculate the higher order Lie derivatives grows extremely large with the size of a model. The calculation for combinatorial models of signaling cascades comprising thousands or even millions of ODEs would be infeasible. Another drawback is that, in most cases, the transformation $\vec{\phi}(\vec{x})$ is not globally but only locally invertible. Furthermore, the model states lose their biological interpretability, which is a significant disadvantage especially in conjunction with model validation. While one usually has rough estimates regarding how most species' concentrations evolve over time, or at least about their lower and upper boundaries, no such knowledge is available for higher derivatives of the output.

Exact model reduction of combinatorial reaction networks obviously requires an alternative approach. Due to the aforementioned degrees of freedom in the choice of coordinates, the main question is that of which choice is most suitable for combinatorial networks. The work of Borisov *et al.* [16] serves as a basis for our further considerations and will be briefly reviewed in the subsequent section.

4.1.1 Starting Point

A very promising approach to coping with combinatorial complexity has been introduced by Borisov *et al.* [16]. Their work also builds the basis or starting point for the considerations presented here. Borisov *et al.* showed that mechanistic models of scaffolds and receptors can be reduced by exact lumping if all binding processes are completely independent or one controlling domain exists, which unidirectionally influences all other binding processes. This reduction will be further explained for a receptor R providing two distinct binding domains which do not interact. The complete reaction network comprises four reactions

$$\begin{aligned} r_1 &= k_1[L]\,[R(0,0)] - k_{-1}[R(L,0)] \\ r_2 &= k_1[L]\,[R(0,E)] - k_{-1}[R(L,E)] \\ r_3 &= k_2[E]\,[R(0,0)] - k_{-2}[R(0,E)] \\ r_4 &= k_2[E]\,[R(L,0)] - k_{-2}[R(L,E)]. \end{aligned} \tag{4.5}$$

These reactions can be divided into two groups, namely those that change the level of occupancy of the L binding domain $[R(L,*)]$ (r_1 and r_2), and those that change the level of occupancy of the E binding domain $[R(*,E)]$ (r_3 and r_4). Interestingly, all reactions within one of these groups are parameterized by the same kinetic parameters. Due to this special parameterization and the simple structure of the considered mass action kinetics the sums of these reaction rates can be written as

$$\begin{aligned} r_{1,2} = r_1 + r_2 &= k_1[L]\underbrace{([R(0,0)] + [R(0,E)])}_{=[R(*,*)]-[R(L,*)]} - k_{-1}\underbrace{([R(L,0)] + [R(L,E)])}_{=[R(L,*)]} \\ r_{3,4} = r_3 + r_4 &= k_2[E]\underbrace{([R(0,0)] + [R(L,0)])}_{=[R(*,*)]-[R(*,E)]} - k_{-2}\underbrace{([R(0,E)] + [R(L,E)])}_{=[R(*,E)]}. \end{aligned} \tag{4.6}$$

If we assume that the concentrations $[L]$ and $[E]$ are input signals, the reaction rates $r_{1,2}$ and $r_{3,4}$ only depend on the system states $[R(*,*)]$, $[R(L,*)]$ and $[R(*,E)]$, which correspond to the constant overall concentration of receptor species and the two occupancy levels respectively. Thus, an exact mathematical description of the two occupancy levels only requires the following ordinary differential equations

$$\begin{aligned} \frac{d[R(L,*)]}{dt} &= k_1[L]\left([R(*,*)] - [R(L,*)]\right) - k_{-1}[R(L,*)] \\ \frac{d[R(*,E)]}{dt} &= k_2[E]\left([R(*,*)] - [R(*,E)]\right) - k_{-2}[R(*,E)]. \end{aligned} \tag{4.7}$$

If $[L]$ was the only input of the system, the ODE for $[R(*,E)]$ would be uncontrollable. Hence, one only needs the ODE for $[R(L,*)]$, whereas the concentrations of $[R(*,E)]$ and $[E]$ can be algebraically calculated from the stationary second ODE and the mass conservation relation for E. With similar considerations it is possible to deduce reduced models for other systems. These findings prove that combinatorial models of signal transduction networks may be reduced by exact model reduction techniques in the case of macroscopic output variables. Additionally, the results of Borisov *et al.* [16] also indicate that the occurring process interactions determine whether, and to what extent, these models can be reduced. If one considers the discussed example using different kinetic parameters realizing a mutual interaction between the two binding processes, the complete mechanistic model represents a minimal realization, and no exact model reduction is feasible. However, Borisov *et al.* [16] provided neither a general rule to determine whether a reaction network can be reduced, nor did they provide a method that facilitates the derivation of the reduced model equations for systems of arbitrary size and complexity. These will be introduced in this thesis.

4.1.2 A Linear Hierarchically Structured Transformation

The reduced models of Borisov *et al.* [16] do have very nice properties. First, all occurring new variables are biologically interpretable. They probably even have a higher biological relevance than the original ones, since levels of occupancy directly correspond to experimental readouts.

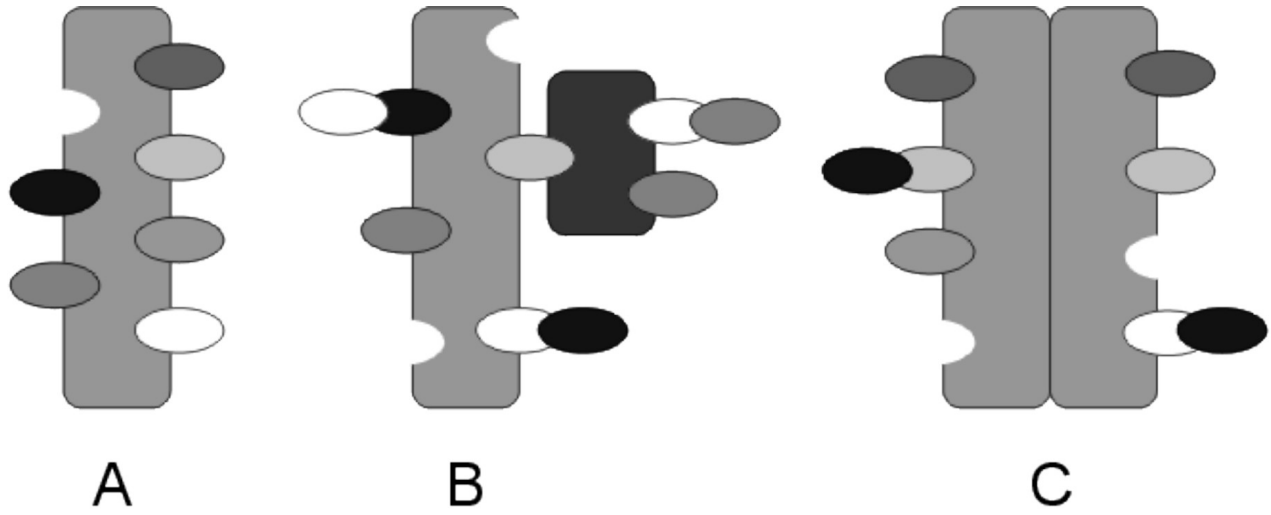

Figure 4.1: The three basic scenarios that will be discussed in this chapter. Figure A depicts a receptor or scaffold protein with single protein ligands, meaning each binding domain can recruit single proteins which do not possess further binding domains. A scaffold with multiprotein ligands is shown in Figure B. Some of the ligands are scaffolds themselves. The last scenario additionally includes receptor homodimerization. Heterodimerization on the other site corresponds to the scenario depicted in Figure B.

Additionally, the model equations of the reduced model can easily be divided into different modules. In the example discussed above the remaining two ODEs are completely decoupled resembling the complete independence of the two considered binding processes. Perhaps the most interesting characteristic from a mathematical point of view, is that the new coordinates correspond to linear combinations of the original ones. This also holds true for all other examples presented by Borisov *et al.* [16], suggesting the assumption that an exact reduction of combinatorial reaction networks might always be achievable by linear transformations. A linear transformation rule is most desirable since it is much easier to handle than nonlinear ones.

In fact, we have found linear transformations that realize a Kalman decomposition for all combinatorial reaction networks we analyzed. Again, one can find infinitely many different linear transformations $\vec{z} = T\vec{x}$ having this property. The transformation rule suggested here introduces new hierarchically structured states, including the levels of occupancy which correspond to our output variables $\vec{y}$. Choosing an invertible transformation matrix T assures that the system's dynamics are preserved, and the original states can be retrieved from the new ones at any time as long as none of the transformed equations are eliminated. The pattern of this linear and hierarchically structured transformation will be considered for the three most biologically relevant scenarios, namely scaffolds with single protein ligands, scaffolds with multiprotein ligands and receptor or scaffold homodimerization. These three scenarios are depicted and elucidated in Figure 4.1.

4.1.3 Scaffolds with Single Protein Ligands

The first and probably most simple scenario we are going to look at are scaffolds with single protein ligands. The term *single protein ligand* indicates that we only consider the multi domain protein and its direct binding partners but no additional binding or modification processes at these ligands. This scenario also corresponds to the one described by Borisov *et al.* [16] and Conzelmann *et al.* [32].
For the sake of simplicity we take the assumption that each domain j can only bind one specific effector protein E^j. However, note that the method can also be applied to systems in which effector proteins compete for certain binding domains. In the following we also discuss one example in which two effector proteins compete for a binding domain. Additionally, we neglect domain phosphorylation, since phosphorylation and subsequent effector binding belongs to the second scenario discussed below. Let us assume that the considered receptor R possesses n binding domains. The consequent number of different receptor complexes is 2^n, since each domain can be either unoccupied (0) or occupied (1). Additionally, one has to consider the n effector proteins that can bind to the receptor. These $2^n + n$ individual species or micro-states can be written as $E^j(0)$ with $j = 1, ..., n$ and $R(i_1, ..., i_n)$ with $i_j \in \{0, 1\}$. The alternative coordinates we propose in order to facilitate a Kalman decomposition correspond to a formally very similar representation in which the identifier zero is replaced by an asterisk.

4.1.3.1 General Transformation Pattern

The suggested replacement of identifiers implies a linear state space transformation which can be structured in a hierarchical way. It consists of different tiers, where each of these tiers represents a certain level of detail. Firstly, we define the 0^{th} tier of our transformation, which includes the $n + 1$ overall concentrations of all participating proteins, namely $[E^j(*)]$ and $[R(*, ..., *)]$. Mathematically, $[E^j(*)]$ corresponds to the sum of all occurring species including the effector molecule E^j, and $[R(*, ..., *)]$ to the sum of all receptor species. If the model does not include production and degradation, these quantities will be constant over time due to mass conservation. Consequently, the corresponding ODEs can be eliminated and replaced by constant values. In the general case, when production and degradation is included, these are also important macroscopic and measureable quantities of interest. The subsequent 1^{st} tier of our transformation comprises all n occupancy levels of the binding domains, which correspond to the output variables of our system. According to Borisov *et al.* [16] the occupancy level of a certain binding domain j is defined as the sum of all concentrations of receptor species with an occupied binding domain j. The 2^{nd} tier describes the occupancy levels of all pairs of domains, corresponding to the accumulated concentration of receptor species with concurrently occupied binding domains i and j. Following this pattern, the subsequent tiers describe all triples, all quadruples and all higher tuples of concurrently occupied binding domains. The final n^{th} tier only comprises of one state, namely the state $R(1, ..., 1)$. According to Borisov *et al.* [16], who introduced the terms macro- and micro-states describing the 0^{th} and 1^{st} as well as the n^{th} tier

of our transformation, we introduce the term *mesoscopic states* for the remaining $n-2$ tiers.

Importantly, one can also prove that this transformation is always invertible. First of all, it is quite obvious that the number of new states is equivalent to the number of old ones, since we simply replace the identifier zero by an asterisk. One can also show by mathematical induction that the transformation matrix is not only quadratic but also has a triangular form. The basic idea is that each transformed state of the i^{th} tier corresponds to a sum of micro-states occurring in the tiers that describe higher tuples of concurrently occupied domains plus one further micro-state. The induction basis is given by the following considerations. While the one and only state of the n^{th} tier directly corresponds to the micro-state $[R(1,...,1)]$, all n states of the $(n-1)^{\text{th}}$ tier correspond to a sum of $[R(1,...,1)]$ and one further micro-state like for example $[R(0,1,...,1)]$ for the mesoscopic state $[R(*,1,...,1)]$. This facilitates the reconstruction of n additional micro-states. All states of the $(n-2)^{\text{th}}$ tier also correspond to sums composed of already-reconstructed micro-states plus one additional still unknown micro-state. One example is the mesoscopic state $[R(*,*,1,...,1)]$, which corresponds to the sum of the already-known micro-states $[R(1,...,1)]$ from the n^{th} tier as well as $[R(0,1,...,1)]$ and $[R(1,0,1,...,1)]$ from the $(n-1)^{\text{th}}$ tier and the still unknown micro-state $[R(0,0,1,...,1)]$.
In the induction step, we consider a mesoscopic state of the i^{th} tier such as

$$[R(\underbrace{1,...,1}_{n-i},\underbrace{*,...,*}_{i})].$$

It corresponds to a sum of micro-states, composed of only one state characterized by i zero identifiers, and numerous micro-states characterized by a lower number of zero identifiers. All micro-states with less than i zero identifiers are also part of other mesoscopic states belonging to one of the $(i+1)^{\text{th}}$ to n^{th} tier. Since the sequence of asterisk and one identifiers of the particular mesoscopic state does not affect these considerations, this is true for all states of the i^{th} tier.
Thus, we have shown that the pattern described always provides a linear and invertible transformation. Whether this transformation really leads to a Kalman decomposition of the considered combinatorial reaction network will be discussed below. First of all, the transformation will be exemplified.

4.1.3.2 Example with Three Binding Domains

Let us consider a scaffold or receptor protein R which provides three binding domains that can recruit three different effectors. One can distinguish eleven molecular species, namely $E^1(0)$, $E^2(0)$, $E^3(0)$, $R(0,0,0)$, $R(1,0,0)$, $R(0,1,0)$, $R(0,0,1)$, $R(1,1,0)$, $R(1,0,1)$, $R(0,1,1)$ and $R(1,1,1)$. The complete combinatorial reaction network comprises twelve reactions, which are parameterized by a total number of 24 kinetic parameters (see Table 4.1). In our example we do not consider production or degradation of any component. According to the presented general transformation pattern, the linear transformation which realizes a Kalman decomposition for this simple example is given in Table 4.2. Note, that the structure of the transformation matrix

Binding of E^1	Binding of E^2	Binding of E^3
$[R(0,0,0)]+[E^1] \rightleftharpoons [R(1,0,0)]$	$[R(0,0,0)]+[E^2] \rightleftharpoons [R(0,1,0)]$	$[R(0,0,0)]+[E^3] \rightleftharpoons [R(0,0,1)]$
$[R(0,1,0)]+[E^1] \rightleftharpoons [R(1,1,0)]$	$[R(0,0,1)]+[E^2] \rightleftharpoons [R(0,1,1)]$	$[R(0,1,0)]+[E^3] \rightleftharpoons [R(0,1,1)]$
$[R(0,0,1)]+[E^1] \rightleftharpoons [R(1,0,1)]$	$[R(1,0,0)]+[E^2] \rightleftharpoons [R(1,1,0)]$	$[R(1,0,0)]+[E^3] \rightleftharpoons [R(1,0,1)]$
$[R(0,1,1)]+[E^1] \rightleftharpoons [R(1,1,1)]$	$[R(1,0,1)]+[E^2] \rightleftharpoons [R(1,1,1)]$	$[R(1,1,0)]+[E^3] \rightleftharpoons [R(1,1,1)]$

Table 4.1: Reactions for a scaffold with three binding sites. A complete mechanistic model of a scaffold protein with three binding domains, where each domain can bind one effector protein (E^1, E^2, E^3), has to consider the twelve reactions shown. The kinetic parameters for each reaction can be denoted with k_{+i} for the association and k_{-i} for the dissociation reaction.

$$
\begin{aligned}
[E^1(*)] &= [E^1(0)] + [R(1,0,0)] + [R(1,1,0)] + [R(1,0,1)] + [R(1,1,1)] \\
[E^2(*)] &= [E^2(0)] + [R(0,1,0)] + [R(1,1,0)] + [R(0,1,1)] + [R(1,1,1)] \\
[E^3(*)] &= [E^3(0)] + [R(0,0,1)] + [R(1,0,1)] + [R(0,1,1)] + [R(1,1,1)] \\
[R(*,*,*)] &= [R(0,0,0)] + [R(1,0,0)] + [R(0,1,0)] + [R(0,0,1)] + [R(1,1,0)] \\
&\quad + [R(1,0,1)] + [R(0,1,1)] + [R(1,1,1)] \\
[R(1,*,*)] &= [R(1,0,0)] + [R(1,1,0)] + [R(1,0,1)] + [R(1,1,1)] \\
[R(*,1,*)] &= [R(0,1,0)] + [R(1,1,0)] + [R(0,1,1)] + [R(1,1,1)] \\
[R(*,*,1)] &= [R(0,0,1)] + [R(0,1,1)] + [R(1,0,1)] + [R(1,1,1)] \\
[R(1,1,*)] &= [R(1,1,0)] + [R(1,1,1)] \\
[R(1,*,1)] &= [R(1,0,1)] + [R(1,1,1)] \\
[R(*,1,1)] &= [R(0,1,1)] + [R(1,1,1)] \\
[R(1,1,1)] &= [R(1,1,1)]
\end{aligned}
$$

Table 4.2: Hierarchical linear transformation for a receptor or scaffold protein with three binding domains and three single protein ligands. The new states $[E^j(*)]$ and $[R(*,*,*)]$ correspond to the overall concentrations of the 0^{th} tier. The 1^{st} tier comprises three levels of occupancy, the 2^{nd} tier three pairs of concurrently occupied domains and the last tier comprises the micro-state $[R(1,1,1)]$.

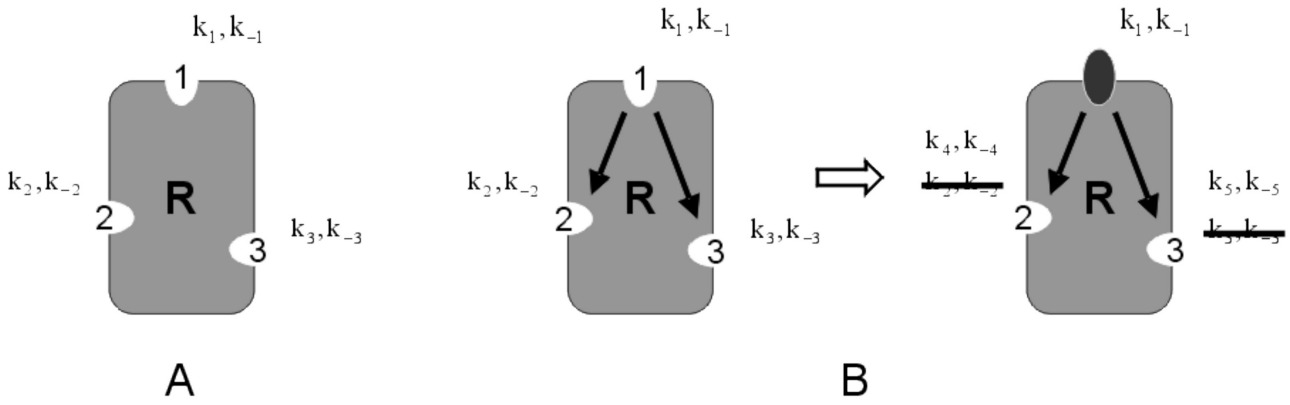

Figure 4.2: Figure A depicts a scaffold or receptor with three completely independent binding domains. Due to their independence all reactions changing the occupancy level of a certain domain are parameterized by the same kinetic parameters. In Figure B we assume that binding domain one controls the other two domains as indicated by the arrows. Again, the kinetic parameters for the model follow immediately from this assumption. As soon as binding domain one is occupied, the kinetic properties of the docking sites two and three will change. Since binding domain one is independent of the other binding sites, the on- and off-rate constants of this domain always stay the same.

is completely independent of the occurring process interactions. In vector representation the transformation can be written as $\vec{z} = T\vec{x}$ where $\vec{z}$ is the vector of new transformed variables and $\vec{x}$ corresponds to the vector of original micro-states. The resulting transformed model equations are

$$\dot{\vec{z}} = T\vec{f}(T^{-1}\vec{z}, \vec{u}). \tag{4.8}$$

In this example the overall concentration $[E^1(*)]$ is assumed to be the system input u, while the levels of occupancy $[R(1,*,*)]$, $[R(*,1,*)]$ and $[R(*,*,1)]$ are considered as output variables $\vec{y}$. Since $[E^1(*)]$ is the system input, one does not require an ODE for this quantity. Due to the absence of production and degradation processes, the overall concentrations of E^2, E^3 and R are constant and the corresponding ODEs can also be eliminated. The structure of the remaining seven transformed model equations are highly dependent on the interactions between the three considered binding processes. The absence of process interactions as well as unidirectional process interactions prove to be of special interest in this context since they facilitate the modularization of the model and in many cases its reduction as well. Although we have already discussed that from a thermodynamic point of view, unidirectional process interactions are highly restricted and, in general, occur in conjunction with domain phosphorylation instead of effector binding, unidirectional interactions will also be considered here. The usage of unidirectional interactions in this context, however, facilitates the treatment of all important aspects of exact model reduction considering one simple reaction network. We consider two different interaction patterns, which are also depicted in Figure 4.2.

$$
\begin{aligned}
\frac{d[R(1,*,*)]}{dt} &= k_1\left([R(*,*,*)]-[R(1,*,*)]\right)\left([E^1(*)]-[R(1,*,*)]\right)-k_{-1}[R(1,*,*)]\\
\frac{d[R(*,1,*)]}{dt} &= k_2\left([R(*,*,*)]-[R(*,1,*)]\right)\left([E^2(*)]-[R(*,1,*)]\right)-k_{-2}[R(*,1,*)]\\
\frac{d[R(*,*,1)]}{dt} &= k_3\left([R(*,*,*)]-[R(*,*,1)]\right)\left([E^3(*)]-[R(*,*,1)]\right)-k_{-3}[R(*,*,1)]\\
\frac{d[R(1,1,*)]}{dt} &= k_1\left([R(*,1,*)]-[R(1,1,*)]\right)\left([E^1(*)]-[R(1,*,*)]\right)-k_{-1}[R(1,1,*)]\\
&\quad +k_2\left([R(1,*,*)]-[R(1,1,*)]\right)\left([E^2(*)]-[R(*,1,*)]\right)-k_{-2}[R(1,1,*)]\\
\frac{d[R(1,*,1)]}{dt} &= k_1\left([R(*,*,1)]-[R(1,*,1)]\right)\left([E^1(*)]-[R(1,*,*)]\right)-k_{-1}[R(1,*,1)]\\
&\quad +k_3\left([R(1,*,*)]-[R(1,*,1)]\right)\left([E^3(*)]-[R(*,*,1)]\right)-k_{-3}[R(1,*,1)]\\
\frac{d[R(*,1,1)]}{dt} &= k_2\left([R(*,*,1)]-[R(*,1,1)]\right)\left([E^2(*)]-[R(*,1,*)]\right)-k_{-2}[R(*,1,1)]\\
&\quad +k_3\left([R(*,1,*)]-[R(*,1,1)]\right)\left([E^3(*)]-[R(*,*,1)]\right)-k_{-3}[R(*,1,1)]\\
\frac{d[R(1,1,1)]}{dt} &= k_1\left([R(*,1,1)]-[R(1,1,1)]\right)\left([E^1(*)]-[R(1,*,*)]\right)-k_{-1}[R(1,1,1)]\\
&\quad +k_2\left([R(1,*,1)]-[R(1,1,1)]\right)\left([E^2(*)]-[R(*,1,*)]\right)-k_{-2}[R(1,1,1)]\\
&\quad +k_3\left([R(1,1,*)]-[R(1,1,1)]\right)\left([E^3(*)]-[R(*,*,1)]\right)-k_{-3}[R(1,1,1)].
\end{aligned}
$$

Table 4.3: Transformed model equations for a scaffold protein with independent binding domains. The levels of occupancy which correspond to the output variables do not depend on the remaining four states. Consequently, the system comprises three observable states. The states $[R(1,*,*)]$, $[R(1,1,*)]$, $[R(1,*,1)]$ and $[R(1,1,1)]$ are controllable, since the input signal directly influences them.

Non-Interacting Binding Processes. Non-interacting binding processes imply that the binding reactions for E^1, for E^2 and for E^3 are parameterized by the same kinetic parameters respectively. The transformed ODEs provide a very special and hierarchical structure (compare Table 4.3). The differential equations describing the macro-states of the 1st transformation tier are completely decoupled from the other ODEs. The states of the other two remaining tiers only depend on themselves and on states of the preceding tier. As a result of its hierarchical structure the Jacobian matrix of the ODE system has a lower triangular form. From this structure one can simply deduce which states of the system are controllable and/or observable.

The state $[R(1,*,*)]$ is the only one which is both controllable and observable. It directly depends on the input signal $[E^1(*)]$ and corresponds to one of the output variables. The other macro-states depend neither on the input variable $[E^1(*)]$ nor on any controllable state such as the example $[R(1,*,*)]$, which indicates that they are only observable but not controllable. The states $[R(1,1,*)]$, $[R(1,*,1)]$ and $[R(1,1,1)]$ directly depend on the input but do not influence any of the output variables, which means that they are controllable but not observable. The remaining state $[R(*,1,1)]$ is neither controllable nor observable. Thus, the given model representation is a Kalman decomposition of the considered system, as defined above. A minimal realization for the defined input and outputs only comprises one ODE for $[R(1,*,*)]$

$R(0,*,*)$	$+$	E^1	$\leftrightharpoons$	$R(1,*,*)$	k_1, k_{-1}
$R(0,0,*)$	$+$	E^2	$\leftrightharpoons$	$R(0,1,*)$	k_2, k_{-2}
$R(1,0,*)$	$+$	E^2	$\leftrightharpoons$	$R(1,1,*)$	k_3, k_{-3}
$R(*,0,0)$	$+$	E^3	$\leftrightharpoons$	$R(*,0,1)$	k_4, k_{-4}
$R(*,1,0)$	$+$	E^3	$\leftrightharpoons$	$R(*,1,1)$	k_5, k_{-5}

Table 4.4: Reaction rules describing the example depicted in Figure 4.2 B. The kinetic parameters are also specified to the right of the rules.

and two algebraic equations that determine the constant steady state concentrations for the uncontrollable output variables $[R(*,1,*)]$ and $[R(*,*,1)]$.

One Binding Process Influences the others Unidirectionally. Let us assume that the receptor R has one extracellular binding domain that recruits a ligand. Ligand binding changes association and dissociation constants of the other two intracellular binding processes as depicted in Figure 4.2 B. Since the interactions are assumed to be unidirectional, the association of intracellular effector proteins does not affect ligand binding. This interaction pattern can be realized by parameterizing reactions as indicated by the reaction rules in Table 4.4.

In this case the structure of the transformed model equations is different (equations see Table 4.5). The model can be dissected into four modules. The first one only comprises the equation for $[R(1,*,*)]$ which is completely decoupled from all other equations. Additionally, there exist two equally structured modules comprising the states $[R(*,1,*)]$, $[R(1,1,*)]$ and $[R(*,*,1)]$, $[R(1,*,1)]$ respectively. These two modules, which describe the levels of occupancy of the intracellular domains, do not interact with each other. However, both modules are unidirectionally coupled with the state $[R(1,*,*)]$ of the first module. This resembles the interaction pattern of the considered system. Binding of the extracellular ligand has an unidirectional influence on the other two domains, which do not interact with each other. The remaining two ODEs for $[R(*,1,1)]$ and $[R(1,1,1)]$ form the last module, and do not influence any of the other three mentioned modules. An accurate description of the defined output variables only requires the first three modules. Hence, it follows that the two states $[R(*,1,1)]$ and $[R(1,1,1)]$ are unobservable and therefore have been omitted in Table 4.5. In this example the model does not comprise uncontrollable states. Interestingly, the described state space transformation not only modularizes the model equations but also the kinetic parameters. The module describing the level of occupancy of the extracellular domain only comprises the parameters k_1 and k_{-1}. The two equally structured modules, which describe the two intracellular domains, additionally include either the parameters k_2, k_{-2}, k_3 and k_{-3} or k_4, k_{-4}, k_5 and k_{-5}. This special model structure also reveals valuable information for parameter identification. Thus, one easily sees that measuring $[R(1,*,*)]$ only facilitates the identification of the kinetic parameters k_1 and k_{-1}. Additionally, one does not have to consider a seven ODE model to identify these parameters from measurement data but instead only the single ODE for $[R(1,*,*)]$.

$$
\begin{aligned}
\frac{d[R(1,*,*)]}{dt} &= k_1\left([R(*,*,*)]-[R(1,*,*)]\right)E^1 - k_{-1}[R(1,*,*)] \\
\frac{d[R(*,1,*)]}{dt} &= k_2\left([R(*,*,*)]-[R(1,*,*)]-[R(*,1,*)]+[R(1,1,*)]\right)[E^2] - k_{-2}\left([R(*,1,*)]-[R(1,1,*)]\right) \\
&\quad + k_3\left([R(1,*,*)]-[R(1,1,*)]\right)E^2 - k_{-3}[R(1,1,*)] \\
\frac{d[R(*,*,1)]}{dt} &= k_4\left([R(*,*,*)]-[R(1,*,*)]-[R(*,*,1)]+[R(1,*,1)]\right)[E^3] - k_{-4}\left([R(*,*,1)]-[R(1,*,1)]\right) \\
&\quad + k_5\left([R(1,*,*)]-[R(1,*,1)]\right)E^3 - k_{-5}[R(1,*,1)] \\
\\
\frac{d[R(1,1,*)]}{dt} &= k_1\left([R(*,1,*)]-[R(1,1,*)]\right)[E^1] - k_{-1}[R(1,1,*)] + k_3\left([R(1,*,*)]-[R(1,1,*)]\right)[E^2] - k_{-3}[R(1,1,*)] \\
\frac{d[R(1,*,1)]}{dt} &= k_1\left([R(*,*,1)]-[R(1,*,1)]\right)[E^1] - k_{-1}[R(1,*,1)] + k_5\left([R(1,*,*)]-[R(1,*,1)]\right)[E^3] - k_{-5}[R(1,*,1)]
\end{aligned}
$$

Table 4.5: Transformed model equations for a scaffold protein with one controlling binding domain. For the sake of simplicity, expressions such as $[E^1(*)] - [R(1,*,*)]$ are replaced by the equivalent term $[E^1]$. Furthermore, the ODEs for $[R(*,1,1)]$ and $[R(1,1,1)]$ have been neglected since they are unobservable and rather complex.

4.1.3.3 Example Taken from T-Cell Receptor Signaling.

The following example is taken from Conzelmann *et al.* [32], and shows that the discussed elimination of unobservable states facilitates significant model reductions in real signaling networks [32]. LAT (Linker for Activation of T cells) is a scaffold molecule that plays a pivotal role in T cell signaling [87]. LAT has nine conserved cytoplasmatic tyrosines, of which the four membrane-distal tyrosines (at residues 132/171/191/226 in human LAT) are essential and are phosphorylated upon ligand binding to the T cell receptor [87]. Different signaling molecules, such as PLCγ1, Grb2 and Gads can bind to the different residues. Grb2 recruits Sos, which in turn activates Ras, and subsequently the Raf/MEK/ERK MAP Kinase cascade. On the other hand, binding of PLCγ1 and Gads (bound to the adaptor SLP76 that additionally recruits Itk), allows the activation of PLCγ1, leading to cleavage of phosphatidyl-inositol-4,5 bisphosphate (PIP2) and the generation of dyacilglycerol (DAG) and inositol trisphosphate IP3. DAG activates RasGTP, which in turn activates Ras, as well as PKC, while IP3 regulates Calcium signaling [132].
PLCγ1 binds at the Y132 tyrosine, Grb2 at Y171, Y191 and Y226, and Gads at Y171 and Y191 (see Figure 4.3) [87]. Even by ignoring preceding domain phosphorylation the number of different protein complexes occurring in this simple example is already $2 \cdot 3 \cdot 3 \cdot 2 = 36$, and the number of reactions that have to be considered is 86. We will show how one can precisely describe the levels of occupancy without considering all 36 complexes. Recent experimental data from LAT mutation studies indicate that the binding domains can influence one another [149]. Binding of Grb2 to Y226 appears to help the binding of Gads to LAT [149]. This effect can be readily incorporated into the model by changing the kinetic parameters for Gads binding if the binding site Y226 is occupied by Grb2. Transforming the model equations shows that

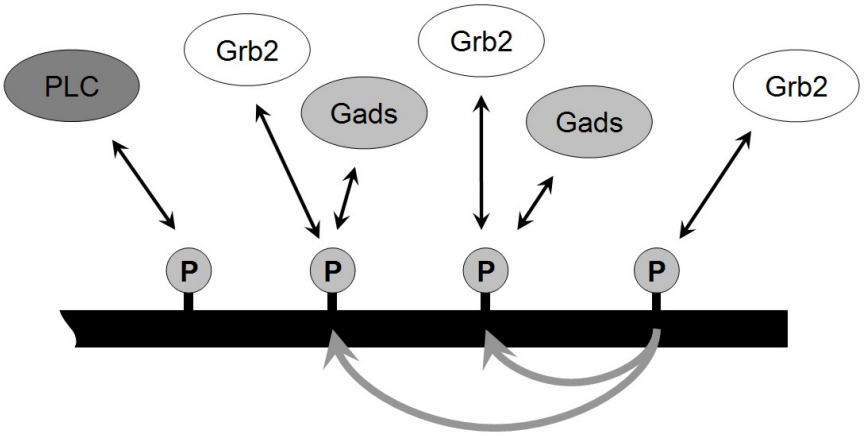

Figure 4.3: The four distal tyrosine rests on LAT and the binding possibilities, according to Lindquist *et al.* [87].

only ten ODEs are required to describe the system dynamics exactly. The transformed model equations can be found in Conzelmann *et al.* [32]. Hence, our method is capable of reducing signal transduction models including scaffold proteins. The modular structure of the derived model equations also strongly facilitates model analysis as well as parameter estimation.

4.1.3.4 Generality of the Method

In the previously discussed examples it was shown that the proposed linear transformation facilitates the separation, and subsequently, the elimination of unobservable and/or uncontrollable model states. However, the question remains as to whether the resulting reduced models are minimal realizations. A general proof is difficult if not infeasible. Yet control theory provides numerous techniques which allow a system to be checked for observability or controllability. One possibility is checking for local observability or controllability by analyzing the linearized model equations

$$\dot{\vec{x}} = A\vec{x} + B\vec{u} \qquad \text{with} \qquad A = \left(\frac{\partial \vec{f}(\vec{x},\vec{u})}{\partial \vec{x}}\right)_{\vec{x}_o,\vec{u}_o}, B = \left(\frac{\partial \vec{f}(\vec{x},\vec{u})}{\partial \vec{u}}\right)_{\vec{x}_o,\vec{u}_o}, \tag{4.9}$$

$$\vec{y} = C\vec{x} \qquad \text{and} \qquad \vec{x} \in \mathbb{R}^n, \vec{u} \in \mathbb{R}^m. \tag{4.10}$$

The system is locally controllable at the operating point $(\vec{x}_o, \vec{u}_o)$ if the rank of the matrix

$$P = \left(B, AB, A^2B, ..., A^{n-1}B\right) \tag{4.11}$$

is n. However, using this analysis method one has to be aware of the fact that controllable nonlinear systems might lose controllability at individual operating points. Since the given criterion only facilitates local conclusions, the results of this analysis have to be interpreted very carefully. A matrix rank of n proves that the considered system does not include any further

globally uncontrollable states. At least all states are controllable at the chosen operating point and therefore affect the system's input/output behavior. If a reduced model still comprises uncontrollable states, the rank of this matrix will be smaller than n for all considered operating points. However, if the matrix rank is lower than n this may imply that the system is not a minimal realization and still comprises uncontrollable states, but it is also possible that the system has been linearized at an unpropitiously chosen operating point. Hence, it might be necessary to repeat the test at several operating points. A matrix rank smaller than n for numerous operating points suggests the further existence of uncontrollable states in the nonlinear system, but it is no proof.

Accordingly, the system can be checked for observability by considering the rank of

$$Q = \left(C, CA, CA^2, ..., CA^{n-1}\right)^T. \tag{4.12}$$

Again, this criterion only provides local information about the operating point being considered. More global conclusions require the application of nonlinear methods like those proposed by Isidori [65].

All examples discussed in this thesis have been checked for further uncontrollable or unobservable states. In all cases the reduced models proved to be minimal realizations for the chosen input and output variables. However, an interesting border case exists, which will be discussed here.

We reconsider the previously analyzed receptor with three binding domains where one extracellular domain controls the two intracellular domains in an unidirectional manner. We presume that the two intracellular domains are identical. Both recruit the same effector protein E and both have exactly the same kinetic properties. Let us further assume that the system output is the total number of E proteins bound to the receptor, which corresponds to the sum of both occupancy levels. In this case, our proposed transformation again facilitates the elimination of the two unobservable ODEs $[R(*,1,1)]$ and $[R(1,1,1)]$ such as in the Example depicted in Table 4.5. However, in this case the remaining ODEs can only be dissected into two modules. Although the two identical domains do not interact with each other their ODEs are coupled due to the fact that both recruit the same effector. The module that describes the two intracellular domains resembles the symmetry of the considered system. Its equations form two identical but coupled submodules

$$\begin{aligned} \dot{\vec{x}}_1 &= \vec{f}(\vec{x}_1, \vec{x}_2, \vec{u}) \qquad \vec{x}_1(0) = \vec{x}_{0,1}, \\ \dot{\vec{x}}_2 &= \vec{f}(\vec{x}_2, \vec{x}_1, \vec{u}) \qquad \vec{x}_2(0) = \vec{x}_{0,2}, \\ y &= C\left(\vec{x}_1 + \vec{x}_2\right), \end{aligned} \tag{4.13}$$

each describing one of the two identical binding domains. Note, however, that the initial conditions do not necessarily have to coincide. Under these assumptions the system still comprises unobservable states if the vector field $\vec{f}$ fulfills the superposition principle

$$\vec{f}(\vec{x}_1, \vec{x}_2, \vec{u}) + \vec{f}(\vec{x}_2, \vec{x}_1, \vec{u}) = \vec{f}(\vec{x}_1 + \vec{x}_2, \vec{x}_1 + \vec{x}_2, \vec{u}) = \vec{g}(\vec{x}_1 + \vec{x}_2, \vec{u}). \tag{4.14}$$

In this case the system output y and its derivatives only depend on the sum of $\vec{x}_1$ and $\vec{x}_2$

$$\dot{y} = C\left(\vec{f}(\vec{x}_1, \vec{u}) + \vec{f}(\vec{x}_2, \vec{u})\right) = C\vec{g}(\vec{x}_1 + \vec{x}_2, \vec{u}). \tag{4.15}$$

Thus, a minimal realization of the system would be

$$\begin{aligned} &\dot{\vec{\xi}} = \vec{g}(\vec{\xi}, \vec{u}) \qquad \vec{\xi}(0) = \vec{\xi}_0 = \vec{x}_{10} + \vec{x}_{20} \\ &y = C\vec{\xi}. \end{aligned} \tag{4.16}$$

The superposition principle is fulfilled if the operator $\vec{f}$ is linear in $\vec{x}$. In the more general case if $\vec{f}$ does not fulfill the superposition principle our transformation provides a minimal realization of the system. Note, however, that even for a general operator $\vec{f}$ the number of equations can be reduced if the initial conditions of both submodules are equivalent ($\vec{x}_{10} = \vec{x}_{20}$). Under this condition both submodules are completely identical ($\vec{x}_1 = \vec{x}_2 = \vec{\xi}$) and therefore one of them can be eliminated and the reduced module can be written as

$$\begin{aligned} &\dot{\vec{\xi}} = \vec{f}(\vec{\xi}, \vec{\xi}, \vec{u}) = \vec{g}(\vec{\xi}, \vec{u}) \qquad \vec{\xi}(0) = \vec{\xi}_0 = \vec{x}_{10} = \vec{x}_{20} \\ &y = 2C\vec{\xi}. \end{aligned} \tag{4.17}$$

This reduction is not due to the elimination of unobservable states but instead results from the restricted choice of initial conditions. From these considerations it can be seen that, apart from the case of two identical linear subsystems, no example has been found for which the proposed transformation does not provide a minimal realization. We have also found that under special conditions ODE models of combinatorial reaction networks might be exactly reducible although they do not comprise unobservable or uncontrollable states.

4.1.4 Scaffolds with Multiprotein Ligands

Many scaffold proteins or receptors do not only bind single protein ligands, but often recruit other scaffolds, which in turn can be phosphorylated and/or bind further ligands. A good example is the scaffold IRS which binds to the insulin receptor and can recruit numerous other ligands such as Grb2 or PI3K. All scaffolds which can be recruited by a receptor or another scaffold will be called multiprotein ligands. Note that in general these multiprotein ligands can either bind single protein ligands or other multiprotein ligands. This justifies the consideration of arbitrarily large signaling complexes. Remember, however, that we do not consider reaction systems in which the multiprotein complex can get infinitely large (compare Chapter 2). Heterodimerization as it occurs in the previously discussed ErbB signaling network also fits into this category. However, homodimerization will be excluded from the following considerations. Due to the symmetry of homodimeric complexes homodimerization has to be handled differently and will be discussed separately. The aforementioned problem of scaffolds with single protein ligands can be considered as a special case of what we examine here. The main difference between these multiprotein and the previously discussed single protein ligand

systems is the formation of long protein chains. For this reason we will initially focus on this phenomenon and its mathematical treatment. Afterwards, we will explain how branched multiprotein ligand systems can be handled by considering a small part of the insulin signaling system.

Let us consider a receptor protein R which provides n binding domains. We take the assumption that each domain i can bind an effector protein E_1^i which in turn can recruit another effector protein E_2^i until finally E_{m-1}^i binds E_m^i. In order to reduce the number of indices, we also presume that each chain of effector proteins consists of m proteins. Finally, we only consider binding processes and neglect all domain phosphorylations. Thus, each receptor domain can be either unoccupied or occupied by a multiprotein ligand consisting of one to m proteins, which results in $(m+1)^n$ distinct receptor complexes. Furthermore, the m effectors that form the different multiprotein ligands for one single receptor domain can build $\frac{m(m+1)}{2}$ distinct complexes. According to these examinations the total number of feasible multiprotein species is $(1+m)^n + \frac{m(m+1)}{2}n$. In analogy to the considerations made before, we search an equal number of macroscopic and mesoscopic states which facilitate a Kalman decomposition of the reaction network.

4.1.4.1 General Transformation Pattern

The concept of using levels of occupancy as new variables is problematic for the considered multiprotein ligand systems. The term *level of occupancy* implies a certain hierarchy among the signaling proteins, which is certainly given in the single protein ligand scenario where one scaffold can bind numerous other effector proteins. It is obvious that in such reaction networks the scaffold takes up a prominent position suggesting the need to consider its occupancy levels. In a system that involves numerous scaffolds, a clear hierarchy is missing, and the question arises as to which occupancy levels should be considered. In most cases, an intuitive hierarchy will be automatically chosen. For example, in the case of insulin signaling, it is quite natural to choose the insulin receptor as the central protein of the cascade. Due to representational reasons, we also assume a hierarchy in our examples with R being the central protein. However, if one considers heterodimerization of two ErbB receptors, it is not apparent which receptor takes up a more prominent position. Another problem is that the definition of occupancy levels for multiprotein ligand systems is not as unique as for single protein ligand systems. The quantity $[R(E_1^1, *, ..., *)]$, which can be interpreted as an occupancy level, describes all receptor species whose first domain is occupied by the single protein E_1^1 excluding all species in which E_1^1 has bound any further effectors or scaffolds. $[R(E_1^1(*), *, ..., *)]$ on the other hand represents an alternative type of occupancy level which does not exclude the previously mentioned multiprotein complexes.

A more general transformation pattern is required which avoids the implication of molecular hierarchy, which at the same time, is also consistent with the transformation pattern already discussed for the single protein ligand scenario. These requirements are met by the introduction

of so-called *occurrence levels*. Occurrence levels always refer to a certain molecular subcomplex and correspond to the sums of all multiprotein species that comprise this subcomplex. Thus, for each individual molecular species one can define a respective occurrence level. If these occurrence levels are used to replace the original model states, a linear and invertible transformation is defined. The proposed transformation pattern does not imply any hierarchy among the involved signaling proteins, however, it preserves the hierarchical structure of the transformation matrix. The previously defined 0^{th} tier of the transformation matrix includes the overall concentrations of all involved signaling proteins. It corresponds to the occurrence levels of individual proteins which are a very special type of subcomplex. The 1^{st} tier includes the occurrence levels of all possible two protein subcomplexes. In the case of scaffolds with single protein ligands, this directly corresponds to the previously introduced levels of occupancy. According to this pattern the following tiers of the transformation matrix respectively comprise all subcomplexes consisting of three, four and more proteins. If phosphorylations occur in the considered reaction network the phosphate groups have to be treated as additional molecules. For example, a scaffold with one phosphorylated domain is considered to be a two-molecule complex. The related occurrence level encompasses all molecular species that contain this phosphorylated scaffold.
For the simplified case introduced above the new transformed states can be specified as discussed below. The 0^{th} tier comprises the states $[R(*,...,*)]$ and $[E_j^i(*)]$, while the first one includes the states $[R(*,...,*,E_1^i(*),*,...,*)]$ as well as $[E_j^i(E_{j+1}^i(*))]$. The occurrence levels that refer to all three molecule complexes are $[R(*,...,*,E_1^i(*),*,...,*,E_1^k(*),*,...,*)]$, $[R(*,...,*,E_2^i(*),*,...,*)]$ and $[E_j^i(E_{j+2}^i(*))]$. The subsequent tiers are defined according to this pattern, with the last tier comprising of only the single micro-state $[R(E_m^1,...,E_m^n)]$. The fact that each individual molecular species can be uniquely linked to an associated occurrence level suggests that the transformation is invertible. This can also be proven through the use of the mathematical induction as described for single protein ligands above.

4.1.4.2 Examples

In this section, we analyze three different systems of receptors with multiprotein ligands (see Figure 4.4). For the sake of simplicity, the first two examples solely consider chains of signaling proteins. The first system consists of six signaling proteins which bind consecutively to each other. In order to provide a simple representation of the occurring complexes and the corresponding occurrence levels, the protein R is considered as the central receptor which binds the single protein ligand L and a multiprotein ligand consisting of the effectors E_1 to E_4. None of these proteins are assumed to be phosphorylated. The second example only comprises four signaling proteins, of which three are phosphorylated. The third system we analyze, is a simplified model of insulin signaling which includes insulin, the insulin receptor, IRS and Shc.

Example 1: Six Signaling Proteins. We consider a receptor R that provides an extracellular binding domain, which is able to recruit the ligand L. A second intracellular domain can

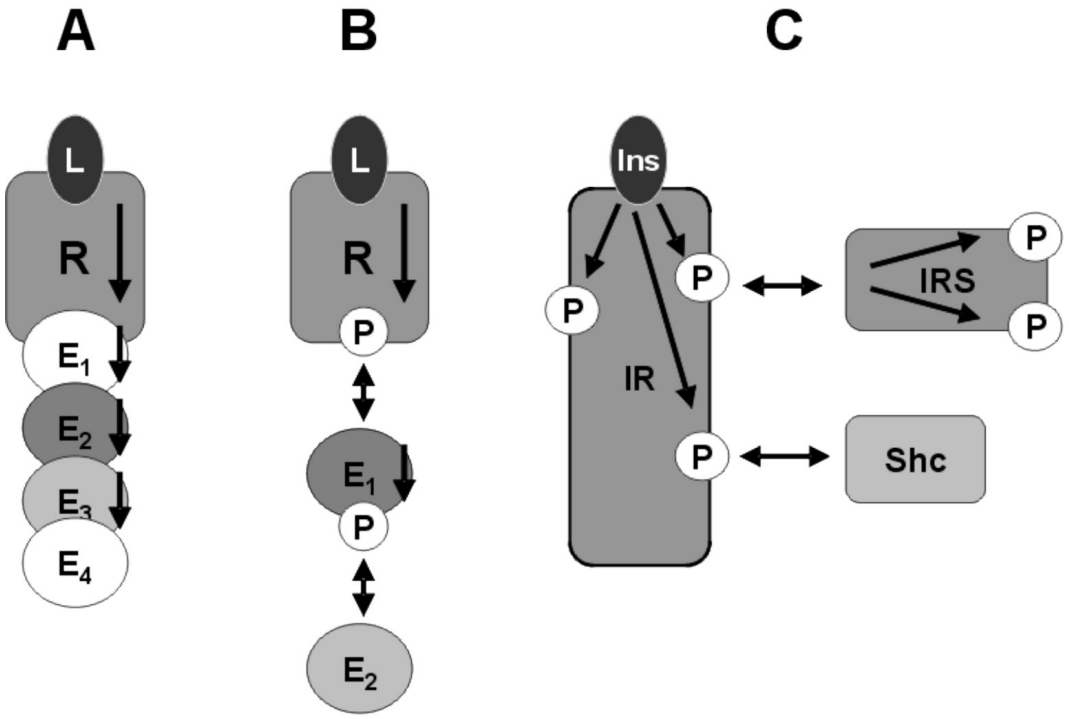

Figure 4.4: Examples for multiprotein ligand systems. Figure A depicts a chain of signaling proteins without any post-translational modifications such as phosphorylations. All bindings are assumed to interact unidirectionally with each other (black unidirectional arrows). Figure B shows a similar system including domain phosphorylation. Thereby, it is assumed that phosphorylation and subsequent effector binding interact via an all-or-none reaction. Since all-or-none interactions are always bidirectional they are depicted by bidirectional arrows. The last example is a small part of the insulin signaling pathway.

$R(0,*)$	$+$	L	$\leftrightharpoons$	$R(L,*)$	k_1, k_{-1}
$R(0,0)$	$+$	$E_1(*)$	$\leftrightharpoons$	$R(0,E_1(*))$	k_2, k_{-2}
$R(L,0)$	$+$	$E_1(*)$	$\leftrightharpoons$	$R(L,E_1(*))$	k_3, k_{-3}
$E_1(0,0)$	$+$	$E_2(*)$	$\leftrightharpoons$	$E_1(E_2(*))$	k_4, k_{-4}
$R(*,E_1)$	$+$	$E_2(*)$	$\leftrightharpoons$	$R(*,E_1(E_2(*)))$	k_5, k_{-5}
$E_2(0,0)$	$+$	$E_3(*)$	$\leftrightharpoons$	$E_2(E_3(*))$	k_6, k_{-6}
$E_1(*,E_2)$	$+$	$E_3(*)$	$\leftrightharpoons$	$E_1(*,E_3(*))$	k_7, k_{-7}
$E_3(0,0)$	$+$	E_4	$\leftrightharpoons$	$E_3(E_4)$	k_8, k_{-8}
$E_2(*,E_3)$	$+$	E_4	$\leftrightharpoons$	$E_2(*,E_4)$	k_9, k_{-9}

Table 4.6: Reaction rules describing the Example depicted in Figure 4.4 A. The kinetic parameters are specified to the right of the rules.

bind the effector protein E_1, which in turn recruits E_2. This chain of consecutively binding effector proteins is continued to E_4. We assume that E_1 binding is unidirectionally influenced by the recruitment of L. Equivalently, E_i binding is unidirectionally influenced by the binding of E_{i-1} to its predecessor. The resulting reaction rules for this system are given in Table 4.6. We take the assumption that $[L]$ is the input of the system. Determining output variables in this example is more difficult. For systems with single protein ligands, the levels of occupancy are chosen. These correspond to all states included in the 1^{st} transformation tier. In accordance to this choice, one could again take all states of the 1^{st} tier as output variables. For multi-protein ligands, these states correspond to the occurrence levels of all two-protein complexes. However, for many real networks, other states might also be of interest. Let us consider the insulin receptor which can recruit a multiprotein ligand consisting of Shc, Grb2 and SOS. In this case the recruitment of SOS to a membrane bound signaling complex initiates the MAPK cascade. Thus, it is important to know how many SOS proteins have bound to the receptor complex and not how many Grb2-SOS complexes occur in the network. For this reason we will consider two types of output variables.

Below, the output vector $\vec{y}_1$ represents the five occurrence levels of the 1^{st} transformation tier. The output vector $\vec{y}_2$ on the other hand includes the variables $[R(L,*)]$, $[R(*,E_1(*))]$, $[R(*,E_2(*))]$, $[R(*,E_3(*))]$ and $[R(*,E_4)]$. In order to show the large influence of process interactions on exact model reduction, we additionally consider the case that $k_8 = k_9$ and $k_{-8} = k_{-9}$. This assumption implies that E_4 binding is completely independent of all other binding processes. Note that due to the thermodynamic constraints of reaction networks discussed above the aforementioned scenarios are, in reality, not very likely to occur. However, they help to show the advantages the proposed transformation pattern provides. Since the transformation pattern is independent of both the kinetic system properties and the chosen output variables, all mentioned cases can be handled using the same transformation. It consists of six tiers that are shown in Table 4.7. Due to the absence of protein production and degradation, the six states of the 0^{th} tier remain constant. Thus, these six ODEs can be eliminated in the considered example. First, we will discuss the case that E_4 binding is unidirectionally influenced by E_3 binding. In this case, our transformation does not allow any exact reduction of the model, for either of the output variables $\vec{y}_1$ or $\vec{y}_2$. From the linearized model equations one can additionally deduce that all states are observable and controllable. Interestingly, the transformed model equations can be dissected into five modules, which are all unidirectionally coupled. This model structure directly resembles the interaction pattern between the five considered binding processes. In fact each of the modules describes one of these five processes. However, the modules differ in size and structure. The first module, which describes the recruitment of L to the receptor, only consists of one differential equation. The second, third, fourth and fifth modules comprise of two, three, four and five states respectively. Another nice property of the transformed system is the concurrently achieved modularization of the kinetic parameters. The L binding module only contains the parameters k_1 and k_{-1}. In addition to k_1 and k_{-1}, the second module comprises all parameters that describe binding of E_1 to R but no others. This special hierarchical structure can also be found by considering the other three modules, and is very advantageous in parameter

$$
\begin{aligned}
[R(*,*)] =& [R(0,0)] + [R(0,E_1)] + [R(0,E_2)] + [R(0,E_3)] + [R(0,E_4)] + [R(L,0)] + [R(L,E_1)] + [R(L,E_2)] \\
&+ [R(L,E_3)] + [R(L,E_4)] \\
[E_1(*)] =& [E_1(0)] + [E_1(E_2)] + [E_1(E_3)] + [E_1(E_4)] + [R(0,E_1)] + [R(0,E_2)] + [R(0,E_3)] + [R(0,E_4)] \\
&+ [R(L,E_1)] + [R(L,E_2)] + [R(L,E_3)] + [R(L,E_4)] \\
[E_2(*)] =& [E_1(E_2)] + [E_1(E_3)] + [E_1(E_4)] + [E_2(0)] + [E_2(E_3)] + [E_2(E_4)] + [R(0,E_2)] + [R(0,E_3)] \\
&+ [R(0,E_4)] + [R(L,E_2)] + [R(L,E_3)] + [R(L,E_4)] \\
[E_3(*)] =& [E_1(E_3)] + [E_1(E_4)] + [E_2(E_3)] + [E_2(E_4)] + [E_3(0)] + [E_3(E_4)] + [R(0,E_3)] + [R(0,E_4)] \\
&+ [R(L,E_3)] + [R(L,E_4)] \\
[E_4(*)] =& [E_1(E_4)] + [E_2(E_4)] + [E_3(E_4)] + [E_4(0)] + [R(0,E_4)] + [R(L,E_4)]
\end{aligned}
$$

$$
\begin{aligned}
[R(L,*)] =& [R(L,0)] + [R(L,E_1)] + [R(L,E_2)] + [R(L,E_3)] + [R(L,E_4)] \\
[R(*,E_1(*))] =& [R(0,E_1)] + [R(0,E_2)] + [R(0,E_3)] + [R(0,E_4)] + [R(L,E_1)] + [R(L,E_2)] + [R(L,E_3)] + [R(L,E_4)] \\
[E_1(E_2(*)] =& [E_1(E_2)] + [E_1(E_3)] + [E_1(E_4)] + [R(0,E_2)] + [R(0,E_3)] + [R(0,E_4)] + [R(L,E_2)] \\
&+ [R(L,E_3)] + [R(L,E_4)] \\
[E_2(E_3(*))] =& [E_1(E_3)] + [E_1(E_4)] + [E_2(E_3)] + [E_2(E_4)] + [R(0,E_3)] + [R(0,E_4)] + [R(L,E_3)] + [R(L,E_4)] \\
[E_3(E_4(*))] =& [E_1(E_4)] + [E_2(E_4)] + [E_3(E_4)] + [R(0,E_4)] + [R(L,E_4)]
\end{aligned}
$$

$$
\begin{aligned}
[R(L,E_1(*))] =& [R(L,E_1)] + [R(L,E_2)] + [R(L,E_3)] + [R(L,E_4)] \\
[R(*,E_2(*))] =& [R(0,E_2)] + [R(0,E_3)] + [R(0,E_4)] + [R(L,E_2)] + [R(L,E_3)] + [R(L,E_4)] \\
[E_1(E_3(*)] =& [E_1(E_3)] + [E_1(E_4)] + [R(0,E_3)] + [R(0,E_4)] + [R(L,E_3)] + [R(L,E_4)] \\
[E_2(E_4(*))] =& [E_1(E_4)] + [E_2(E_4)] + [R(0,E_4)] + [R(L,E_4)]
\end{aligned}
$$

$$
\begin{aligned}
[R(L,E_2(*))] =& [R(L,E_2)] + [R(L,E_3)] + [R(L,E_4)] \\
[R(*,E_3(*))] =& [R(0,E_3)] + [R(0,E_4)] + [R(L,E_3)] + [R(L,E_4)] \\
[E_1(E_4(*)] =& [E_1(E_4)] + [R(0,E_4)] + [R(L,E_4)]
\end{aligned}
$$

$$
\begin{aligned}
[R(L,E_3(*))] =& [R(L,E_3)] + [R(L,E_4)] \\
[R(*,E_4(*))] =& [R(0,E_4)] + [R(L,E_4)]
\end{aligned}
$$

$$
[R(L,E_4(*))] = [R(L,E_4)]
$$

Table 4.7: Hierarchical transformation that realizes a Kalman decomposition for the example system depicted in Figure 4.4 A. The new states correspond to the occurrence levels of different subcomplexes. The transformation can be structured in different tiers. The previously discussed case of single protein ligand systems can be considered as border cases of the underlying transformation pattern. The transformation is independent of the chosen output variables as well as the kinetic properties of the reaction network. However, a different choice of output variables may lead to a higher or lower number of observable states. The same holds true for varying kinetic parameters. For given input and output signals, the kinetic properties determine whether states are observable and/or controllable. Furthermore, the kinetic parameters also define whether the model equations can be modularized or not. In the considered example, the system does not comprise unobservable states and can be divided into five modules if $k_8 \neq k_9$ and $k_{-8} \neq k_{-9}$. If $k_8 = k_9$ and $k_{-8} = k_{-9}$, the system can be reduced to ten ODEs.

$R(0,*)$	$+$	L	$\leftrightharpoons$	$R(L,*)$	k_1, k_{-1}
$R(0,0)$			$\leftrightharpoons$	$R(0,P)$	k_2, k_{-2}
$R(L,0)$			$\leftrightharpoons$	$R(L,P)$	k_3, k_{-3}
$R(*,P)$	$+$	$E_1(*)$	$\leftrightharpoons$	$R(*,E_1(*))$	k_4, k_{-4}
$E_1(0,0)$			$\leftrightharpoons$	$E_1(0,P)$	k_5, k_{-5}
$R(*,E_1)$			$\leftrightharpoons$	$R(*,E_1(P))$	k_6, k_{-6}
$E_1(*,P)$	$+$	E_2	$\leftrightharpoons$	$E_1(*,E_2)$	k_7, k_{-7}

Table 4.8: Reaction rules describing the Example depicted in Figure 4.4 B. The kinetic parameters are specified to the right of the rules.

estimation. Measurements of the transient behavior of either states $\vec{y}_1$ or $\vec{y}_2$ facilitate a stepwise identification of the kinetic model parameters, module by module. A stepwise procedure is computationally much less costly than the concurrent identification of all parameters.

Taking the assumption that the association of E_3 and E_4 is independent of all other occurring binding processes, the structure of the fifth module changes. The state $E_3(E_4(*))$ is not controllable any more, since the respective binding process can neither be directly nor indirectly influenced by changes in the L concentration. If $\vec{y}_1$ is the output vector of the system, the output variable $E_3(E_4(*))$ is determined by the steady state equation of the respective ODE. The remaining four states of the fifth module are not observable and can simply be omitted. Thus, the model can be exactly reduced to ten ODEs. The situation changes if one considers the output vector $\vec{y}_2$. The choice of different output variables does not affect the controllability of a system. Thus, the state $E_3(E_4(*))$ is still uncontrollable and the respective ODE can be replaced by its steady state equation. However, all model states are observable in this case and as a result no further equation can be eliminated. An exactly reduced model would, in this case, comprise fourteen ODEs.

Example 2: Domain Phosphorylation. As a second example we consider a receptor R which again provides an extracellular binding domain, which can recruit the ligand L. In contrast to the previously considered example, the receptor's intracellular domain has to be phosphorylated in order to bind the effector protein E_1. Phosphorylation is considered to be a necessary precondition for E_1 binding, while bound E_1 preserves the receptor domain from dephosphorylation due to steric reasons. E_1 also has to be phosphorylated in order to recruit E_2, which prevents dephosphorylation of E_1. In this case, we do not consider binding of further effector proteins. One presumption we make is that receptor phosphorylation is unidirectionally influenced by recruitment of L. Equivalently E_1 phosphorylation is unidirectionally influenced by E_1 binding to the receptor R. The interactions between receptor phosphorylation and E_1 binding as well as between E_1 phosphorylation and E_2 recruitment are all-or-none interactions. The reaction rules for this system are given in Table 4.8.

Again the concentration $[L]$ is considered as the input of the system. According to our con-

$$
\begin{aligned}
[R(*,*)] =& [R(0,0)] + [R(0,P)] + [R(0,E_1)] + [R(0,E_1(P))] + [R(0,E_2)] + [R(L,0)] + [R(L,P)] \\
&+ [R(L,E_1)] + [R(L,E_1(P))] + [R(L,E_2)] \\
[E_1(*)] =& [E_1(0)] + [E_1(P)] + [E_1(E_2)] + [R(0,E_1)] + [R(0,E_1(P))] + [R(0,E_2)] + [R(L,E_1)] \\
&+ [R(L,E_1(P))] + [R(L,E_2)] \\
[E_2(*)] =& [E_1(E_2)] + [E_2(0)] + [R(0,E_2)] + [R(L,E_2)]
\end{aligned}
$$

$$
\begin{aligned}
[R(L,*)] =& [R(L,0)] + [R(L,P)] + [R(L,E_1)] + [R(L,E_1(P))] + [R(L,E_2)] \\
[R(*,P(*))] =& [R(0,P)] + [R(0,E_1)] + [R(0,E_1(P))] + [R(0,E_2)] + [R(L,P)] + [R(L,E_1)] + [R(L,E_1(P))] + [R(L,E_2)] \\
[E_1(P(*)] =& [E_1(P)] + [E_1(E_2)] + [R(0,E_1(P))] + [R(0,E_2)] + [R(L,E_1(P))] + [R(L,E_2)]
\end{aligned}
$$

$$
\begin{aligned}
[R(L,P(*))] =& [R(L,P)] + [R(L,E_1)] + [R(L,E_1(P))] + [R(L,E_2)] \\
[R(*,E_1(*))] =& [R(0,E_1)] + [R(0,E_1(P))] + [R(0,E_2)] + [R(L,E_1)] + [R(L,E_1(P))] + [R(L,E_2)] \\
[E_1(E_2(*)] =& [E_1(E_2)] + [R(0,E_2)] + [R(L,E_2)]
\end{aligned}
$$

$$
\begin{aligned}
[R(L,E_1(*))] =& [R(L,E_1)] + [R(L,E_1(P))] + [R(L,E_2)] \\
[R(*,E_1(P(*)))] =& [R(0,E_1(P))] + [R(0,E_2)] + [R(L,E_1(P))] + [R(L,E_2)]
\end{aligned}
$$

$$
\begin{aligned}
[R(L,E_1(P(*)))] =& [R(L,E_1(P))] + [R(L,E_2)] \\
[R(*,E_2(*))] =& [R(0,E_2)] + [R(L,E_2)]
\end{aligned}
$$

$$
[R(L,E_2(*))] = [R(L,E_2)]
$$

Table 4.9: Hierarchical transformation for the example system depicted in Figure 4.4 B. The new states correspond to the occurrence levels of different subcomplexes. The transformation can be structured in different tiers. The previously discussed case of single protein ligand systems can be considered as border case of the underlying transformation pattern.

siderations in the previous example the states $[R(L,*)]$, $[R(*,P)]$, $[R(*,E_1)]$, $[R(*,E_1(P))]$ and $[R(*,E_2)]$ are chosen as output variables $\vec{y}$. Since the system also comprises six different processes, the transformation pattern again consists of six different tiers that are depicted in Table 4.9. Due to the absence of protein production and degradation, the three states of the 0^{th} tier remain constant. Thus, these three ODEs can be eliminated.

In this example, the transformed model equations can be dissected into three unidirectionally coupled modules including all five output variables, and one additional module comprising the two unobservable states $[R(L,E_1(P))]$ and $[R(L,E_2)]$. All model states are controllable. Thus, this example shows that the existence of all-or-none interactions facilitate significant model reductions. Although the considered system comprises the same number of molecular processes than the previously discussed one, even the complete mechanistic model consists of a lower number of ODEs. Additionally, the system comprises two unobservable states, which allows for further a model reduction. Consequently, a minimal realization of the reaction system for the defined input and outputs consists of nine ODEs.

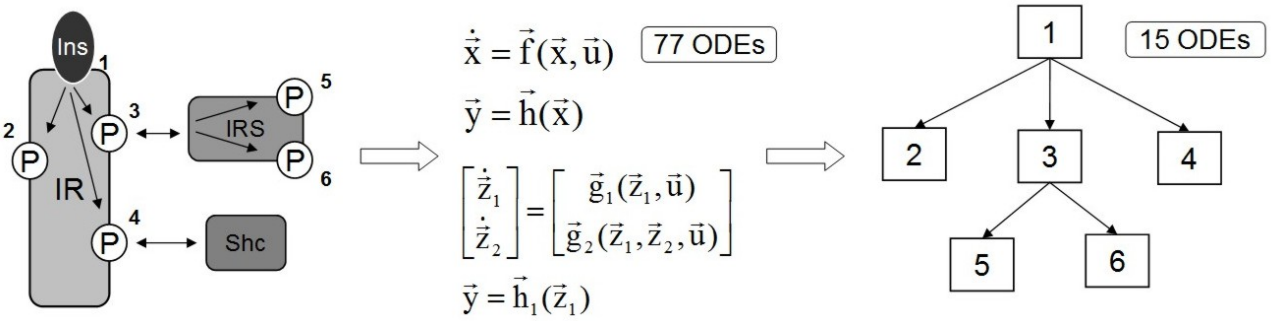

Figure 4.5: The considered part of the insulin signaling network depicted on the left side is translated into ordinary differential equations with the state vector $\vec{x}$. According to the introduced transformation pattern, these model equations are transformed to the new state variables $\vec{z}$. Three ODEs can be eliminated due to mass conservation relations for the proteins IR, IRS and Shc. A huge number of 59 ODEs ($\vec{z}_2$) are unobservable and can be neglected. The remaining 15 ODEs can be divided into six modules as shown on the right. Each of the considered binding and phosphorylation processes can be uniquely assigned to one of these modules. This correlation is denoted by the numbers $1-6$ that can be found in the left drawing and the schematic figure of the modules.

Example 3: The Insulin Signaling Pathway. As a more general example of branched systems, we will analyze a small part of the insulin signaling pathway. We consider the insulin receptor IR and four of its binding domains. For the sake of simplicity we only consider one extracellular ligand domain recruiting insulin. Additionally, we include three intracellular binding domains, which are all phosphorylated after ligand binding. According to the results of Gherzi *et al.* [47] (discussed in Chapter 3), we assume that IR phosphorylation is unidirectionally influenced by insulin binding. Furthermore, the recruitment of Shc and IRS is included to the model, as well as the subsequent phosphorylation of two additional IRS domains. In analogy to the phosphorylation of IR, we also presume that IRS binding to IR unidirectionally influences the phosphorylation of IRS. The system is depicted in Figure 4.5. A complete mechanistic model of this reaction network consists of 77 different molecular species, namely 72 receptor complexes, four different IRS species and the single effector protein Shc. Due to this complexity we refrain from quoting the reaction rules and the state space transformation. However, we will give a short summary regarding the transformed system's properties. The considered system output comprises eight occurrence levels, namely $[IR(Ins,*,*,*)]$, $[IR(*,P,*,*)]$, $[IR(*,*,P(*),*)]$, $[IR(*,*,Shc,*)]$, $[IR(*,*,*,P(*)]$, $[IR(*,*,*,IRS(*,*))]$, $[IR(*,*,*,IRS(P,*))]$ and $[IR(*,*,*,IRS(*,P))]$. Firstly, the neglect of production and degradation processes facilitates the elimination of three ODEs due to mass conservation relations for the proteins IR, Shc and IRS. A huge number of 59 states are unobservable and can be omitted. The remaining 15 ODEs can again be dissected into six unidirectionally coupled modules (compare Figure 4.5). Each of the considered binding and phosphorylation processes can be uniquely assigned to one of the modules. Furthermore, the kinetic parameters are also mo-

dularized. Each module only comprises kinetic parameters which are assigned to the processes described in this module or processes which directly or indirectly influence them. If we assume that measurement data is available for all considered output variables, the model parameters can be estimated step by step and module by module. Thus, the most sophisticated parameter estimation task in this example is the identification of six unknown parameters in a four ODE system. Altogether one can summarize that the described transformation realizes model modularizations and reductions facilitating the generation of practically manageable models.

4.1.5 Homodimerization of Receptors and Scaffolds

Homodimerization of receptors and scaffold proteins is quite common in signal transduction networks. For instance, homodimers occur in the ErbB signaling network as described above. Additionally, there exist numerous other receptors such as vascular endothelial growth factor (VEGF) or platelet derived growth factor (PDGF) receptors which form homodimers [141]. Homodimerization is additionally characterized by a number of unique features having a strong impact on model reduction, which justifies a separate and detailed consideration. Due to their symmetric configuration, the number of distinguishable homodimers is much lower than in equally large heterodimers. If one considers a receptor monomer which forms n distinct monomeric multiprotein complexes, there exist $\frac{n(n+1)}{2}$ feasible homodimers. Heterodimerization of two different receptors, which both form n monomeric species, leads to n^2 feasible heterodimers. However, the indistinguishability of symmetric receptor dimers not only has the positive effect of reducing the number of ODEs compared to heterodimers, but also leads to non-intuitive kinetic system properties, which will be discussed below.
We consider a receptor R with n distinct binding domains. Furthermore, we presume that R can form homodimers. These homodimers will be depicted as $R(*,...,*).R(*,...,*)$. Due to the symmetry of the dimers, one cannot distinguish between $R(L,0,...,0).R(0,...,0)$ and $R(0,...,0).R(L,0,...,0)$. Hence, we come to an agreement where the receptor with more occupied domains will always be mentioned first.

4.1.5.1 Kinetic Properties

Dimerization is a molecular process similar to ligand binding, and dimerization can influence, or can be influenced, by all other processes within the network. The most simple theoretic case one can analyze is the case where receptor homodimerization is completely independent of all other processes. In order to achieve this independence, it is necessary to parameterize all dimerization reactions adequately. This requires one to distinguish between the formation of mirror symmetric dimers and non-mirror symmetric dimers. The reason for this discrimination is that reactions describing the formation of non-mirror symmetric dimers have to be

parameterized by a twofold higher k_{on} value than those of mirror symmetric dimers.

$$\begin{aligned} R(X_1,...,X_n) + R(X_1,...,X_n) &\underset{k_{-1}}{\overset{k_1}{\rightleftharpoons}} R(X_1,...,X_n).R(X_1,...,X_n) \\ R(X_1,...,X_n) + R(Y_1,...,Y_n) &\underset{k_{-1}}{\overset{2k_1}{\rightleftharpoons}} R(X_1,...,X_n).R(Y_1,...,Y_n) \end{aligned} \tag{4.18}$$

The reason for this duplication of the k_{on} value can be explained considering the reaction rates. Let us take the assumption that the two concentrations $[R(X_1,...,X_n)]$ and $[R(Y_1,...,Y_n)]$ are equal. The rates for the considered two reactions comprise the terms $[R(X_1,...,X_n)]^2$ and $[R(X_1,...,X_n)] \cdot [R(Y_1,...,Y_n)]$ respectively. According to the collision theory for chemical reactions these terms are measures for the likelihood of a collision of two reactants in the system. Due to our assumption that the concentrations of both species are equal, the evaluation of both terms leads to exactly the same numerical result. However, the likelihood for the formation of a non-mirror symmetric dimer is two times higher than for mirror symmetric ones. This becomes apparent if one considers the collision probability for both cases. In the second case the number of molecules which may collide are two times higher than in the first scenario.

Not only does the dimerization process itself (and therefore the dimerization reactions) have to be treated differently. Due to the symmetry of homodimers, one also has to be careful in parameterizing ligand binding and modification reactions. Let us again assume that binding of the ligand L is completely independent of all other processes. Note that this is a theoretic assumption in order to illustrate the occurring problems regarding the most simplistic scenario. Furthermore, let k_1 and k_{-1} be the kinetic parameters describing the association and dissociation of L with a receptor monomer

$$R(0,*,...,*) + L \underset{k_{-1}}{\overset{k_1}{\rightleftharpoons}} R(L,*,...,*). \tag{4.19}$$

Here, one must again distinguish between two cases, namely binding of L to a completely unliganded dimer, and binding to a single liganded one. According to our assumption dimerization shall not have any effect on ligand binding. Hence, each receptor molecule of a dimer behaves exactly the same way as a monomeric receptor does, which indicates that an unliganded dimer has a two times higher k_{on} value than a single-liganded, or a monomeric one. The same rationale also implies that the k_{off} value for a double liganded dimer is two times higher than it is for a single liganded one. Thus, the reactions have to be parameterized as follows

$$R(0,*,...,*).R(0,*,...,*) + L \underset{k_{-1}}{\overset{2k_1}{\rightleftharpoons}} R(L,*,...,*).R(0,*,...,*) \tag{4.20}$$

$$R(L,*,...,*).R(0,*,...,*) + L \underset{2k_{-1}}{\overset{k_1}{\rightleftharpoons}} R(L,*,...,*).R(L,*,...,*). \tag{4.21}$$

The realization of process interactions either between two binding or modification processes or between dimerization and some other processes is straight forward. If dimerization has an influence on L binding, Reaction 4.19 will be parameterized by k_1 and k_{-1}, while the parameters k_2 and k_{-2} will be used for the Reactions 4.20 and 4.21. However, the two times

higher association constant of Reaction 4.20 and the two times higher dissociation constant of Reaction 4.21 still has to be accounted for. The negligence of these additional factors corresponds to a mutual interaction between the two ligand binding processes within a dimer.

4.1.5.2 General Transformation Pattern

The general transformation for systems that include homodimerization follows exactly the same pattern as introduced for scaffolds with multiprotein ligands. It is hierarchically structured where the different tiers of the transformation comprise occurrence levels of one, two, three or higher molecule complexes. However, one has to be careful, since some of the species concentrations have to be counted twice. Let us consider the occurrence level of a receptor ligand complex, which we will depict as $[R(L,*,...,*).*]$. This accumulated quantity comprises monomeric, as well as dimeric species, namely $[R(L,*,...,*)]$, $[R(L,*,...,*).R(0,*,...,*)]$ and $[R(L,*,...,*).R(L,*,...,*)]$. Observe that the species $R(L,*,...,*).R(L,*,...,*)$ include two receptor ligand complexes and therefore have to be counted twice. Consequently, the considered occurrence level is defined as

$$[R(L,*,...,*).*] = [R(L,*,...,*)] + [R(L,*,...,*).R(0,*,...,*)] + 2\,[R(L,*,...,*).R(L,*,...,*)]. \tag{4.22}$$

The invertibility of the transformation matrix suggested here can again be proved using mathematical induction.

4.1.5.3 Example

As an example we will analyze homodimerization of the EGFR receptor which, for this example, will be called R. In addition to the dimerization process we also consider EGF binding and receptor phosphorylation. EGF binding and receptor dimerization are assumed to interact mutually. This assumption is in accordance with the previously discussed thermodynamic constraints, and also fits with experimental data presented by Odaka *et al.* and Lemmon *et al.* [99, 82]. Furthermore, we assume that dimerization influences receptor phosphorylation, since the receptors of a dimer phosphorylate each other mutually. In analogy to the experimental results of Gherzi *et al.* [47] for insulin signaling, this interaction is expected to be an unidirectional one. The reaction rules which describe this system are given in Table 4.10. The reaction system comprises 14 receptor species and the ligand EGF. The transformation of these states according to the proposed general transformation pattern is shown in Table 4.11. Since the concentration of extracellular EGF is considered as model input the transformation does not include the overall concentration of EGF. The best choice of output variables in this example are the three occurrence levels of the 1st transformation tier, namely $[R(EGF,*).*]$, $[R(*,P).*]$ and $[R(*,*).R(*,*)]$. These outputs correspond to the total number of liganded EGF binding domains, the total number of phosphorylated intracellular receptor domains as well as the number of receptor dimers. Due to the absence of production and degradation, the overall concentration of EGFR stays constant and the respective ODE can be eliminated. The remaining 13 transformed model equations can be dissected into three modules, with the first module consisting of four ODEs and describing EGF binding as well as receptor homodimerization. This

$R(0,*)$	$+$	EGF	$\leftrightharpoons$	$R(EGF,*)$	k_1, k_{-1}
$R(0,*).R(0,*)$	$+$	EGF	$\leftrightharpoons$	$R(EGF,*).R(0,*)$	$2k_2, k_{-2}$
$R(EGF,*).R(0,*)$	$+$	EGF	$\leftrightharpoons$	$R(EGF,*).R(EGF,*)$	$k_2, 2k_{-2}$
$R(0,X_1)$	$+$	$R(0,X_1)$	$\leftrightharpoons$	$R(0,X_1).R(0,X_1)$	k_3, k_{-3}
$R(0,X_1)$	$+$	$R(0,X_2)$	$\leftrightharpoons$	$R(0,X_1).R(0,X_2)$	$2k_3, k_{-3}$
$R(EGF,X_1)$	$+$	$R(0,X_1)$	$\leftrightharpoons$	$R(EGF,X_1).R(0,X_1)$	k_4, k_{-4}
$R(EGF,X_1)$	$+$	$R(0,X_2)$	$\leftrightharpoons$	$R(EGF,X_1).R(0,X_2)$	$2k_4, k_{-4}$
$R(EGF,X_1)$	$+$	$R(EGF,X_1)$	$\leftrightharpoons$	$R(EGF,X_1).R(EGF,X_1)$	k_5, k_{-5}
$R(EGF,X_1)$	$+$	$R(EGF,X_2)$	$\leftrightharpoons$	$R(EGF,X_1).R(EGF,X_2)$	$2k_5, k_{-5}$
$R(*,0)$			$\leftrightharpoons$	$R(*,P)$	k_6, k_{-6}
$R(*,0).R(*,0)$			$\leftrightharpoons$	$R(*,P).R(*,0)$	$2k_7, k_{-7}$
$R(*,P).R(*,0)$			$\leftrightharpoons$	$R(*,P).R(*,P)$	$k_7, 2k_{-7}$

Table 4.10: Reaction rules for the considered example of EGFR dimerization. Here, the identifiers X_n also indicate that the related domains can be in various states in the same way that the identifier $*$ does. However, all domains with the identifier X_n within one rule have to be in the same state. If two different identifiers X_i and X_j occur within one rule the respective domains are not allowed to be in the same state.

first module comprises the model states $[R(EGF,*).*]$, $[R(*,*).R(*,*)]$, $[R(EGF,*).R(*,*)]$ and $[R(EGF,*).R(EGF,*)]$. The second module describes receptor phosphorylation and contains six ODEs, while the remaining three ODEs for $[R(*,P).R(*.P)]$, $[R(EGF,P).R(*,P)]$ and $[R(EGF,P).R(EGF,P)]$ form the third unobservable module. Since all states are controllable the model can be reduced by omitting the three unobservable states. This reduced model then comprises ten ODEs.

4.1.6 Conclusions

The introduced exact model reduction approach is based on the work of Borisov *et al.* [16, 17], who showed that combinatorial reaction networks are exactly reducible under certain conditions. From a system theoretical point of view exact reducibility corresponds to the existence of unobservable or uncontrollable system dynamics. The separation of observable and unobservable, and controllable and uncontrollable states can always be accomplished by a state space transformation. Interestingly, such a separation can be achieved by a linear transformation in the case of combinatorial reaction networks. We considered three important general scenarios, namely scaffolds with single protein ligands, scaffolds with multiprotein ligands and scaffold or receptor homodimerization. General transformation patterns for all these scenarios have been introduced and extensively discussed by considering numerous examples. The performed examinations indicate that most models of combinatorial reaction networks can be significantly reduced by elimination of unobservable and uncontrollable states. However, it is important to state that the described procedure alone is not an adequate solution for the problem of combi-

$$
\begin{aligned}
[R(*,*).*] =& [R(0,0)] + [R(EGF,0)] + [R(0,P)] + [R(EGF,P)] + 2\,[R(0,0).R(0,0)] \\
&+ 2\,[R(EGF,0).R(0,0)] + 2\,[R(0,P).R(0,0)] + 2\,[R(EGF,0).R(EGF,0)] \\
&+ 2\,[R(EGF,P).R(0,0)] + 2\,[R(EGF,0).R(0,P)] + 2\,[R(0,P).R(0,P)] \\
&+ 2\,[R(EGF,P).R(EGF,0)] + 2\,[R(EGF,P).R(0,P)] + 2\,[R(EGF,P).R(EGF,P)]
\end{aligned}
$$

$$
\begin{aligned}
[R(EGF,*).*] =& [R(EGF,0)] + [R(EGF,P)] + [R(EGF,0).R(0,0)] + 2\,[R(EGF,0).R(EGF,0)] \\
&+ [R(EGF,P).R(0,0)] + [R(EGF,0).R(0,P)] + 2\,[R(EGF,P).R(EGF,0)] \\
&+ [R(EGF,P).R(0,P)] + 2\,[R(EGF,P).R(EGF,P)] \\
[R(*,*).R(*,*)] =& [R(0,0).R(0,0)] + [R(EGF,0).R(0,0)] + [R(0,P).R(0,0)] + [R(EGF,0).R(EGF,0)] \\
&+ [R(EGF,P).R(0,0)] + [R(EGF,0).R(0,P)] + [R(0,P).R(0,P)] \\
&+ [R(EGF,P).R(EGF,0)] + [R(EGF,P).R(0,P)] + [R(EGF,P).R(EGF,P)] \\
[R(*,P).*] =& [R(0,P)] + [R(EGF,P)] + [R(0,P).R(0,0)] + [R(EGF,P).R(0,0)] + [R(EGF,0).R(0,P)] \\
&+ 2\,[R(0,P).R(0,P)] + [R(EGF,P).R(EGF,0)] + 2\,[R(EGF,P).R(0,P)] \\
&+ 2\,[R(EGF,P).R(EGF,P)]
\end{aligned}
$$

$$
\begin{aligned}
[R(EGF,P).*] =& [R(EGF,P)] + [R(EGF,P).R(0,0)] + [R(EGF,P).R(EGF,0)] + [R(EGF,P).R(0,P)] \\
&+ 2\,[R(EGF,P).R(EGF,P)] \\
[R(EGF,*).R(*,*)] =& [R(EGF,0).R(0,0)] + 2\,[R(EGF,0).R(EGF,0)] + [R(EGF,P).R(0,0)] \\
&+ [R(EGF,0).R(0,P)] + 2\,[R(EGF,P).R(EGF,0)] + [R(EGF,P).R(0,P)] \\
&+ 2\,[R(EGF,P).R(EGF,P)] \\
[R(*,P).*] =& [R(0,P).R(0,0)] + [R(EGF,P).R(0,0)] + [R(EGF,0).R(0,P)] + 2\,[R(0,P).R(0,P)] \\
&+ [R(EGF,P).R(EGF,0)] + 2\,[R(EGF,P).R(0,P)] + 2\,[R(EGF,P).R(EGF,P)]
\end{aligned}
$$

$$
\begin{aligned}
[R(EGF,*).R(EGF,*)] =& [R(EGF,0).R(EGF,0)] + [R(EGF,P).R(EGF,0)] + [R(EGF,P).R(EGF,P)] \\
[R(*,P).R(*,P)] =& [R(0,P).R(0,P)] + [R(EGF,P).R(0,P)] + [R(EGF,P).R(EGF,P)] \\
[R(EGF,P).R(*,*)] =& [R(EGF,P).R(0,0)] + [R(EGF,P).R(EGF,0)] + [R(EGF,P).R(0,P)] \\
&+ 2\,[R(EGF,P).R(EGF,P)] \\
[R(EGF,*).R(*,P)] =& [R(EGF,0).R(0,P)] + [R(EGF,P).R(EGF,0)] + [R(EGF,P).R(0,P)] \\
&+ 2\,[R(EGF,P).R(EGF,P)]
\end{aligned}
$$

$$
\begin{aligned}
[R(EGF,P).R(EGF,*)] =& [R(EGF,P).R(EGF,0)] + 2\,[R(EGF,P).R(EGF,P)] \\
[R(EGF,P).R(*,P)] =& [R(EGF,P).R(0,P)] + 2\,[R(EGF,P).R(EGF,P)]
\end{aligned}
$$

$$
[R(EGF,P).R(EGF,P)] = [R(EGF,P).R(EGF,P)]
$$

Table 4.11: Hierarchical transformation for the example system. The new states also correspond to the occurrence levels of different subcomplexes. Due to the symmetric structure of the receptor dimers some species have to be counted twice. For instance the macroscopic state $[R(EGF,*).*]$ is an aggregation of all species that comprise a subcomplex consisting of one receptor and one EGF molecule. The two micro-states $[R(EGF,0).R(0,0)]$ and $[R(EGF,0).R(EGF,0)]$ obviously fit into this pattern. However, the state $[R(EGF,0).R(EGF,0)]$ has to be counted twice since the regarded subcomplex also occurs twice in this species. Furthermore, the transformation can be structured in six different tiers.

natorial complexity. Real signaling cascades often comprise millions or even billions of species and reactions. The requirement of firstly generating a complete mechanistic model, which is subsequently reduced, impedes the application of the discussed methods in many cases. This problem will be discussed in the following section.

4.2 Reduced Order Modeling of Combinatorial Reaction Networks

In the previous section, we discussed a general and systematic method which allows for significant and exact model reductions of combinatorial reaction networks. Now, an alternative approach will be considered which facilitates the direct generation of the exactly reduced model equations. This reduced order modeling approach is based on the close relations between controllability and observability of a model and the process interactions of the examined system. These correlations will be discussed below.

4.2.1 Controllability, Observability and Process Interactions

From the previously discussed examples, it can be seen that the number of observable and controllable states highly depends on the occurring process interactions. The question is that of whether the qualitative information about process interactions can reveal clues about the observability and controllability of a reaction network, or maybe even facilitate a direct translation to reduced model equations. Controllability and observability as well as process interactions provide information about interactions within the considered system, however, at different levels of abstraction.

Controllability and observability are properties of an ODE system, and both of them characterize the ODE couplings with respect to the system inputs and outputs. According to the definitions given in Chapter 2 a state is called observable if its dynamic behavior can be reconstructed or recalculated by measuring the output variables. Hence, all observable states must exert a certain well-defined influence on at least one of the output variables. On the other hand a state is said to be controllable, if it can be influenced either directly or indirectly by one of the system's input variables.

Process interactions describe the system at a different level of abstraction. Instead of ODEs one considers binding and modification processes. The analyses performed in the previous section clearly show that process interactions are closely related to ODE couplings. This can be seen from the fact that ODE models of unidirectionally interacting processes can be divided into unidirectionally coupled ODE modules.
Controllability and observability are closely related to the determination of input and output variables respectively. In accordance to this determination at the ODE level, one can also formally define input and output processes at the process level. A connection between the

two abstraction levels is given by the occurrence levels we previously introduced as a state space representation for combinatorial reaction networks. These coordinates allow a direct assignment of model states to specific molecular processes. Each occurrence level, such as $[R(*,...,*,E_i,*...,*)]$, can be directly assigned to its respective process, namely E_i binding to R. Analogously, occurrence levels of higher tiers, such as $[R(E_1,E_2,E_3,*,...,*)]$, can be linked with three different processes. All processes that are related to the chosen output variables are said to be output processes, and all processes that can be directly assigned to the input variables analogously correspond to the input processes. This direct link between model variables and processes facilitates the unique translation of all input and output variables to a set of input and output processes. Let us consider an example and presume that the concentration of E_1 is our input variable, while $[R(*,E_2,*,...,*)]$ and $[R(*,*,*,E_4,E_5,*,...,*)]$ are output variables. In this case E_1 binding to R is an input process, and E_2, E_4 and E_5 binding to R are output processes.

Furthermore, we can formally introduce *process controllability* and *process observability*. According to the familiar concept of controllability at the ODE level, a process will be called process controllable if it is either directly or indirectly influenced by one of the input processes. Analogously, a process will be called process observable if it directly or indirectly affects one of the output processes. In contrast to controllability and observability of an ODE model, the respective system properties at the process level can be analyzed in a very simple way by considering the process interaction graph. In this graph processes are regarded as nodes, while process interactions are represented as directed edges. This definition of an interaction graph is very similar to that proposed by Klamt *et al.* [74]. A process P is process controllable if the interaction graph comprises a directed path from one of the input processes to the process P. The same process is observable if there exists a directed path from P to one of the output processes.

A relation between the controllability and observability concepts at the different abstraction levels can also be seen. Process controllability suggests that all states that are assigned to this process are influenced and therefore controllable. Process observability on the other hand indicates that the respective occurrence level of the 1^{st} tier is observable. State variables that describe occurrence levels of higher tiers, such as $[R(E_1,E_2,E_3,*,...,*)]$, are only observable if the related processes all jointly affect at least one of the output processes. Thus, we have found a way to predict whether a certain state might be observable or controllable by considering the process interactions. Note that this technique provides a conservative estimation which, in some cases, will classify states as controllable or observable when in fact they are not. This statement can be confirmed by reconsidering *Example 2: Domain phosphorylation* above. In this example all processes are process observable and controllable. Additionally, all of the occurring processes jointly affect the E_2 binding process which is one of the output processes. Nevertheless, two of the system states are unobservable and the model is exactly reducible. However, the method gives correct predictions for many other considered examples and therefore proves to be a helpful tool in analyzing combinatorial reaction networks.

4.2.2 Reduced Order Modeling Technique

The enormous complexity of most real signal transduction networks impedes the application of the previously proposed model reduction technique. New alternative techniques are required which allow for the direct generation of reduced model equations. The already-introduced concepts of process interactions, interaction graphs as well as process controllability and observability serve as a basis for the following considerations. The fundamental idea is that at the macroscopic level, a mathematical description of a certain process merely requires the incorporation of those other processes that exert some influence on the considered one. A detailed specification of the method will be given below and is structured in nine elementary steps. Each step will be illustrated considering the example shown in Figure 4.6.

Step 1: Definition of all proteins, binding domains as well as binding and modification processes that will be included into the model. In the considered example, the model will comprise of the molecules A, B, C and D with their binding domains as depicted in Figure 4.6 A. The occurring processes are usually labeled or numbered as indicated in Figure 4.6 A. In the example, we consider eight different processes, namely binding of A to B (process 1), phosphorylation of B at different domains (processes 2, 3 and 7), binding of C to B (process 4), phosphorylation of C at two distinct domains (processes 5 and 6), as well as binding of D (process 8).

Step 2: In a second step, one has to define all occurring process interactions, including whether these are uni- or bidirectional. These process interactions have to be consistent with both measured kinetic data of the involved proteins, and the thermodynamic constraints as discussed in Chapter 3. Since a mathematical model requires a complete definition for all interactions, fragmentary knowledge has to be completed by assumptions. In Figure 4.6 A, the occurring process interactions of the example are indicated by arrows. The processes (1, 2), (1, 3), (3, 7), (4, 5) and (4, 6) are assumed to interact unidirectionally. The processes (3, 4) and (7, 8) are considered to be all-or-none interactions, which by definition are mutual interactions. All other processes do not interact directly.

Step 3: The interaction pattern of the system has to be translated into an interaction graph. As mentioned before, the labeled or numbered processes are nodes and the occurring interactions are represented by directed edges (arrows) pointing to the process under influence. The interaction graph for the considered example is depicted in Figure 4.6 B.

Step 4: One defines input and output processes according to the considered system stimulations, as well as available measurements or research interests. The goal of generating a model that accurately describes the output processes at a macroscopic level necessitates the further inclusion of all other processes that are process observable. In the example we choose the processes 2, 3, 5 and 8 as output processes. They are marked by grey circles in Figure 4.6 B.

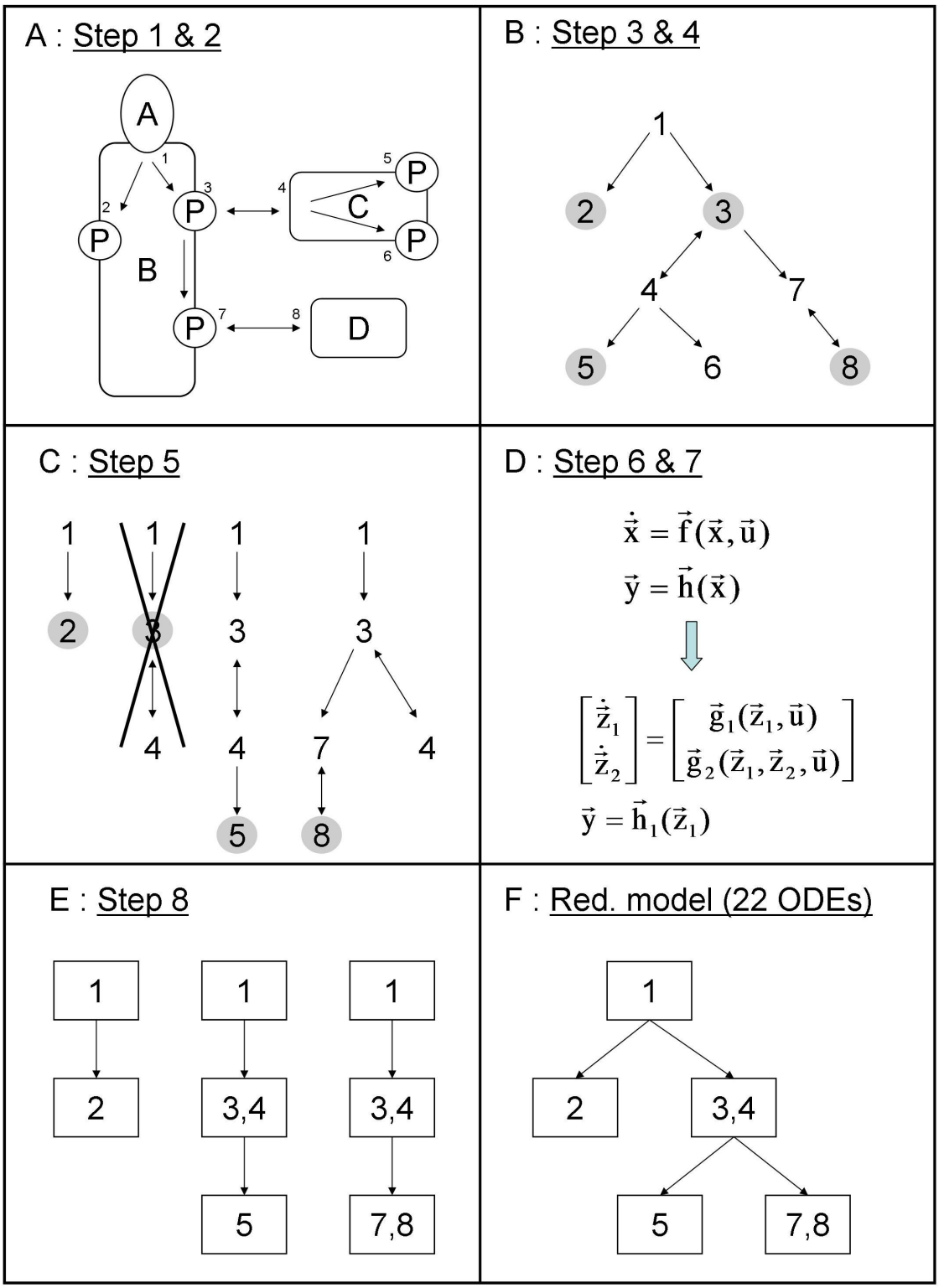

Figure 4.6: Exemplification of the developed reduced order modeling technique. The considered example is very similar to the previously discussed insulin example. Only the interaction pattern is different. The depicted steps of the reduced order modeling technique are explained in the text.

Step 5: The interaction graph can be divided into output subgraphs. An output subgraph contains all nodes from which a specific output node can be reached following the directed edges. Hence, an output subgraph comprises all processes, which are process observable considering a special output process. If a node does not occur in any output subgraph the corresponding process cannot influence any of the output processes and can be completely omitted. Finally, one has to eliminate redundant information, i.e. subgraphs which are completely included by other, bigger subgraphs. In principle one can also analogously define input subgraphs and determine which processes are uncontrollable. However, uncontrollable but observable processes cannot simply be eliminated from further consideration. Uncontrollability merely allows for quasi-steady state assumptions at the ODE level. The graph shown in Figure 4.6 B can be divided into four output subgraphs, as shown in Figure 4.6 C. In this example process six does not influence any of the considered output processes and can be omitted in the following considerations. The subgraph for output process three is completely contained in two other subgraphs and therefore can be eliminated.

Step 6: Each of the output subgraphs describes an autonomous signaling path, which can be modeled separately. Hence, the next step is to create complete mechanistic models for each subgraph. Processes not being part of a subgraph are not included in the respective model. This step will be further explained considering the smallest subgraph of the example system that comprises the processes 1 and 2. The mathematical model is given by

$$\begin{aligned} r_1 &= k_1[A][B(0,0)] - k_{-1}[B(A,0)] \\ r_2 &= k_1[A][B(0,P)] - k_{-1}[B(A,P)] \\ r_3 &= k_2[B(0,0)] - k_{-2}[B(0,P)] \\ r_4 &= k_3[B(A,0)] - k_{-3}[B(A,P)] \end{aligned} \qquad \frac{d}{dt}\begin{pmatrix} [A] \\ [B(0,0)] \\ [B(A,0)] \\ [B(0,P)] \\ [B(A,P)] \end{pmatrix} = \begin{pmatrix} -r_1 - r_2 \\ -r_1 - r_3 \\ r_1 - r_4 \\ -r_2 + r_3 \\ r_2 + r_4 \end{pmatrix}, \tag{4.23}$$

in which the rates r_1 and r_2 describe the binding of A to the scaffold protein B (process 1), and the rates r_3 and r_4 describe the phosphorylation of B (process 2).

Step 7: The model equations have to be transformed to new more convenient coordinates, which allow the elimination of redundant information, still present in the subgraphs. This redundancy is due to the fact that some processes are included in several subgraphs. A suitable choice of new coordinates is given by the previously introduced occurrence levels. As an example, we again consider only the smallest subgraph of the system which comprises processes 1 and 2. The first tier in this example includes the overall concentrations of the molecules A and B

$$\begin{aligned} [A(*)] &= [A] + [B(A,0)] + [B(A,P)] \\ [B(*,*)] &= [B(0,0)] + [B(A,0)] + [B(0,P)] + [B(A,P)]. \end{aligned} \tag{4.24}$$

The next tier comprises the first order occurrence levels, which are given by

$$\begin{aligned}[B(A,*)] &= [B(A,0)] + [B(A,P)] \\ [B(*,P)] &= [B(0,P)] + [B(A,P)].\end{aligned} \tag{4.25}$$

In this example there only one further tier occurs describing the second order occurrence levels, namely

$$[B(A,P)] = [B(A,P)]. \tag{4.26}$$

Processes that are not included in the current subgraph are simply omitted since they are not observable. If the sub-model still contains unobservable states these can also be eliminated at this stage of the procedure.

Step 8: The proposed transformation allows for the dissection of the model equations of each subgraph into modules, as shown above. These modules are characterized by unidirectional communication with other modules. Processes which directly or indirectly interact mutually form one module. If some processes are included in more than one subgraph, the models of these subgraphs will contain identical modules. Multiple copies of modules can be eliminated and the remaining modules can be merged to a complete model. For instance, the transformed ODEs for the discussed smallest subgraph do have a special structure. The variables $[A(*)]$ and $[B(*,*)]$ are constant and equal their initial concentration. The corresponding ODEs are not required. Additionally, the ODE for $[B(A,*)]$ does not depend on $[B(*,P)]$ and $[B(A,P)]$, which is due to the unidirectional process interaction between A binding to B and phosphorylation of B. Hence, the remaining three ODEs can be divided into two modules. One module only comprises the ODE for $[B(A,*)]$, which describes the dynamics of process 1. The second module comprises the other two ODEs, which describe the dynamics of process 2. The ODEs deduced from the two remaining output subgraphs shown in Figure 4.6 C, can be divided into six more modules as indicated in Figure 4.6 E. Each box represents a set of ODEs. The modules are labeled with the process numbers which are described by the appropriate ODEs. Two copies of module (1) and one of module (3,4) can be eliminated here. The resulting model, which consists of only 22 ODEs, is schematically shown in Figure 4.6. A complete mechanistic model of the network would comprise 77 ODEs of which three can be eliminated due to mass conservation relations.

Step 9: In a final step, one can take a quasi-steady state assumption for all uncontrollable states that are still part of the reduced model.

The presented procedure has the advantage to facilitate a direct generation of reduced model equations. Admittedly, the number of equations that have to be set up in step six, in general include redundant information about processes which can be observed at numerous outputs. However, the absolute number of ODEs that have to be generated is usually much lower than the number when a complete mechanistic model is created. In the considered example, one only has to set up 27 ODEs using the described procedure. A complete combinatorial model would comprise 77 states. The method has to be slightly modified if one of the output variables

is a higher order occurrence level which is not contained in any of the submodels. Let us assume that one of the output variables in the example is $[B(*, P(*), P(*), *)]$ which describes both process 2 and process 3. Since none of the three subgraphs depicted in Figure 4.6 C comprises both processes simultaneously, the quantity $[B(*, P(*), P(*), *)]$ will not be a state of the reduced 22 ODE model. This problem can be overcome by the fusion of two subgraphs. This will necessarily increase the number of ODEs that has to be generated as well as the final size of the reduced model. However, the number of ODEs would still be smaller than 77.

Furthermore, the inclusion of production and degradation into the mathematical model necessitates another extension of this method. The same holds true if the considered system includes multifunctional protein binding domains, such that certain binding domains are involved in several binding processes. Both cases will be discussed in the following sections.

4.2.2.1 Multifunctional Protein Binding Domains

Multifunctional protein binding domains are domains which can recruit more than one binding partner. A typical example is the effector protein Grb2 that can either bind to several ErbB receptors or to the adaptor protein Shc. A constellation like this can lead to problems with the reduced order modeling approach introduced above. The problem occurs if such a multifunctional binding domain is part of two or more output subgraphs, as shown in Figure 4.6 C.

Probably the most simple example to illustrate this problem is a scaffold protein R which provides two binding domains. Both of these domains recruit the effector protein E which possesses one binding domain. The binding domain of E is a multifunctional one, since it can bind to both R domains. If we assume that the two binding processes of the regarded system are completely independent and that both are considered as output processes, the system can be divided into two subgraphs. These subgraphs are somehow degenerated since both only comprise a single node. According to the reduced order modeling approach, both binding processes can be modeled separately. However, the problem is that the binding domain of the effector E is involved in both processes. This is a typical crosstalk situation. Since the number of effector proteins E and therefore the number of E binding domains is limited, the recruitment of E to one receptor domain reduces the concentration of unbound effectors and therefore has an indirect influence on the other binding process.

One possible solution for this problem is to merge all output subgraphs that share such multifunctional binding domains. This approach has the drawback where the number of equations that have to be generated in the sixth step of the modeling procedure can be significantly increased. Alternatively, one can formulate the reaction rates for both subgraphs independently. However, all species which are simultaneously involved in both submodels have to be balanced in one joint ODE. If the first subgraph of the example is translated into a reaction rate, one has to consider only the rate

$$r_1 = k_1[R(0, \#)][E] - k_{-1}[R(E, \#)]. \tag{4.27}$$

In this representation, the identifier # indicates that the real scaffold protein offers further binding domains, but the resulting combinatorial complexity is neglected. The second subgraph can be described by the reaction rate

$$r_2 = k_2[R(\#, O)][E] - k_{-2}[R(\#, E)]. \tag{4.28}$$

An ODE model is obtained by balancing all occurring species. Since the species E is involved in both submodels it is necessary to create one joint ODE for $[E]$. Note, that species like $R(0, \#)$ and $R(\#, 0)$ are considered to be completely different molecules. This also emphasizes the point that domains are the fundamental elements of these reaction networks because both species describe the same molecule but different binding domains. Thus, one can also argue that domains are balanced, instead of molecules. From another point of view it can be suggested that $R(0, \#)$ and $R(\#, 0)$ are two different proteins which compete for E binding. The resulting ODE model is given by

$$\begin{aligned} \frac{d[R(0,\#)]}{dt} &= -r_1 \qquad \frac{d[R(E,\#)]}{dt} = r_1 \\ \frac{d[R(\#,0)]}{dt} &= -r_2 \qquad \frac{d[R(\#,E)]}{dt} = r_2 \\ \frac{d[E]}{dt} &= -r_1 - r_2. \end{aligned} \tag{4.29}$$

Following this procedure, one does not have to consider the complete combinatorial complexity of the network. For each subgraph only those reactions that are necessary to describe all processes included in the respective subgraph are generated. One also has to use a joint transformation in this case which is given by

$$\begin{aligned} [R(*,\#)] &= [R(0,\#)] + [R(E,\#)] \\ [R(\#,*)] &= [R(\#,0)] + [R(\#,E)] \\ [E(*)] &= [E] + [R(E,\#)] + [R(\#,E)] \\ [R(E,\#)] &= [R(E,\#)] \\ [R(\#,E)] &= [R(\#,E)]. \end{aligned} \tag{4.30}$$

This means that occurrence levels can be composed of species from both submodels such as $[E(*)]$ in the considered example.

This simple modification or extension of the proposed modeling approach facilitates its application to a larger set of reaction systems. It will also be of great importance in modeling the crosstalk between EGF and the insulin receptor, discussed below.

4.2.2.2 Production and Degradation

A process that has been completely neglected in the preceding considerations which plays a crucial role in many real signal transduction networks is the production and degradation of signaling proteins. Like association and dissociation, production and degradation are two

aspects of the same process. This process increases or decreases the number of available proteins, and thus, can have a strong impact on the dynamic behavior of a reaction network. A quite simple way of modeling production and degradation, which we will adopt here, is the assumption of a constant production rate, and a degradation rate which is proportional to the concentration of the degraded species. Production is necessarily restricted to a very limited number of species, namely all one-protein species. Larger complexes which correspond to aggregates of numerous signaling proteins are not produced. Their formation process is part of the combinatorial reaction network. However, each feasible signaling complex can be degraded either by natural decay or by controlled degradation. In many cases ubiquitin is used as a marker for controlled degradation. In the case of EGF signaling it is known that internalized and phosphorylated ErbB1 receptors can recruit the E3 ubiquitin ligase Cbl, leading to ubiquitination of ErbB1. This facilitates binding of the adaptor protein UIM (ubiquitin-interacting motif) which targets the receptor complex to the lysosomes for degradation [27]. A still unanswered question in this context is whether the whole signaling complex is degraded, or only the ErbB receptor while the adaptor proteins are recycled.

For the sake of simplicity, we make a number of assumptions. First, the considerations will be focused on production and degradation of the considered receptor or scaffold protein and its complexes. The individual receptor protein R will be produced at a constant rate, and all receptor species are presumed to have a natural decay rate. All other adaptor and effector proteins are neither produced nor degraded. If a receptor complex is degraded, all bound adaptor proteins will be recycled to the cytosol. Furthermore, we take the assumption that if the receptor is marked by ubiquitination, its degradation rate is modulated. This change of the degradation rate from natural decay to ordered degradation can be considered as a process interaction. Ubiquitination has a direct influence on degradation. Another interesting question is that of which processes are influenced by degradation or production of R. It is quite obvious that all processes which involve one of the R binding domains are affected. Theoretically, degradation can be considered as a process which sets the k_{on} values of all R binding domains to zero and all k_{off} values to infinity. All other effects caused by degradation are indirect. Note that if one takes the assumption that a complex is degraded with all its bound adaptor proteins, all processes that modify or enlarge the R complex are directly influenced. All these interactions are unidirectional, which can be simply introduced in the process interaction graph. Production and degradation is one additional node in this graph which, for example, is influenced by ubiquitination and can affect numerous other binding and modification processes.

Note, that the inclusion of production and degradation for all involved proteins is possible but often highly restricts the possibility of exact model reductions. However, this is not a problem caused by the modeling technique but rather a structural problem of these systems.

4.2.3 Conclusions

A direct generation of reduced model equations for signal transduction networks is inevitable due to the enormous complexity of most real pathways. Such a reduced order modeling approach is introduced and formalized here. The approach is based on qualitative information about processes and process interactions, which is integrated into a process interaction graph. The formal definition of new characteristics such as process controllability and observability allows us to make statements about controllability and observability of model equations. Additionally, these concepts facilitate reduced order modeling by dissecting the interaction graph into independent subgraphs. These subgraphs can be separately translated into submodels. The further application of the previously introduced hierarchical transformation for combinatorial reaction networks facilitates a modularization and a subsequent reintegration of the submodels. In many cases the resulting subgraphs can be separately modeled and transformed. One has to be careful in the vase where certain binding domains are involved in more than one subsystem. A further complication results from the inclusion of protein production and degradation, or the translocation of proteins to other compartments. However, for all these special cases, alternative procedures can be found, meaning that if it is possible to handle all kinds of real signaling networks. The only limitation is given by high grades of process interconnectivity. If an interaction graph cannot be split into smaller subgraphs, this method will not provide any simplification. However, this is not a limitation of the reduction method but rather indicates that the system under consideration cannot be exactly reduced.

4.3 Example: EGF and Insulin Receptor Crosstalk

The discussed methods will be used to generate a reduced model of EGF and insulin receptor crosstalk. We will compare a complete mechanistic description of this crosstalk and an exactly reduced version. Approximate reductions of this network will be discussed in the next chapter.

4.3.1 Model Definition

In a first step, the molecules and processes which are included in the model, and the assumptions made concerning the process interactions will be defined. Since a manageable complete mechanistic model will also be generated, the considerations will be limited to a small part of the real signaling network. For instance, only the EGF receptor (EGFR/ErbB1) will be taken into account and the other three ErbB receptors shall be ignored. Similar simplifications have been made by many other modelers in the past [122, 73, 12]. In order to avoid an unmanageable combinatorial explosion of feasible EGF receptor species, only two intracellular domains will be modeled. According to Schulze *et al.* the EGF receptor possesses, among others, six potential residues for Grb2 and also six residues for Shc [123]. Hence, we consider one binding domain for each of these two effector proteins. In the consideration of the insulin receptor family, we

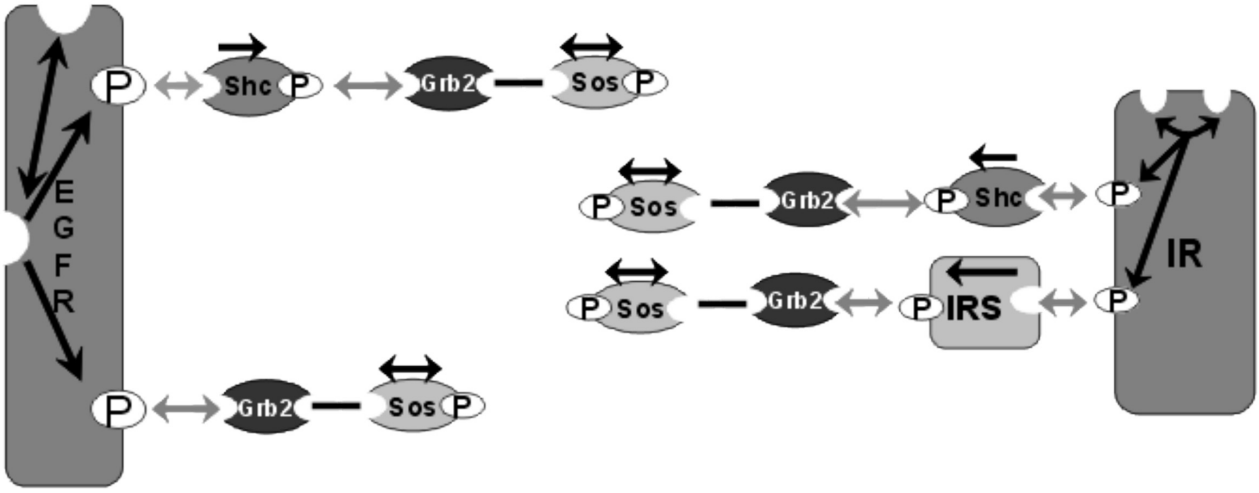

Figure 4.7: The drawn part of the EGF and insulin receptor network is modeled. The process interactions are depicted by arrows. Black arrows represent uni- and bidirectional interactions, while grey arrows describe all-or-none interactions. A complete mechanistic model of this network comprises 5,182 ODEs, while the exactly reduced one consists of solely 87 ODEs.

will focus on the insulin receptor (IR) and exclude potential crosstalk with the insulin-like growth factor receptor (IGFR), and the insulin related receptor (IRR). Again we restrict the considerations to two intracellular IR domains, namely one for Shc and one for IRS.

EGFR provides an extracellular binding domain that recruits EGF [27, 108]. Furthermore, the receptor monomers can form homodimers after being activated by the ligand. This dimerization induces the phosphorylation of numerous intracellular domains [83, 66, 120]. According to thermodynamic constraints we discussed in Chapter 3, EGF binding and receptor dimerization have to interact mutually, fulfilling the Wegscheider conditions. A mutual interaction is also suggested by experimental data [18, 100, 46]. An unidirectional influence between two processes is only feasible if the reaction cycles formed by these processes are futile ones. Phosphorylation can be unidirectionally influenced, as discussed for the insulin receptor in Chapter 3. Analogously, EGFR dimerization is assumed to unidirectionally influence EGFR autophosphorylation of the considered intracellular domains. We also presume that all phosphorylation processes occurring in our example are unidirectionally induced, except for the phosphorylation of SOS (see below). A direct interaction between EGF binding and phosphorylation is not presumed to occur. After the two intracellular domains are phosphorylated, one of them recruits Grb2 and the other Shc. The interaction between receptor phosphorylation and subsequent effector binding will be an all-or-none interaction. Phosphorylation is assumed to be essential for effector binding and effector binding prevents receptor dephosphorylation for steric reasons. Furthermore, it is also known that Shc can be phosphorylated after having bound to EGFR [115]. In accordance with the assumption concerning phosphorylations, Shc binding is thought to unidirectionally affect Shc phosphorylation. The phosphorylated Shc protein can also recruit

Grb2 [115]. Grb2 possesses an additional domain, which recruits the adaptor protein SOS. SOS is a guanine exchange factor (GEF) which can activate the membrane-bound small G-protein Ras, by effecting the exchange of GDP for GTP [86, 24]. Active RasGTP in turn initiates the MAP kinase cascade. Phosphorylated ERK, which is a component of the MAP kinase cascade, stimulates a serine/threonine phosphorylation of SOS, resulting in dissociation of the Grb2-SOS complex [137, 24]. Thus, we take the assumption that the Grb2-SOS binding is not influenced by the association of Grb2 to either a phosphorylated EGF receptor, or phosphorylated Shc. However, if SOS is phosphorylated by ERK, which is considered as an additional input signal, the Grb2-SOS complex dissociates. Here we assume a mutual interaction between SOS phosphorylation and Grb2-SOS binding.

The insulin receptor consists of two constitutively dimerized monomers and is activated exclusively by ligand binding without further oligomerization [103]. Due to the dimeric structure of the insulin receptor, two insulin binding domains will be included into the model. According to the thermodynamic constraints and experimental results, these two domains have to interact mutually [134]. Ligand binding is assumed to unidirectionally influence the phosphorylation of the two considered intracellular domains [47]. Shc is assumed to bind with other kinetic parameters to IR than when binding to EGFR. However, Shc phosphorylation, as well as Grb2 binding to phosphorylated Shc and so on is parameterized in the same way as in the case of EGFR. In order to reduce the complexity of the network, numerous binding domains of the scaffold IRS are ignored. The model only accounts for IRS binding to the phosphorylated insulin receptor, subsequent IRS phosphorylation and binding of the Grb2-SOS complex. In order to reduce the complexity of the model, receptor internalization and degradation is also neglected for both IR and EGFR.

All considered molecules, processes and process interactions are also depicted in Figure 4.7. The reaction rules generating this complete mechanistic model are depicted in Table 4.12.

4.3.2 Complete Mechanistic Model vs. Exactly Reduced Model

A complete mechanistic model of the described network of EGF and insulin receptor crosstalk comprises 42,956 reactions and 5,182 ODEs. According to the assumed process interactions the complete network can be parameterized by 68 kinetic parameters which can be seen in Table 4.12. The exact numerical value of these parameters does not play an important role in this context. The main purpose of this model is to illustrate the possibilities offered by the new reduction methods. Hence, the model equations are normalized to relative concentrations. The overall concentration of the considered components EGFR, IR, Shc, Grb2, SOS and IRS are set to 100 percent. The kinetic parameters are chosen such that the model qualitatively shows the expected behavior. We will focus on time plots of the quantities $[IR(*,*,SOS(*),*)]$, $[IR(*,*,*,SOS(*))]$, $[EGFR(*,SOS(*),*).*]$ and $[EGFR(*,*,SOS(*)).*]$.

The complete mechanistic model can be generated by BioNetGen or other similar rule-based modeling tools. This example was modeled using the software tool ALC [79]. ALC allows

$IR(0,0,*,*)$	+	Ins	$\leftrightharpoons$	$IR(I,0,*,*)$	k_1, k_{-1}	$ER(*, Grb2(0), *)$	+	$SOS(P)$	$\leftrightharpoons$	$ER(*, SOS(P), *)$	k_{10}, k_{-10}
$IR(0,0,*,*)$	+ +	Ins	$\leftrightharpoons$	$IR(0,I,*,*)$	k_1, k_{-1}	$ER(*, SOS(0), *)$			$\leftrightharpoons$	$ER(*, SOS(P), *)$	k_{11}, k_{-11}
$IR(I,0,*,*)$	+ +	Ins	$\leftrightharpoons$	$IR(I,I,*,*)$	k_2, k_{-2}	$ER(*,*,0)$			$\leftrightharpoons$	$ER(*,*,P)$	k_{25}, k_{-25}
$IR(0,I,*,*)$	+	Ins	$\leftrightharpoons$	$IR(I,I,*,*)$	k_2, k_{-2}	$ER(*,*,P)$	+	$Grb2(*)$	$\leftrightharpoons$	$ER(*,*,Grb2(*))$	k_{26}, k_{-26}
$IR(0,0,0,*)$			$\leftrightharpoons$	$IR(0,0,P,*)$	k_3, k_{-3}	$ER(*,*,Grb2(0))$	+ +	$SOS(0)$	$\leftrightharpoons$	$ER(*,*,SOS(0))$	k_9, k_{-9}
$IR(I,0,0,*)$			$\leftrightharpoons$	$IR(I,0,P,*)$	k_4, k_{-4}	$ER(*,*,Grb2(0))$	+	$SOS(P)$	$\leftrightharpoons$	$ER(*,*,SOS(P))$	k_{10}, k_{-10}
$IR(0,I,0,*)$			$\leftrightharpoons$	$IR(0,I,P,*)$	k_4, k_{-4}	$ER(*,*,SOS(0))$			$\leftrightharpoons$	$ER(*,*,SOS(P))$	k_{11}, k_{-11}
$IR(I,I,0,*)$			$\leftrightharpoons$	$IR(I,I,P,*)$	k_5, k_{-5}	$ER(E,*,*)$	+ +	$ER(0,*,*)$	$\leftrightharpoons$	$ER_2(E,*,*,0,*,*)$	k_{27}, k_{-27}
$IR(*,*,P,*)$	+	$Shc(*)$	$\leftrightharpoons$	$IR(*,*,Shc(*),*)$	k_6, k_{-6}	$ER(0,*,*)$	+ +	$ER(0,*,*)$	$\leftrightharpoons$	$ER_2(0,*,*,0,*,*)$	k_{28}, k_{-28}
$IR(I,I,Shc(0),*)$			$\leftrightharpoons$	$IR(I,I,Shc(P),*)$	k_7, k_{-7}	$ER(E,*,*)$	+ +	$ER(E,*,*)$	$\leftrightharpoons$	$ER_2(E,*,*,E,*,*)$	k_{29}, k_{-29}
$IR(*,*,Shc(P),*)$	+ +	$Grb2(*)$	$\leftrightharpoons$	$IR(*,*,Grb2(*),*)$	k_8, k_{-8}	$ER_2(0,*,*,*,*,*)$	+ +	EGF	$\leftrightharpoons$	$ER_2(E,*,*,*,*,*)$	k_{30}, k_{-30}
$IR(*,*,Grb2(0),*)$	+ +	$SOS(0)$	$\leftrightharpoons$	$IR(*,*,SOS(0),*)$	k_9, k_{-9}	$ER_2(*,0,*,*,*,*)$			$\leftrightharpoons$	$ER_2(*,P,*,*,*,*)$	k_{31}, k_{-31}
$IR(*,*,Grb2(0),*)$	+ +	$SOS(P)$	$\leftrightharpoons$	$IR(*,*,SOS(P),*)$	k_{10}, k_{-10}	$ER_2(*,P,*,*,*,*)$	+	$Shc(*)$	$\leftrightharpoons$	$ER_2(*,Shc(*),*,*,*,*)$	k_{23}, k_{-23}
$IR(*,*,SOS(0),*)$			$\leftrightharpoons$	$IR(*,*,SOS(P),*)$	k_{11}, k_{-11}	$ER_2(*,Shc(0),*,*,*,*)$			$\leftrightharpoons$	$ER_2(*,Shc(P),*,*,*,*)$	k_{32}, k_{-32}
$IR(0,0,*,0)$			$\leftrightharpoons$	$IR(0,0,*,P)$	k_{12}, k_{-12}	$ER_2(*,Shc(P),*,*,*,*)$	+ +	$Grb2(*)$	$\leftrightharpoons$	$ER_2(*,Grb2(*),*,*,*,*)$	k_8, k_{-8}
$IR(I,0,*,0)$			$\leftrightharpoons$	$IR(I,0,*,P)$	k_{13}, k_{-13}	$ER_2(*,Grb2(0),*,*,*,*)$	+ +	$SOS(0)$	$\leftrightharpoons$	$ER_2(*,SOS(0),*,*,*,*)$	k_9, k_{-9}
$IR(0,I,*,0)$			$\leftrightharpoons$	$IR(0,I,*,P)$	k_{13}, k_{-13}	$ER_2(*,Grb2(0),*,*,*,*)$	+ +	$SOS(P)$	$\leftrightharpoons$	$ER_2(*,SOS(P),*,*,*,*)$	k_{10}, k_{-10}
$IR(I,I,*,0)$			$\leftrightharpoons$	$IR(I,I,*,P)$	k_{14}, k_{-14}	$ER_2(*,SOS(0),*,*,*,*)$			$\leftrightharpoons$	$ER_2(*,SOS(P),*,*,*,*)$	k_{11}, k_{-11}
$IR(*,*,*,P)$	+	$IRS(*)$	$\leftrightharpoons$	$IR(*,*,*,IRS(*))$	k_{15}, k_{-15}	$ER_2(*,*,0,*,*,*)$			$\leftrightharpoons$	$ER_2(*,*,P,*,*,*)$	k_{33}, k_{-33}
$IR(I,I,*,IRS(0))$			$\leftrightharpoons$	$IR(I,I,*,IRS(P))$	k_{16}, k_{-16}	$ER_2(*,*,P,*,*,*)$	+	$Grb2(*)$	$\leftrightharpoons$	$ER_2(*,*,Grb2(*),*,*,*)$	k_{34}, k_{-34}
$IR(*,*,*,IRS(P))$	+	$Grb2(*)$	$\leftrightharpoons$	$IR(*,*,*,Grb2(*))$	k_{17}, k_{-17}	$ER_2(*,*,Grb2(0),*,*,*)$	+ +	$SOS(0)$	$\leftrightharpoons$	$ER_2(*,*,SOS(0),*,*,*)$	k_9, k_{-9}
$IR(*,*,*,Grb2(0))$	+ +	$SOS(0)$	$\leftrightharpoons$	$IR(*,*,*,SOS(0))$	k_9, k_{-9}	$ER_2(*,*,Grb2(0),*,*,*)$	+ +	$SOS(P)$	$\leftrightharpoons$	$ER_2(*,*,SOS(P),*,*,*)$	k_{10}, k_{-10}
$IR(*,*,*,Grb2(0))$	+	$SOS(P)$	$\leftrightharpoons$	$IR(*,*,*,SOS(P))$	k_{10}, k_{-10}	$ER_2(*,SOS(0),*,*,*,*)$	+ +		$\leftrightharpoons$	$ER_2(*,*,SOS(P),*,*,*)$	k_{11}, k_{-11}
$IR(*,*,*,SOS(0))$			$\leftrightharpoons$	$IR(*,*,*,SOS(P))$	k_{11}, k_{-11}						
$Shc(0)$			$\leftrightharpoons$	$Shc(P)$	k_{18}, k_{-18}						
$Shc(P)$	+	$Grb2(*)$	$\leftrightharpoons$	$Shc(Grb2(*))$	k_8, k_{-8}						
$Shc(Grb2(0))$	+ +	$SOS(0)$	$\leftrightharpoons$	$Shc(SOS(0))$	k_9, k_{-9}						
$Shc(Grb2(0))$	+ +	$SOS(P)$	$\leftrightharpoons$	$Shc(SOS(P))$	k_{10}, k_{-10}						
$Shc(SOS(0))$			$\leftrightharpoons$	$Shc(SOS(P))$	k_{11}, k_{-11}						
$Grb2(0)$	+	$SOS(0)$	$\leftrightharpoons$	$Grb2(SOS(0))$	k_9, k_{-9}						
$Grb2(0)$	+ +	$SOS(P)$	$\leftrightharpoons$	$Grb2(SOS(P))$	k_{10}, k_{-10}						
$Grb2(SOS(0))$			$\leftrightharpoons$	$Grb2(SOS(P))$	k_{11}, k_{-11}						
$SOS(0)$			$\leftrightharpoons$	$SOS(P)$	k_{19}, k_{-19}						
$IRS(0)$			$\leftrightharpoons$	$IRS(P)$	k_{20}, k_{-20}						
$IRS(P)$	+	$Grb2(*)$	$\leftrightharpoons$	$IRS(Grb2(*))$	k_{17}, k_{-17}						
$IRS(Grb2(0))$	+ +	$SOS(0)$	$\leftrightharpoons$	$IRS(SOS(0))$	k_9, k_{-9}						
$IRS(Grb2(0))$	+	$SOS(P)$	$\leftrightharpoons$	$IRS(SOS(P))$	k_{10}, k_{-10}						
$IRS(SOS(0))$			$\leftrightharpoons$	$IRS(SOS(P))$	k_{11}, k_{-11}						
$ER(0,*,*)$	+	EGF	$\leftrightharpoons$	$ER(E,*,*)$	k_{21}, k_{-21}						
$ER(*,0,*)$			$\leftrightharpoons$	$ER(*,P,*)$	k_{22}, k_{-22}						
$ER(*,P,*)$	+	$Shc(*)$	$\leftrightharpoons$	$ER(*,Shc(*),*)$	k_{23}, k_{-23}						
$ER(*,Shc(0),*)$			$\leftrightharpoons$	$ER(*,Shc(P),*)$	k_{24}, k_{-24}						
$ER(*,Shc(P),*)$	+ +	$Grb2(*)$	$\leftrightharpoons$	$ER(*,Grb2(*),*)$	k_8, k_{-8}						
$ER(*,Grb2(0),*)$	+ +	$SOS(0)$	$\leftrightharpoons$	$ER(*,SOS(0),*)$	k_9, k_{-9}						

Table 4.12: Reaction rules for the considered example of EGF and insulin receptor crosstalk.

the generation of combinatorial network models and produces output files for both MATLAB and MATHEMATICA. For a numeric simulation of such a large ODE model, MATLAB is superior to MATHEMATICA. However, one simulation run with the MATLAB integrator `ode15s` took several hours using a 3.06 GHz Intel® Xeon™ CPU with 2 GB main memory. The simulation can be sped up by providing an analytically derived Jacobian matrix of the ODE system. All non-zero elements of the Jacobian matrix have been analytically calculated using MATHEMATICA and afterwards have been exported to MATLAB. The resulting simulation files have a size of over 13 MB, and a single simulation run still took about half an hour.

An exactly reduced version of the crosstalk model was generated using the reduced order modeling approach we introduced above. In order to get comparable results for all occurring binding and phosphorylation processes, each of them was chosen as output processes. The process interaction graph of the considered system can be divided into four subgraphs. Each subgraph describes one intracellular binding domain, either of the EGF or the insulin receptor. However, due to the multifunctionality of the Grb2 binding domain all four subgraphs comprise the Grb2-SOS binding process as well as the serine/threonine phosphorylation of SOS. Consequently, the four subgraphs have to be simultaneously modeled and all species have to be simultaneously balanced. The resulting model comprises 1,826 reactions and 391 ODEs, which is already a significant reduction compared to the complete model. A further reduction can be achieved by transforming the model to the previously-introduced occurrence levels and subsequent elimination of redundant, unobservable and uncontrollable system dynamics. The final and exactly reduced model of the network consists of 87 ODEs, which can be divided into six unidirectionally coupled modules. One of these modules, which consists of four ODEs, describes EGF binding and EGFR homodimerization. Another module specifies insulin binding to the insulin receptor and comprises two ODEs. Six ODEs are required to model IR phosphorylation at the IRS domain, and subsequent IRS binding. Shc binding to EGFR as well as IR and the related domain phosphorylations form another module with a total number of 18 ODEs. The largest module consists of 32 ODEs and describes Grb2 binding to the EGF receptor as well as to phosphorylated Shc. The last module comprises all variables describing SOS binding and SOS phosphorylation and consists of 25 ODEs. One simulation run of this exactly reduced model only takes a few seconds. The size of the simulation file is 37.4 KB. In Figure 4.8, it is shown that both models also provide exactly the same results for the considered output variables.

4.3.3 Conclusions

The methods for exact model reduction and reduced order modeling that have been introduced in this thesis facilitate a strong reduction of the considered crosstalk model. The complete mechanistic model, which comprises 5,182 ODEs, can be reduced to only 87 ODEs. Furthermore, the reduced model can be divided into six modules, which strongly simplifies parameter estimation or model analysis. The simulation time has been reduced by a factor of approximately five hundred. This clearly shows that these new methods are well suited to circumvent

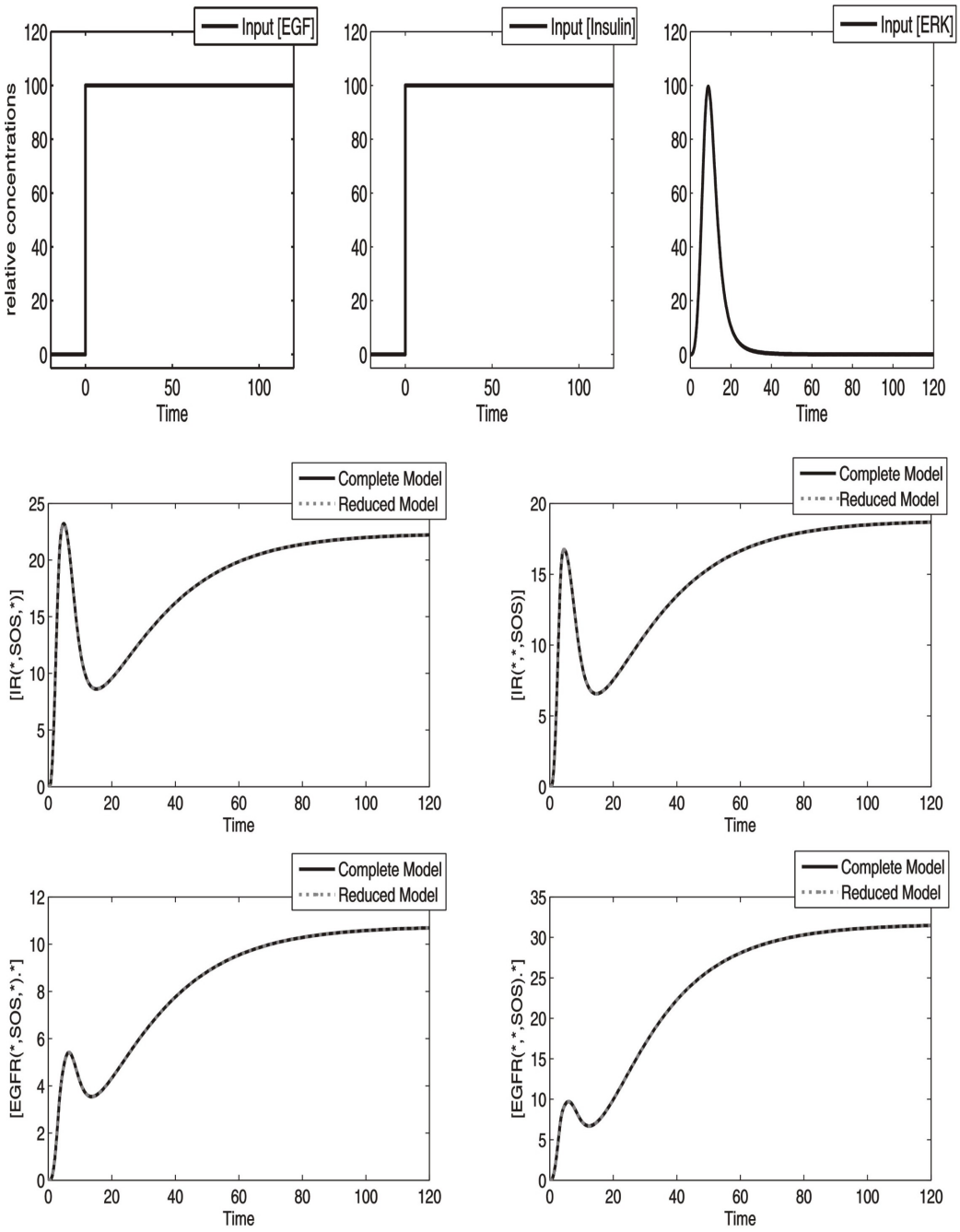

Figure 4.8: Simulation results of the generated crosstalk model. The kinetic parameters of the model have been chosen such that the system qualitatively shows the expected behavior. All quantities are depicted in relative concentrations. The overall concentrations of all involved components have been set to 100. The displayed curves show the chosen input signals $[EGF]$, $[insulin]$ and $[ERK]$ as well as the output concentrations $[IR(*,SOS,*)]$, $[IR(*,*,SOS)]$, $[EGFR(*,SOS,*).*]$ and $[EGFR(*,*,SOS).*]$.

the problems arising from combinatorial complexity in a systematic manner. Furthermore, their applicability to very complex and realistic reaction networks has been shown.

Chapter 5

Approximate Model Reduction

The previous chapter is dedicated to the exact reduction of combinatorial reaction networks. Exact reducibility is only a border case in model reduction which is only feasible if a model comprises unobservable or uncontrollable states. In general, the term model reduction refers to approximate reduction techniques. All approximate reduction methods can be viewed as a trade-off between complexity and error margin. The purpose is to find a system of minimal complexity that optimally approximates the original one in terms of the system output, for a given error margin. Conversely, one may also search for a system that approximates the original one with minimal error within the class of systems with maximal admissible complexity [5]. The development of such approximate techniques for combinatorial reaction networks is necessary, since in many cases exact reductions are not feasible or the exactly reduced models remain unmanageably large.

5.1 Approximate Model Reduction

In literature, one can find numerous contributions about approximate model reduction. A rough overview about available model reduction techniques, their main application range, as well as their drawbacks is given in the Background section. It has already been discussed that all available model reduction techniques for dynamic ODE models can be divided into two classes. Time-scale based approaches on the one hand, and observability and controllability based approaches on the other hand.

In order to develop a new approximate model reduction technique, adapted to the special requirements of combinatorial reaction networks, which provides good approximation results, both of these approaches will be combined. The main challenge of time-scale based approaches is how to find a low dimensional subspace or manifold to which all trajectories converge very quickly. The reduction of the model is achieved by projecting the real system trajectories from the n dimensional state space onto this low dimensional manifold. It is quite clear that the quicker the original trajectory converges towards the defined slow manifold, the faster an initial

error will vanish. Each manifold can be characterized by algebraic equations $\vec{\Psi}(\vec{x}) = 0$, where $\vec{x}$ is the state vector of the original system. A number of d independent algebraic equations facilitates the elimination of d ODEs and therefore a reduction of the model to $n-d$ differential equations. For linear systems, slow subspaces or manifolds can be found by an eigenvalue decomposition. For nonlinear systems, slow manifolds are rather difficult to find and are, in general, approximated. Examples of slow manifold approximations are quasi-steady state or rapid equilibrium assumptions. However, in the case of quasi-steady state assumptions, the main problem is that in many cases $\vec{\Psi}(\vec{x}) = 0$ cannot be analytically solved, or does not provide an unique solution. The application of the rapid equilibrium assumption requires knowledge about the velocity of individual reactions which is not available in many cases. Thus, one has to find a slow manifold approximation $\vec{\Psi}(\vec{x}) = 0$ on the basis of available qualitative knowledge. Another requirement is that $\vec{\Psi}(\vec{x}) = 0$ is analytically and uniquely solvable.

The approximation quality also depends on a second circumstance, namely the choice of variables which are to be eliminated. The d algebraic equations $\vec{\Psi}(\vec{x}) = 0$ can be solved for all d variables $\vec{\xi} = \vec{\phi}(\vec{x})$ that fulfill the condition

$$\operatorname{rank}\left(\frac{\partial\vec{\Psi}}{\partial\vec{\xi}}\right) = d. \tag{5.1}$$

It is quite easy to see that the choice of $\vec{\xi}$ plays a crucial role in this context. Assume that a system has one single output variable $y = x_i$. Furthermore, a slow manifold approximation $\Psi(\vec{x}) = 0$ is known. If this equation is used to replace the ODE for the state x_i, the output signals of the reduced and the original model will in general not coincide for $t = 0$. However, if another ODE is eliminated by using this algebraic equation, the two output signals will have the same starting point. The approximated model will give the best results if those variables that are only scarcely observable and controllable are replaced.

In this chapter, a new general technique will be introduced, which allows for the definition slow manifold approximations for large combinatorial reaction networks. This method is also based on the work of Borisov *et al.* [16], but focuses on another aspect than that focused on by the exact reaction method. We will then make some considerations about observability measures of combinatorial reaction networks in order to decide which states are to be replaced.

5.1.1 Starting Point

As in the case of exact model reduction, the starting point of our considerations will be the work of Borisov *et al.* [16] regarding combinatorial complexity. First, we will reconsider the previously introduced Example 2.5, namely a receptor R providing two distinct binding domains that can recruit the ligands L and E. Furthermore, we assume that both binding processes do not interact. We have already shown that the occupancy levels of this receptor can be exactly

modeled by the following two ODEs

$$\begin{aligned} \frac{d[R(L,*)]}{dt} &= \quad k_1[L]\left([R(*,*)] - [R(L,*)]\right) - k_{-1}[R(L,*)] \\ \frac{d[R(*,E)]}{dt} &= \quad k_2[E]\left([R(*,*)] - [R(*,E)]\right) - k_{-2}[R(*,E)] \end{aligned} \tag{5.2}$$

if we assume that the overall concentration $[R(*,*)]$ is constant and the concentrations $[L]$ and $[E]$ are considered as inputs. However, we have lost the information about the state variable $[R(L,E)]$. Borisov *et al.* [16] suggested the recalculation of this state on the basis of probability calculus. Since both binding processes are completely independent this approach appears reasonable. If one considers an arbitrary receptor molecule of the system, the probability of choosing one that has bound the ligand L is $P(L) = \frac{[R(L,*)]}{[R(*,*)]}$. Analogously, the probability of choosing a receptor that has recruited E is $P(E) = \frac{[R(*,E)]}{[R(*,*)]}$. Due to the independence of the two processes, the probability of choosing a receptor molecule that has bound both ligands is $P(LE) = P(L) \cdot P(E)$. From this it follows

$$[R(L,E)] = P(LE) \cdot [R(*,*)] = \frac{[R(L,*)] \cdot [R(*,E)]}{[R(*,*)]}. \tag{5.3}$$

Alternatively, this equation can be written as

$$\Psi(\vec{x}) = [R(L,E)] \cdot [R(*,*)] - [R(L,*)] \cdot [R(*,E)] = 0 \tag{5.4}$$

and defines a manifold. On the basis of the probability calculus one can formulate similar algebraic equations for much more complex combinatorial reaction networks if they comprise independent processes. Such relations build the basis for the further considerations.

5.1.2 Time-Scale Based Approaches and Slow Manifolds

Slow manifolds are nonlinear subspaces of a model's state space, to which all possible trajectories converge very quickly. Borisov *et al.* introduced algebraic relations which result from probability calculus [16]. Each set of algebraic equations can be considered as the definition of a manifold. A great property of Equation 5.4 is that it is completely independent of kinetic parameters. Furthermore, it can be analytically solved for all four state variables. However, the question remains as to whether it describes a slow manifold or is at least a good approximation of a slow manifold. If Equation 5.4 is not fulfilled, the numerical value of $\vec{\Psi}(\vec{x})$ can be considered as a measure for the approximation error of Equation 5.3. Interestingly, it can be shown by some simple calculations that this manifold is attractive and fulfills the linear differential equation

$$\dot{\Psi} + a\Psi = 0 \qquad \text{with} \qquad a = k_1[L] + k_{-1} + k_2[E] + k_{-2}. \tag{5.5}$$

Consequently, the defined manifold is invariant, for instance, if the initial conditions of the system fulfill Equation 5.4, the system trajectory will remain on the defined manifold for all

times $t > 0$. If the initial condition of the system does not fulfill Equation 5.4 the trajectory converges to this manifold.

Let us furthermore presume that the concentrations $[L]$ and $[E]$ remain constant over time. This assumption results in the example system being linear. For this linear system one can perform an eigenvalue decomposition. The eigenvalues of the system are $\lambda_1 = -k_1[L] - k_{-1}$, $\lambda_2 = -k_2[E] - k_{-2}$ and $\lambda_3 = -k_1[L] - k_{-1} - k_2[E] - k_{-2}$. Importantly, the fastest eigenvalue λ_3 coincides with the eigenvalue of Equation 5.5. Hence, all trajectories converge very quickly to the defined manifold, which therefore can be regarded as slow manifold.

Another very interesting interpretation of Equation 5.4 can be obtained by transforming it to the coordinates $[R(0,0)]$, $[R(L,0)]$, $[R(0,E)]$ and $[R(L,E)]$. The transformed equation is given by

$$[R(0,0)] \cdot [R(L,E)] - [R(L,0)] \cdot [R(0,E)] = 0 \tag{5.6}$$

or equivalently

$$\frac{[R(L,0)]}{[R(0,0)]} = \frac{[R(L,E)]}{[R(0,E)]}. \tag{5.7}$$

The same result can be derived from the rapid equilibrium assumption. If one takes the rapid equilibrium assumption for the reactions r_1 and r_2 (see Equation 2.5), this yields

$$\frac{[R(L,0)]}{[L] \cdot [R(0,0)]} = \frac{k_1}{k_{-1}} = K_{eq,1} \qquad K_{eq,1} = \frac{k_1}{k_{-1}} = \frac{[R(L,E)]}{[L] \cdot [R(0,E)]}. \tag{5.8}$$

Since both reactions have the same equilibrium constant $K_{eq,1}$, the two relations can be equated. If one additionally cancels the concentration $[L]$ the resulting formula coincide with Equation 5.7. The same equation can be derived by taking the rapid equilibrium assumption for the rates r_3 and r_4 from Example 2.5.

However, the question remains as to whether this finding is of any use for model reduction, since complete independence of processes always facilitates exact reducibility. In the considered example, Equation 5.4 does not allow for the elimination of the two states that the minimal realization (Equation 5.2) consists of. It merely facilitates the reconstruction of the eliminated unobservable state variable $[R(L,E)]$. In order to further explain how the discussed results can be used for model reduction we consider a slightly modified example. Again we consider a receptor protein with two binding domains where the first domain can recruit the ligand L. Furthermore, we assume that ligand binding induces phosphorylation of the second domain. This phosphorylated domain consecutively binds the effector E. In terms of process interactions, we take the assumption that L binding unidirectionally influences the phosphorylation of R, and that there is an all-or-none interaction between the phosphorylation and the effector binding process. The complete reaction network is depicted in Figure 5.1. A mechanistic model of this reaction network comprises seven reactions and five ODEs, if one presumes that the overall concentration of R stays constant and that $[L]$ and $[E]$ are input signals. This model cannot be exactly reduced since all five states are both observable and controllable. In contrast to the first example we considered the three processes here are not completely independent. However,

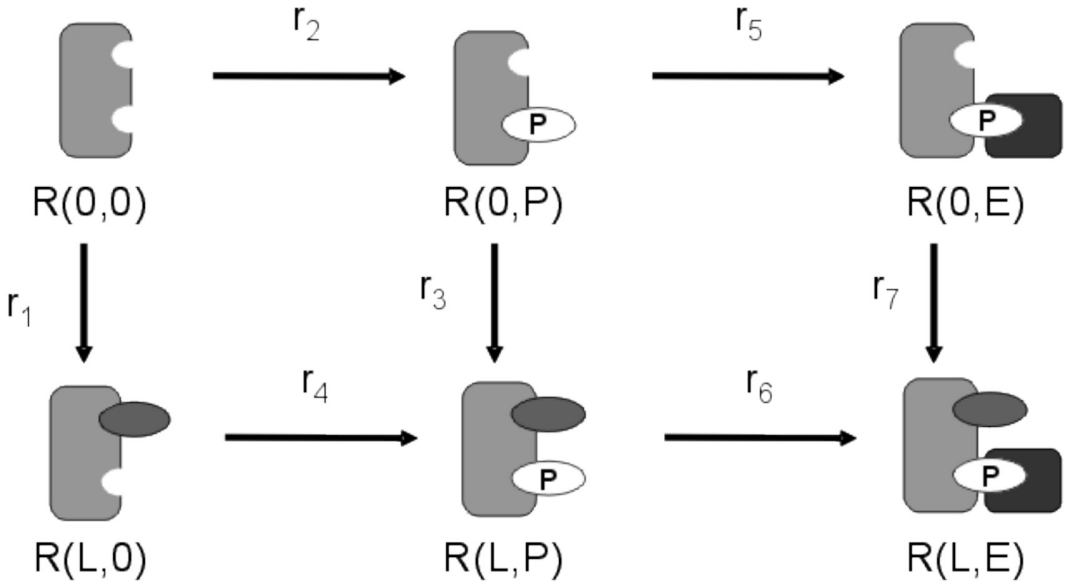

Figure 5.1: Example for approximate model reduction. The depicted reaction network is adapted from Koschorreck *et al.* [78].

L binding and E binding only interact indirectly with each other, such that L binding does not have a direct effect on E binding. The indirect influence is mediated by the phosphorylation process. Recruitment of L induces receptor phosphorylation, which in turn facilitates effector binding. The fact that the two binding processes do not directly interact, indicates that the reactions r_3 and r_7, as well as the reactions r_5 and r_6 (compare Figure 5.1), are parameterized by the same kinetic parameters respectively. These four reactions form a reaction cycle similar to the one given in the previous example. Using the rapid equilibrium assumption, one can derive an equation similar to Equation 5.4

$$[R(L,E)] \cdot [R(0,P)] - [R(L,P)] \cdot [R(0,E)] = 0. \tag{5.9}$$

Similar independent reaction cycles can be found in all combinatorial reaction networks which comprise two or more indirectly or non-interacting processes. Each of these cycles facilitates the formulation of equations like 5.9. If two processes do not interact directly, but instead interact indirectly, the model is in general not exactly reducible and the derived equations can be used to replace ODEs. We will analyze whether the assumption is justified stating that these algebraic equations still describe slow manifolds or at least slow manifold approximations, if the considered processes are not completely independent. It might be possible that indirect interactions between two processes impairs the applicability of this approach for model reduction. In contrast to the isolated reaction cycle we analyzed in the first example, such cycles are generally embedded into a larger network. Thus, if one of these cycles is analyzed, one has to take influxes and outflows into consideration. Figure 5.2 depicts such a cycle. The fluxes J_1 to J_4 can describe both influxes and outflows. The arrow only indicates that influxes correspond to positive values of J_i and outflows to negative ones. From the rapid equilibrium assumption

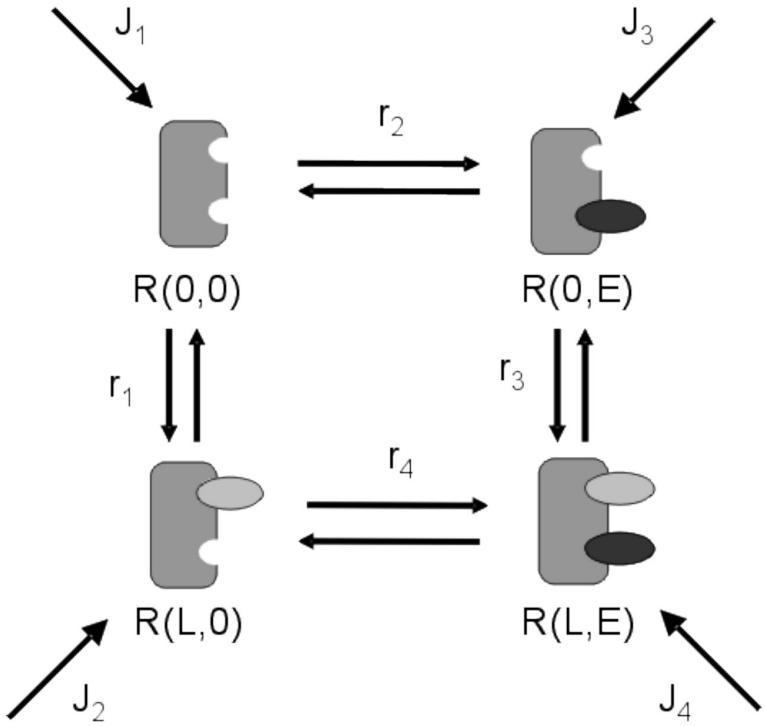

Figure 5.2: The fluxes J_i result from indirect interactions between the two considered binding processes. Since the processes are assumed to be independent, the rates r_1 and r_3 are parameterized by k_1 and k_{-1}. Additionally, the rates r_2 and r_4 are parameterized by k_2 and k_{-2}. The fluxes J_1 to J_4 can describe both influxes and outflows. The arrow only indicates that influxes correspond to positive values of J_i and outflows to negative ones.

one can deduce the equation

$$\Psi(\vec{x}) = [R(L,E)] \cdot [R(0,0)] - [R(L,0)] \cdot [R(0,E)] = 0. \tag{5.10}$$

Interestingly, the function $\Psi(\vec{x})$ still fulfills a linear differential equation. However, now this ODE is inhomogeneous

$$\dot{\Psi} + a\Psi = u(t) \tag{5.11}$$

with

$$a = k_1[L] + k_{-1} + k_2[E] + k_{-2} \tag{5.12}$$

and

$$u(t) = J_1[R(L,E)] - J_2[R(0,E)] - J_3[R(L,0)] + J_4[R(0,0)]. \tag{5.13}$$

It is apparent that the error will completely vanish if $u(t) = 0$, for example if the fluxes J_i vanish. From a thermodynamic point of view, all reaction rates have to vanish if the system reaches thermodynamic equilibrium. Thus, one can guarantee that the stationary error will be zero if the system in consideration ends up in thermodynamic equilibrium. This is the case if two major conditions are fulfilled, such that the Wegscheider conditions have to be satisfied in the whole network (compare Chapter 3), and none of the modeled concentrations is assumed

to stay constant. However, most biological reaction networks operate far from thermodynamic equilibrium, and as such, it is important to discuss the error for these cases. From ODE 5.11 one can easily derive the stationary error as

$$\Psi_s = \frac{u_s}{a}. \tag{5.14}$$

The dynamic error is given by the general solution of ODE 5.11

$$\Psi(t) = e^{-a\,t}\left(\Psi(0) + \int_0^t e^{a\,\tau} u(\tau) d\tau\right). \tag{5.15}$$

In order to provide at least a rough estimation of the maximal error we assume that

$$u(t) = u_{max} = \max\left(J_1[R(L,E)] - J_2[R(0,E)] - J_3[R(L,0)] + J_4[R(0,0)]\right). \tag{5.16}$$

With this we can give the following error bound

$$\Psi(t) \leq \Psi(0)e^{-a\,t} + \frac{u_{max}}{a}\left(1 - e^{-a\,t}\right). \tag{5.17}$$

These equations show that both the steady state error as well as the maximal dynamic error decrease for increasing values of a. These results indicate that Equation 5.11 does not describe a slow and invariant manifold but it provides a very good approximation of a slow manifold.

It has been shown that in a complex combinatorial reaction network, one can deduce simple algebraic equations for each pair of non-directly interacting processes. Due to their simple structure and their good approximation of a slow manifold, this approach seems to be very promising. The remaining question is that of which states of the original model will be replaced by these algebraic relations in order to minimize the error of the output variables.

5.1.3 Observability Based Considerations

One essential requirement for observability based considerations in model reduction is the availability of a suitable measure. For linear systems, such measures can be easily obtained and are widely used, namely the previously introduced observability and controllability gramians

$$\begin{aligned} \mathcal{Q} &= \int_0^\infty e^{A^T t} C^T C e^{At} dt \\ \mathcal{P} &= \int_0^\infty e^{At} B B^T e^{A^T t} dt. \end{aligned} \tag{5.18}$$

Here, the matrices A, B and C represent the dynamic matrix, the input matrix and the output matrix of the considered linear system (see Equation 2.10 in Chapter 2) respectively. These gramians help to quantify the amount of energy obtained, by observing the output if the initial condition of the system is $\vec{x}_0$, as well as the energy needed to steer the system from the state $\vec{0}$ to $\vec{x}$:

$$\mathcal{E}_O = \vec{x}_0^T \mathcal{Q} \vec{x}_0 \qquad \mathcal{E}_C = \vec{x}^T \mathcal{P}^{-1} \vec{x}. \tag{5.19}$$

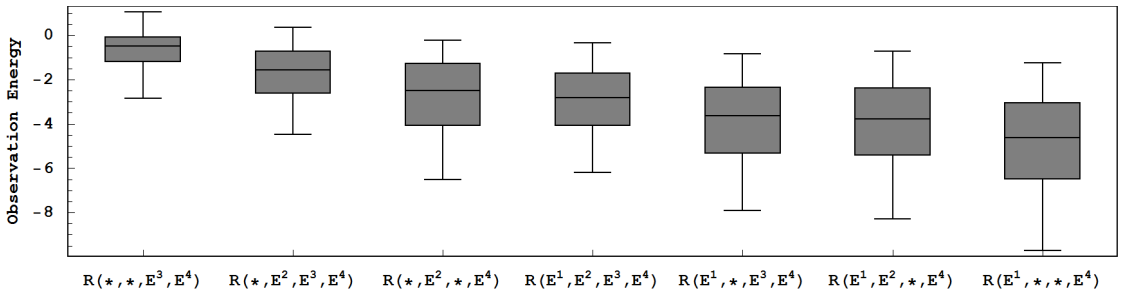

Figure 5.3: This Figure depicts the results of a statistical analysis of the dependence between observation energies and kinetic parameters. First, the model equations of the example introduced in Table 5.1 is linearized. The linearized model is used to calculate the observability gramian $\mathcal{Q}$. The state $[R(*,*,*,E^4)]$ has been chosen as model output. The diagonal matrix elements of $\mathcal{Q}$ correspond to the observation energies for unitary disturbance of all individual model states. These values are chosen as a measure to rate the observability of the considered system's coordinates. For different sets of parameters these values vary over several orders of magnitude. Therefore, we took $50,000$ arbitrary parameter sets and compared the relative difference of the resulting observation energies. In this Figure, the results for the states of the fourth module are shown. All observation energies are divided by the observation energy obtained for a unitary disturbance of the output variable $[R(*,*,*,E^4)]$. Hence, the data is normalized such that the observation energy for $[R(*,*,*,E^4)]$ is always equal to one. The logarithm of these normalized observation energies is plotted on the ordinate. The boxes span the distance between the 25% and the 75% quantile surrounding the median. The whiskers span the data from the 10% quantile to the 90% quantile.

The related reduction approach, called balanced truncation, which is also introduced in Chapter 2, eliminates the most scarcely observable and controllable system dynamics. This approach is only applicable to linear systems and an equivalently practical approach for nonlinear systems is not available. However, the gramians $\mathcal{Q}$ and $\mathcal{P}$ can be calculated for linearized model equations. They can give hints as to which system states are more or less observable or controllable. We will focus on the observability gramian $\mathcal{Q}$ in order to determine which states will be replaced by the algebraic equations derived previously.

As a starting point, we will consider a complete mechanistic model of a combinatorial reaction network that has been transformed according to the transformation suggested in Chapter 4. Furthermore, we assume that the system is not exactly reducible. Due to the hierarchical configuration of the transformation pattern and, of the resulting transformed model equations, one might hypothesize that this transformation not only realizes a Kalman decomposition, but also sorts the system states according to their grade of observability. If this hypothesis is true, the model equations will not have to be transformed anew. The perpetuation of the hierarchically structured system coordinates has the additional advantage that the modular model structure is preserved, and that the model variables keep their biological interpretability. However, note that due to the enormous variability of combinatorial reaction networks, such a hypothesis cannot be proved generally, but rather substantiated. For this purpose, we will consider and analyze

$R(0,*,*,*)$	$+$	E^1	$\leftrightharpoons$	$R(E^1,*,*,*)$	k_1, k_{-1}
$R(0,0,*,*)$	$+$	E^2	$\leftrightharpoons$	$R(0,E^2,*,*)$	k_2, k_{-2}
$R(E^1,0,*,*)$	$+$	E^2	$\leftrightharpoons$	$R(E^1,E^2,*,*)$	k_3, k_{-3}
$R(*,0,0,*)$	$+$	E^3	$\leftrightharpoons$	$R(*,0,E^3,*)$	k_4, k_{-4}
$R(*,E^2,0,*)$	$+$	E^3	$\leftrightharpoons$	$R(*,E^2,E^3,*)$	k_5, k_{-5}
$R(*,*,0,0)$	$+$	E^4	$\leftrightharpoons$	$R(*,*,0,E^4)$	k_6, k_{-6}
$R(*,*,E^3,0)$	$+$	E^4	$\leftrightharpoons$	$R(*,*,E^3,E^4)$	k_7, k_{-7}

Table 5.1: Reaction rules for the considered receptor with four binding domains. The four binding domains activate each other unidirectionally. The resulting complete mechanistic model comprises 15 ODEs and cannot be exactly reduced.

the model of a receptor with four binding domains as an example. Furthermore, we assume that the first domain has an unidirectional influence on the second, which in turn unidirectionally interacts with the third, and finally the third domain unidirectionally affects the fourth one. This network can be described by the reaction rules depicted in Table 5.1. A complete mechanistic model of this network is made up of 20 different individual species and 32 reactions. Due to conservation relations, the number of ODEs can be reduced to 15. However, the model does not comprise unobservable or uncontrollable states, but the transformed system can still be split into four modules. The first module describes the level of occupancy of the first domain and solely consists of one ODE for $[R(E^1,*,*,*)]$. The second module describes the occupancy level of the second domain, however, consists of two ODEs for $[R(*,E^2,*,*)]$ and $[R(E^1,E^2,*,*)]$. The third and fourth module accordingly describe the occupancy level of the third and fourth domain and comprise four and eight ODEs respectively. The third module consists of the states $[R(*,*,E^3,*)]$, $[R(*,E^2,E^3,*)]$, $[R(E^1,*,E^3,*)]$ and $[R(E^1,E^2,E^3,*)]$. Consequently, the last module includes the states $[R(*,*,*,E^4)]$, $[R(E^1,*,*,E^4)]$, $[R(*,E^2,*,E^4)]$, $[R(*,*,E^3,E^4)]$, $[R(E^1,E^2,*,E^4)]$, $[R(E^1,*,E^3,E^4)]$, $[R(*,E^2,E^3,E^4)]$ and $[R(E^1,E^2,E^3,E^4)]$. The size of these modules obviously depends on the number of processes that directly or indirectly influence the described occupancy level. No process has an influence on the first domain. The second domain is only affected by the first one. For this reason the second module also comprises the state $[R(E^1,E^2,*,*)]$ which can be interpreted as mediator of this direct interaction. According to this interpretation the state $[R(*,*,E^3,E^4)]$ would mediate the direct interaction between the third and fourth domain, while the other states of the fourth module can be considered as mediators of the indirect interactions. Furthermore, we can hypothesize that indirect interactions might have a lower impact than direct interactions, which would suggest that the states $[R(E^1,*,*,E^4)]$, $[R(*,E^2,*,E^4)]$, $[R(E^1,E^2,*,E^4)]$, $[R(E^1,*,E^3,E^4)]$, $[R(*,E^2,E^3,E^4)]$ and $[R(E^1,E^2,E^3,E^4)]$ only play a minor, or at least a less important role than $[R(*,*,E^3,E^4)]$. In order to substantiate these considerations, the module will be analyzed in more detail using the observability gramian $\mathcal{Q}$. First the model equations are linearized and the observability gramian is calculated with $[R(*,*,*,E^4)]$ being the only output variable. Kinetic parameters

and steady state concentrations are arbitrarily chosen out of a large interval comprising of several orders of magnitude. With these parameters the observability gramian is evaluated. The diagonal matrix elements correspond to the observation energies for unitary disturbance of all individual model states. These values can be considered as measures to rate the observability of the chosen system coordinates. For different sets of parameters these values also vary over several orders of magnitude. Therefore, we took $50,000$ arbitrary parameter sets and observed the relative difference of the resulting observation energies. The results of this analysis for all states of the fourth module are depicted in Figure 5.3, which shows that in the majority of cases the two states $[R(*,*,*,E^4)]$ and $[R(*,*,E^3,E^4)]$ play the most important role. This corresponds to our expectation that the state which mediates the direct interaction is more important than those that mediate indirect interactions. If algebraic relations are formulated for all independent cycles of the network, the six ODEs of this module that mediate indirect effects can be eliminated. Thus, it can be stated that in general one should not replace states that mediate direct process interactions. Similar results can be obtained by analyzing other combinatorial network models with the same method.

In conjunction with the presented method to derive simple parameter-free slow manifold approximations, one can generate strongly reduced models of combinatorial networks and still achieve a very good approximation quality. This will be further explained below by applying this method to the exactly reduced model of EGF and Insulin crosstalk, introduced in Chapter 4.

5.2 Approximate Modeling Techniques

In the previous chapter we discussed the fact that in most cases model *reduction* is problematic since the unreduced models are far too large to be generated. A direct generation of the reduced model equations would be desirable. For exact model reduction we could present a general method that allows for the direct generation of reduced models. For the approximate reduction technique introduced above, an appropriate approximate modeling technique exists, as developed by Koschorreck *et al.* [78]. The presented method is based on a formal division of the complete reaction network into modules or *layers*, according to the occurring process interactions. Different layers are characterized by the fact that they only interact via all-or-none interactions. Thus, it can be guaranteed that each reaction cycle formed by two processes of different layers is an independent cycle, as depicted in Figure 5.2. The modeling method facilitates the direct generation of a reduced model which incorporates all equations $\vec{\Psi}(\vec{x}) = 0$ which can be deduced from these independent cycles. A drawback of this method is that it cannot cover reductions that are based on independent cycles within one layer. However, it allows for a large class of physiological cases to be handled. Koschorreck *et al.* [78] showed that a reduced model of early events in insulin signaling can be generated with this method consisting of 214 ODEs, whereas a complete mechanistic model would comprise nearly $1.5 \cdot 10^8$ ODEs. This enormous reduction shows the great practical use of the method. Since the described

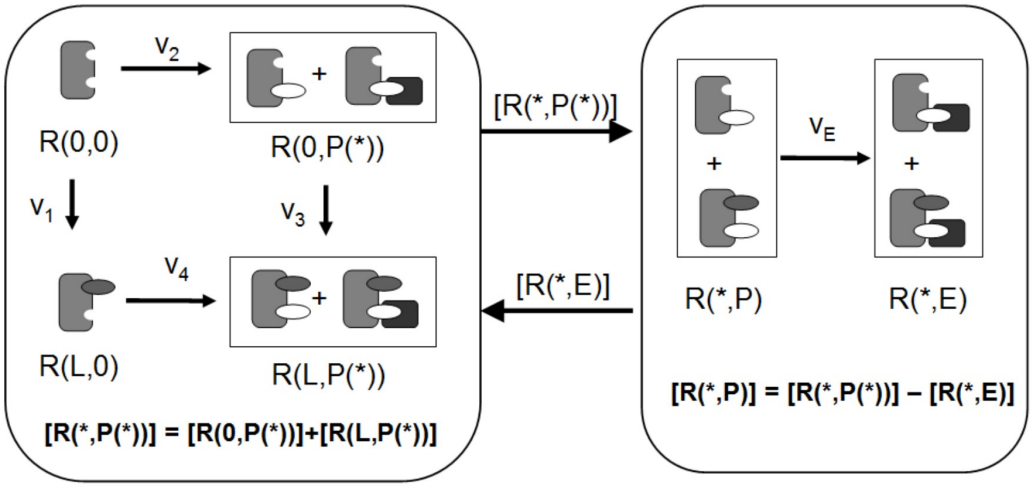

Figure 5.4: In this example system, the left module is the receptor layer which includes ligand binding and receptor phosphorylation. The right module corresponds to the effector layer, where binding of E to the phosphorylated binding site on R is described. Note that one could also compute $[R(*, P)]$ in the receptor layer and transfer this quantity to the effector layer instead of $[R(*, P(*))]$. This choice is up to the modeler. We suggest the transfer of $[R(*, P(*))]$, since this variable is a macroscopic quantity which corresponds to experimental readouts.

approximate reduced order modeling approach has not been developed in the framework of this thesis, the reader is referred to the work of Koschorreck *et al.* [78] for further theoretic details. In the following section, we will further explain the method by considering the simple example depicted in Figure 5.1

5.2.1 Layer-Based Modeling Approach: An Example

In order to introduce the layer-based reduced modeling concept suggested by Koschorreck *et al.* [78], the example shown in Figure 5.1 will be considered in order to illustrate the main features. It is presumed that ligand binding unidirectionally influences receptor phosphorylation, which in turn is an essential precondition for effector binding. Ligand binding and effector binding do not interact directly. From this it follows that the reaction rates r_1, r_3 and r_7 are all parameterized by the same kinetic rate constants. The same holds true for the reaction rates r_5 and r_6. The model can be split into two layers. The receptor layer describes ligand binding and receptor phosphorylation, the effector layer describes effector binding (compare Figure 5.4). There is an unidirectional interaction within the receptor layer and an all-or-none interaction between the two layers. In this simple case, no further interactions occur within the effector layer. The states of the reduced model generally represent lumped states, for instance they correspond to sums of micro-states or, in special cases, to single micro-states. In the example $[R(0, 0)]$ and $[R(L, 0)]$ correspond to micro-states. The lumped states $[R(0, P(*))]$ and

$[R(L,P(*))]$ are pools for all species which are phosphorylated, incorporating the phosphorylated species that have recruited an effector. $[R(*,P)]$ and $[R(*,E)]$ are pools for species with no regard to ligand binding. Mathematically, the states of the reduced model can be defined as

$$\begin{aligned}
[R(0,0)] &= [R(0,0)] \\
[R(L,0)] &= [R(L,0)] \\
[R(0,P(*))] &= [R(0,P)] + [R(0,E)] \\
[R(L,P(*))] &= [R(L,P)] + [R(L,E)] \\
[R(*,P)] &= [R(0,P)] + [R(L,P)] \\
[R(*,E)] &= [R(0,E)] + [R(L,P)].
\end{aligned} \tag{5.20}$$

Observe, that these six equations are linearly dependent. $[R(*,P)]$ or $[R(*,E)]$ can be expressed by using a conservation relation

$$[R(0,P(*))] + [R(L,P(*))] = [R(*,P)] + [R(*,E)] = [R(*,P(*))]. \tag{5.21}$$

The connection between the two layers, in other words, the information exchange, is given by the two states $[R(*,P(*))]$ and $[R(*,E)]$. As depicted in Figure 5.4 the sum of phosphorylated binding sites $[R(*,P(*))]$ is passed to the effector layer, and the sum of occupied binding sites $[R(*,E)]$ is passed to the receptor layer. If one compares the reactions of the reduced model (Figure 5.4) and the reactions of the detailed model (Figure 5.1), one finds

$$\begin{aligned}
v_1 &= r_1 \qquad & v_2 &= r_2 \qquad & v_3 &= r_3 + r_7 \\
v_4 &= r_4 \qquad & v_E &= r_5 + r_6.
\end{aligned}$$

As already mentioned, the reaction rates that are merged together, namely r_3 and r_7 as well as r_5 and r_6, have the same kinetic rate constants. Our model will provide equations for all variables that are given in Equation 5.20. Hence, all the original variables occurring in the new reaction rates v_i have to be replaced by expressions which only comprise the new variables defined in Equation 5.20. v_1, v_3 and v_E can be written using the new state variables defined in Equation 5.20. However, for an exact formulation of the rates v_2 and v_4, the micro-states $[R(0,P)]$ and $[R(L,P)]$ are required. Due to the linear dependence of Equations 5.20 an exact reconstruction of these micro-states is not possible. They can only be approximated by

$$\begin{aligned}
[R(0,P)] &= \frac{[R(*,P(*))] - [R(*,E)]}{[R(*,P(*))]} [R(0,P(*))] \\
[R(L,P)] &= \frac{[R(*,P(*))] - [R(*,E)]}{[R(*,P(*))]} [R(L,P(*))].
\end{aligned} \tag{5.22}$$

The expression $c_I = \frac{[R(*,P(*))]-[R(*,E)]}{[R(*,P(*))]}$ can be considered as a correction term corresponding to the fraction of phosphorylated binding sites which are unoccupied. The correction term c_I can also be regarded as the percentage of phosphorylated but unliganded binding domains.

Here, one takes the assumption that this percentage is not affected by L binding. This directly corresponds to the assumption that L and E binding are independent, which is the basis of the previously discussed model reduction technique. The rates v_2 and v_4 can be written as

$$v_2 = k_2[R(0,0)] - k_{-2}\frac{[R(*,P(*))]-[R(*,E)]}{[R(*,P(*))]}[R(0,P(*))] \tag{5.23}$$

$$v_4 = k_4[R(L,0)] - k_{-4}\frac{[R(*,P(*))]-[R(*,E)]}{[R(*,P(*))]}[R(L,P(*))]. \tag{5.24}$$

As occupied binding sites cannot be dephosphorylated, the concentration $[R(0,P(*))]$ has to be multiplied by the correction term c_I. The resulting model is given by

$$\begin{aligned}
[R(0,0)] &= [R(*,*)] - [R(L,0)] - [R(0,P(*))] - [R(L,P(*))] \\
\frac{d[R(L,0)]}{dt} &= v_1 - v_4 \\
\frac{d[R(0,P(*))]}{dt} &= v_2 - v_3 \\
\frac{d[R(L,P(*))]}{dt} &= v_3 + v_4 \\
\frac{d[R(*,E)]}{dt} &= v_E.
\end{aligned} \tag{5.25}$$

These equations are equivalent to a complete mechanistic model of the system in which the micro-state $[R(L,E)]$ has been replaced by the algebraic equation 5.9. It is only given in a linearly transformed state space representation. One can analytically show that the combination of Equations 5.20 with Equation 5.9 allows for the reconstruction of all micro-states and leads to the result given in Equations 5.22.

5.3 Example: EGF and Insulin Receptor Crosstalk

The exactly reduced model of EGF and insulin receptor crosstalk that has been introduced in Chapter 4, still comprises 87 ODEs. The new approximate reduction methods facilitate the further elimination of numerous model variables. In order to rate the approximation quality of the method, the simulation results of the reduced model will be compared both with the exact model as well as with a reduced model version obtained by Proper Orthogonal Decomposition (POD).

5.3.1 Layer-Based Approach

The term layer-based approach has been introduced by Koschorreck *et al.* [78] and describes the reduced order modeling approach discussed above. In this thesis, the same term will also be used to characterize the related model reduction method. This method will be used to further reduce the exactly reduced model of EGF and insulin receptor crosstalk, discussed in Chapter 4. Since the exact model consisting of 87 ODEs has already been generated a model reduction approach

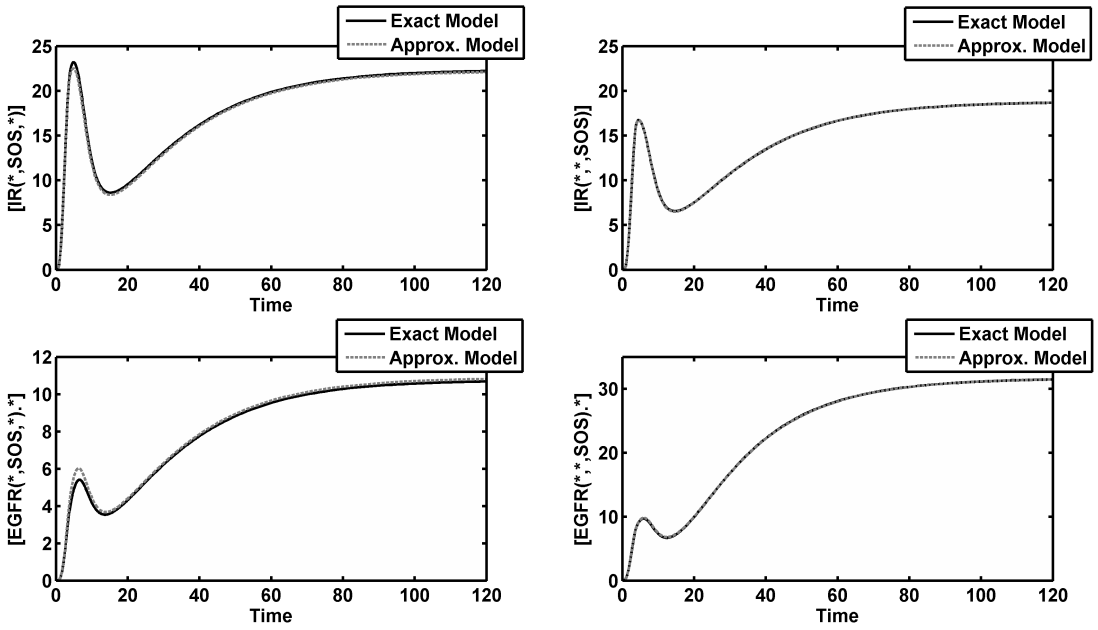

Figure 5.5: In this Figure the simulation results obtained from the approximately reduced 41 ODE model of EGF and insulin receptor crosstalk are compared with the simulation results of the exact 87 ODE model. For [EGF], [Ins] and [ERK] we have chosen the input functions depicted in Figure 4.8. Both models show nearly the same dynamics for the chosen output variables.

is suggested. Many of the occurring binding and modification processes do not interact directly with each other. Each pair of these processes forms at least one independent reaction cycle and thus facilitates the formulation of algebraic equations $\vec{\Psi}(\vec{x}) = 0$ as discussed above. However, note that a great number of these cycles do not play a crucial role in the further reduction of the network, since they have already been eliminated by the exact reduction. Let us consider the phosphorylation of the two intracellular IR binding domains. These two phosphorylation processes do not interact directly, however both processes are completely decoupled and part of different interaction subgraphs. In the modeling step each of these interaction subgraphs was separately translated into model equations. Consecutively, the reduced model does not comprise any reaction cycle formed by the two phosphorylation processes. Only processes that are part of the same interaction subgraph can be considered. We will focus on the subgraph which describes direct binding of Grb2 to the EGF receptor. In this subgraph, EGF binding and receptor phosphorylation do not interact directly. The corresponding independent reaction cycle for EGF receptor (EGFR) monomers yields

$$[EGFR(0,\#,0)] \cdot [EGFR(EGF,\#,P)] - [EGFR(EGF,\#,0)] \cdot [EGFR(0,\#,P)] = 0. \quad (5.26)$$

It has been shown earlier that an equivalent formulation is given by

$$[EGFR(*,\#,*)] \cdot [EGFR(EGF,\#,P)] - [EGFR(EGF,\#,*)] \cdot [EGFR(*,\#,P)] = 0. \quad (5.27)$$

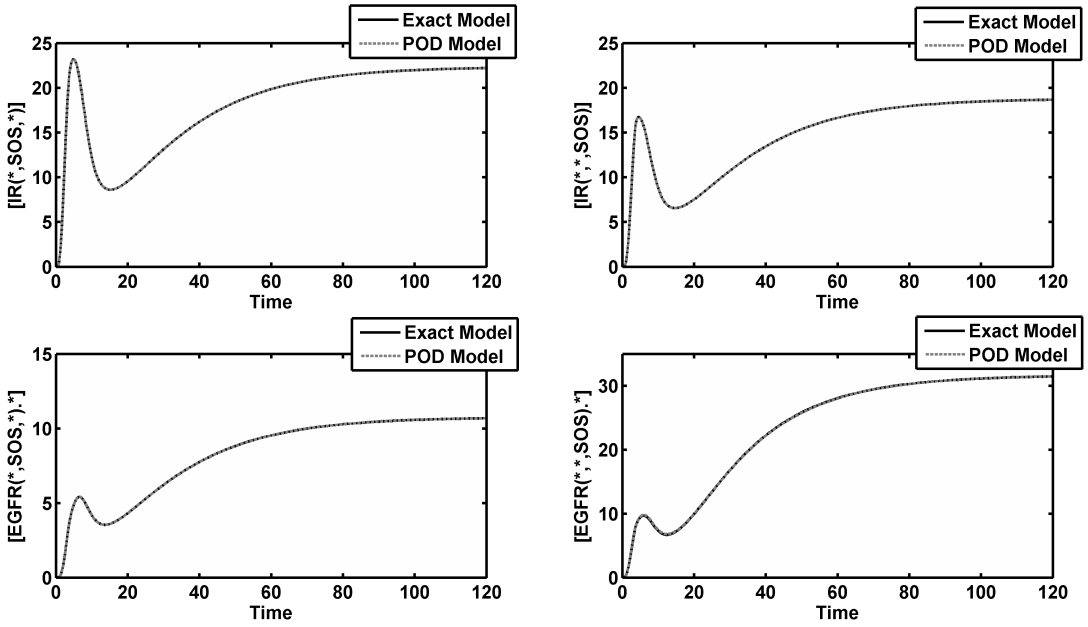

Figure 5.6: Using the POD reduction approach the exact 87 ODE model can be reduced to a 15 ODE model. In this Figure the simulation results obtained from the exact and the POD reduced model are compared. For [EGF], [Ins] and [ERK] we have again chosen the input functions depicted in Figure 4.8. Both models show nearly the same dynamics for the chosen output variables. Thus, POD facilitates the elimination of a higher number of ODEs. However, the reduced model cannot be modularized like the one obtained by the layer-based method.

This formulation is more convenient for the reduction of the considered model, since it also comprises occupancy or occurrence levels. These equations can only be used for model reduction if all occurring variables are state variables of the exactly reduced model. However, in the exactly reduced model, $[EGFR(*,\#,*)]$ has been eliminated due to the existing conservation relation for the EGF receptor

$$[EGFR(*,\#,*).*] = 2[EGFR_2(*,\#,*,*,\#,*)] + [EGFR(*,\#,*)]. \tag{5.28}$$

The inclusion of this conservation relation yields as a final formulation

$$[EGFR(EGF,\#,P)] = \frac{[EGFR(EGF,\#,*)] \cdot [EGFR(*,\#,P)]}{[EGFR(*,\#,*).*] - 2[EGFR_2(*,\#,*,*,\#,*)]}. \tag{5.29}$$

This equation has already been solved for the variable $[EGFR(EGF,\#,P)]$ which will be replaced in the model. Analogously, one can formulate further algebraic relations for other independent reaction cycles of EGFR monomers such as in the example

$$[EGFR(EGF,\#,Grb2)] = \frac{[EGFR(EGF,\#,P)] \cdot [EGFR(*,\#,Grb2)]}{[EGFR(*,\#,P)]}. \tag{5.30}$$

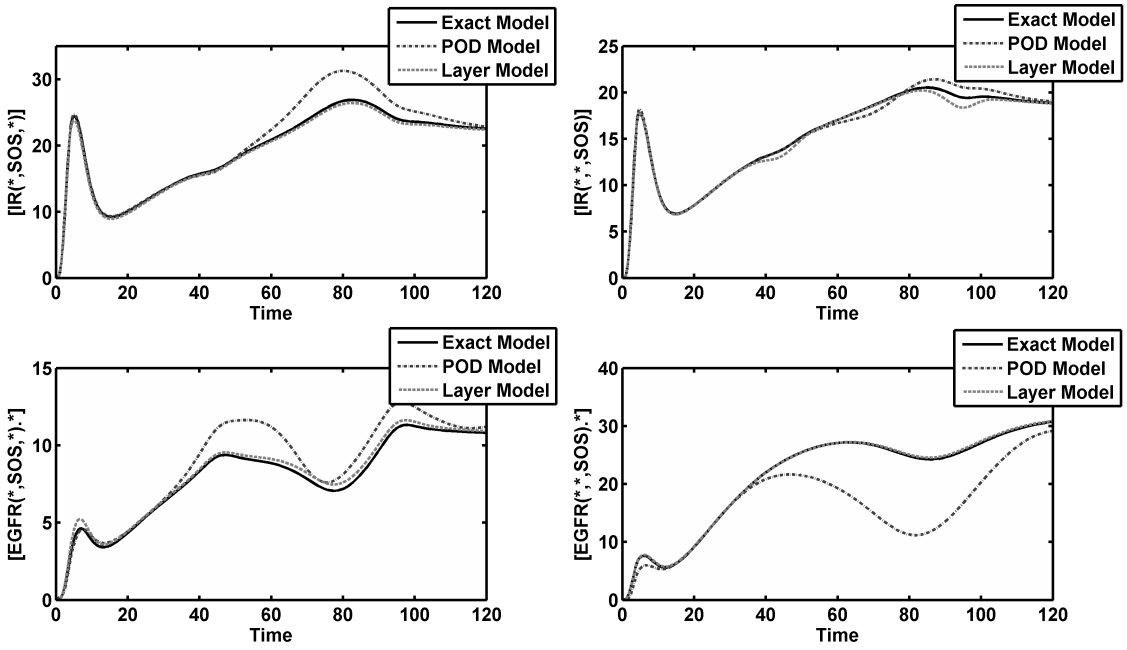

Figure 5.7: Comparison of the exact 87 ODE model with the two reduced models obtained by the layer-based approach and by POD. As input functions we have chosen [EGF]=50 $\left(\sin(\frac{1}{8}t)+1\right)$ and [Ins]=50 $\left(\sin(\frac{1}{14}t)+1\right)$. The input function of [ERK] is the same as before (see Figure 4.8). The simulation results show that the layer-based model provides a much better approximation of the real system dynamics than the POD model.

The same approach also facilitates the replacement of dimeric state variables such as

$$[EGFR_2(EGF,\#,P,*,\#,*)] = \frac{[EGFR_2(EGF,\#,*,*,\#,*)]\cdot[EGFR_2(*,\#,P,*,\#,*)]}{2[EGFR_2(*,\#,*,*,\#,*)]}. \tag{5.31}$$

Following this approach, 46 algebraically independent equations can be formulated. Thus, the exact model can be reduced from 87 to 41 ODEs. As it can be seen in Figure 5.5 the approximation quality is fairly accurate and emphasizes the utility of the developed approach.

5.3.2 Layer-Based Approach vs. POD

A widely used model reduction approach for nonlinear systems is the so-called proper orthogonal decomposition. The method has already been discussed from a mathematical point of view in Chapter 2. This approach is based on a singular value decomposition of a matrix $\mathcal{X}$ which is composed of snapshots of the state trajectory $\vec{x}(t_k)$ with $k = 1...N$. The main drawback of this method is that the complete model has to be simulated and then transformed, which can be very complex. Furthermore, a good approximation quality can only be guaranteed for the input functions that are used to generate the trajectory snapshots for the matrix $\mathcal{X}$. In the

considered example, we again use step functions for $[EGF]$ and $[Ins]$ and a bell-shaped curve for activated ERK ($[ERK]$) to generate $\mathcal{X}$.

The singular value decomposition of the resulting matrix $\mathcal{X}$ indicates that one can reduce the model to only 15 ODEs. A comparison of the exact 87 ODE model and the reduced 15 ODE model shows that the reduced model accurately describes the system behavior for the defined inputs (see Figure 5.6). However, the approximation error can grow much larger if the reduced model is stimulated with other input signals. As an alternative input signal we choose an oscillating EGF and insulin concentration. The ERK signal has remained unchanged. In Figure 5.7 the simulation results of the exact model and the two reduced models are compared. The model deduced with the layer-based approach provides a much more accurate approximation of the real system behavior than the approximation of the 15 ODE model resulting from POD.

5.4 Conclusions

The approximate reduction method presented in this chapter is based on the derivation of slow manifold approximations and therefore can be considered as a time-scale separation method. The derived algebraic equations are parameter-free and can be analytically solved due to their simple structure. Furthermore, the approximation error can be quantified in a very simple manner, and it can be shown that the stationary error is zero for all reaction networks fulfilling the Wegscheider conditions as discussed in Chapter 3.
The numerical analysis of observability gramians for linearized model equations additionally indicates that the derived algebraic equations should be used to replace those variables that solely mediate indirect interactions. Thus, the proposed method combines a time-scale based approach with an observability based one. The considered example of EGF and Insulin receptor crosstalk shows that this method provides excellent approximation qualities and leads to even better results than the POD method.

Chapter 6

Conclusions and Outlook

Mathematical models of biochemical reaction networks play an increasing role in cytological research. Most of the underlying reaction networks are far too complex to facilitate an intuitive understanding. In this thesis, the focus is on ODE based dynamic modeling of receptor mediated signal transduction in mammalian cells, such as insulin, epidermal growth factor (EGF) or tumor necrosis factor (TNF) signaling. These systems are of special interest since malfunctions within these signaling cascades can cause maladies such as cancer, diabetes mellitus or neurodegenerative disorders [92]. These networks share some common features. Ligand binding to a receptor triggers conformational changes that facilitate receptor dimerization and/or phosphorylation of numerous residues. The subsequent formation of multiprotein signaling complexes on these receptors and their scaffolding adaptor proteins initiates a variety of signaling pathways. The main problem that occurs in modeling these networks using common modeling strategies is the enormous number of feasible multiprotein species and the high complexity of the related reaction networks. The number of multiprotein species and reactions grows exponentially with the number of binding domains and can easily reach several millions or even more [56, 30].

The main contribution of this thesis for ODE based modeling of signal transduction pathways is the provision of new model reduction and reduced order modeling techniques that allow for the generation of manageable reduced models, which account for the dynamic effects of combinatorial complexity. A detailed analysis of these combinatorial reaction networks revealed that these systems are highly restricted by elementary thermodynamic constraints. The mathematical constraints that follow from the principle of detailed balance or microscopic reversibility [101, 102] reduce the number of kinetic model parameters and imply certain restrictions on interactions among binding and modification processes.
These analyses build the basis for the developed model reduction and reduced order modeling approaches. For common input and output signals, the number of unobservable and uncontrollable model states depends on the occurring process interactions, and tend to be fairly high for a complete mechanistic model. The elimination of uncontrollable and unobservable state variables can be achieved by a linear and hierarchically structured state space transformations, which additionally facilitate a modularization of the model equations. Since this approach does

not affect the input/output behavior of the system, it is often referred to as an exact model reduction approach. Due to the enormous size of many real signaling cascades the generation of a complete mechanistic model and its subsequent reduction is not practical. An alternative approach is directly based on the process interaction pattern of the considered system. All occurring process interactions can be integrated in an interaction graph which is subsequently split into independent interaction subgraphs. If these subgraphs are modeled individually, the resulting ODE system contains the same information as the exactly reduced one.
Process interactions also play an important role in the approximate reduction approach introduced here. This approach combines time-scale based and observability based model reduction techniques and is adapted to the special requirements of combinatorial reaction networks. If two arbitrary molecular processes do not directly interact with each other this information can be used to formulate slow manifold approximations with good convergence properties. A projection of the system trajectories onto the slow manifold approximation provides a reduced model structure.
Both the exact and the approximate techniques are used to generate a reduced model of EGF and insulin receptor crosstalk. These methods allow for the reduction of the complete mechanistic model with 5,182 ODEs to only 41. Simulation studies show that the approximation quality that can be achieved using these methods is very good.

Thus, the results of this thesis provide new and powerful tools for dynamic modeling of combinatorial reaction networks such as those occurring in signal transduction. The performed analyses of thermodynamic constraints in these networks yield descriptive interpretations of these restrictions on the level of process interactions. Furthermore, we discuss a new and systematic approach to parameterize combinatorial reaction networks in a thermodynamically consistent manner. The introduced reduction techniques facilitate the generation of fairly reduced and modularized dynamic models which in general have a negligible approximation error. The modular structure of the resulting models also reduces the complexity of parameter estimation. Furthermore, the availability of an alternative reduced order modeling approach for both exact and approximate reduction techniques also facilitates the handling of very large and complex signaling networks. This property is of immense practical relevance since most real signaling cascades are too complex to be translated into a complete mechanistic model to be subsequently reduced.

Several promising extensions of the approximate reduction technique as well as the layer-based modeling approach are possible. In analogy to the rapid equilibrium based derivation of algebraic equations $\vec{\Psi}(\vec{x}) = 0$ for independent reaction cycles, similar equations can be derived for mutually interacting processes. It is quite obvious that this extended reduction approach will have a smaller scope of application, but may still be helpful under certain conditions. The layer-based reduced order modeling approach, as introduced by Koschorreck *et al.* [78], does not cover all reductions possible by the proposed approximate reduction technique. The development of an extended layer-based approach which also incorporates the possible reductions within one layer would be a desirable improvement. Finally, all the developed techniques should be combined and implemented in software tools like ProMoT, BioNetGen or Copasi [59, 13, 50].

All discussed reduction or reduced modeling procedures follow a systematic algorithm which therefore can be automated without difficulty. The integration of the developed methods into a commonly used software tool which also supports modeling of metabolic pathways can also be very helpful to model the interactions between metabolic and signaling pathways.

Bibliography

[1] T. E. Adams, V. C. Epa, T. P. Garrett, and C. W. Ward. Structure and function of the type 1 insulin-like growth factor receptor. *Cell Mol Life Sci*, 57(7):1050–1093, Jul 2000.

[2] B. Alberts, A. Johnson, J. Lewis, M. Raff, K. Roberts, and P. Walter. *Molecular biology of the cell*. Garland Publishing Inc,US, 2002.

[3] Andres Alonso, Joanna Sasin, Nunzio Bottini, Ilan Friedberg, Iddo Friedberg, Andrei Osterman, Adam Godzik, Tony Hunter, Jack Dixon, and Tomas Mustelin. Protein tyrosine phosphatases in the human genome. *Cell*, 117(6):699–711, Jun 2004.

[4] I. Alroy and Y. Yarden. The ErbB signaling network in embryogenesis and oncogenesis: signal diversification through combinatorial ligand-receptor interactions. *FEBS Lett*, 410(1):83–86, Jun 1997.

[5] AC Antoulas. *Approximation of Large-Scale Dynamical Systems*. SIAM, 2004.

[6] A. P. Arkin. Synthetic cell biology. *Curr Opin Biotechnol*, 12(6):638–644, Dec 2001.

[7] A. R. Asthagiri and D. A. Lauffenburger. A computational study of feedback effects on signal dynamics in a mitogen-activated protein kinase (MAPK) pathway model. *Biotechnol Prog*, 17(2):227–239, 2001.

[8] J. Baulida, M. H. Kraus, M. Alimandi, P. P. Di Fiore, and G. Carpenter. All ErbB receptors other than the epidermal growth factor receptor are endocytosis impaired. *J Biol Chem*, 271(9):5251–5257, Mar 1996.

[9] Daniel A Beard, Eric Babson, Edward Curtis, and Hong Qian. Thermodynamic constraints for biochemical networks. *J Theor Biol*, 228(3):327–333, Jun 2004.

[10] Daniel A Beard, Shou dan Liang, and Hong Qian. Energy balance for analysis of complex metabolic networks. *Biophys J*, 83(1):79–86, Jul 2002.

[11] Daniel A Beard and Hong Qian. Thermodynamic-based computational profiling of cellular regulatory control in hepatocyte metabolism. *Am J Physiol Endocrinol Metab*, 288(3):E633–E644, Mar 2005.

[12] M. L. Blinov, J. Yang, J. R. Faeder, and W. S. Hlavacek. Graph theory for rule-based modeling of biochemical networks. *Lect Notes Comput Sci*, 4230:89–106, 2006.

[13] Michael L Blinov, James R Faeder, Byron Goldstein, and William S Hlavacek. BioNetGen: software for rule-based modeling of signal transduction based on the interactions of molecular domains. *Bioinformatics*, 20(17):3289–3291, Nov 2004.

[14] Michael L Blinov, James R Faeder, Byron Goldstein, and William S Hlavacek. A network model of early events in epidermal growth factor receptor signaling that accounts for combinatorial complexity. *Biosystems*, 83(2-3):136–151, 2006.

[15] Michael L Blinov, James R Faeder, Jin Yang, Byron Goldstein, and William S Hlavacek. 'on-the-fly' or 'generate-first' modeling? *Nat Biotechnol*, 23(11):1344–5; author reply 1345, Nov 2005.

[16] Nikolay M Borisov, Nick I Markevich, Jan B Hoek, and Boris N Kholodenko. Signaling through receptors and scaffolds: independent interactions reduce combinatorial complexity. *Biophys J*, 89(2):951–966, Aug 2005.

[17] Nikolay M Borisov, Nick I Markevich, Jan B Hoek, and Boris N Kholodenko. Trading the micro-world of combinatorial complexity for the macro-world of protein interaction domains. *Biosystems*, 83(2-3):152–166, 2006.

[18] Antony W Burgess, Hyun-Soo Cho, Charles Eigenbrot, Kathryn M Ferguson, Thomas P J Garrett, Daniel J Leahy, Mark A Lemmon, Mark X Sliwkowski, Colin W Ward, and Shigeyuki Yokoyama. An open-and-shut case? Recent insights into the activation of EGF/ErbB receptors. *Mol Cell*, 12(3):541–552, Sep 2003.

[19] Herbert B Callen. *Thermodynamics and an introduction to thermostatistics*. Jon Wiley And Sons, 1985.

[20] G. Carpenter. Receptor tyrosine kinase substrates: SRC homology domains and signal transduction. *FASEB J*, 6(14):3283–3289, Nov 1992.

[21] Chiranjib Chakraborty. Biochemical and molecular basis of insulin resistance. *Curr Protein Pept Sci*, 7(2):113–21, Apr 2006.

[22] L. Chang and M. Karin. Mammalian MAP kinase signalling cascades. *Nature*, 410(6824):37–40, Mar 2001.

[23] Louise Chang, Shian-Huey Chiang, and Alan R Saltiel. Insulin signaling and the regulation of glucose transport. *Mol Med*, 10(7-12):65–71, 2004.

[24] Dong Chen, S. B. Waters, K. H. Holt, and J. E. Pessin. SOS phosphorylation and disassociation of the Grb2-SOS complex by the ERK and JNK signaling pathways. *J Biol Chem*, 271(11):6328–6332, Mar 1996.

[25] W. S. Chen, C. S. Lazar, M. Poenie, R. Y. Tsien, G. N. Gill, and M. G. Rosenfeld. Requirement for intrinsic protein tyrosine kinase in the immediate and late actions of the EGF receptor. *Nature*, 328(6133):820–823, 1987.

[26] Hyun-Soo Cho and Daniel J Leahy. Structure of the extracellular region of HER3 reveals an interdomain tether. *Science*, 297(5585):1330–1333, Aug 2002.

[27] Ami Citri and Yosef Yarden. EGF-ErbB signalling: towards the systems level. *Nat Rev Mol Cell Biol*, 7(7):505–516, Jul 2006.

[28] David Colquhoun, Kathryn A Dowsland, Marco Beato, and Andrew J R Plested. How to impose microscopic reversibility in complex reaction mechanisms. *Biophys J*, 86(6):3510–3518, Jun 2004.

[29] H Conzelmann, M Koschorreck, M Ederer, and ED Gilles. Thermodynamic constraints of signal transduction networks. *submitted*, 2008.

[30] H. Conzelmann, J. Saez-Rodriguez, T. Sauter, E. Bullinger, F. Allgöwer, and E. D. Gilles. Reduction of mathematical models of signal transduction networks: simulation-based approach applied to EGF receptor signalling. *Syst Biol (Stevenage)*, 1(1):159–169, Jun 2004.

[31] Holger Conzelmann and Ernst D Gilles. *Functional Proteomics, Dynamic pathway modeling of signal transduction networks - A domain-oriented approach*. Humana Press, 2007.

[32] Holger Conzelmann, Julio Saez-Rodriguez, Thomas Sauter, Boris N Kholodenko, and Ernst D Gilles. A domain-oriented approach to the reduction of combinatorial complexity in signal transduction networks. *BMC Bioinformatics*, 7:34, 2006.

[33] J. Downward. The ins and outs of signalling. *Nature*, 411(6839):759–762, Jun 2001.

[34] Michael Ederer and Ernst Dieter Gilles. Thermodynamically feasible kinetic models of reaction networks. *Biophys J*, 92(6):1846–1857, Mar 2007.

[35] T. Eissing, F. Allgöwer, and E. Bullinger. Robustness properties of apoptosis models with respect to parameter variations and intrinsic noise. *Syst Biol (Stevenage)*, 152(4):221–228, Dec 2005.

[36] Thomas Eissing, Holger Conzelmann, Ernst D Gilles, Frank Allgöwer, Eric Bullinger, and Peter Scheurich. Bistability analyses of a caspase activation model for receptor-induced apoptosis. *J Biol Chem*, 279(35):36892–36897, Aug 2004.

[37] D. Endy and R. Brent. Modelling cellular behaviour. *Nature*, 409(6818):391–395, Jan 2001.

[38] J. R. Faeder, M. L. Blinov, B. Goldstein, and W. S. Hlavacek. Combinatorial complexity and dynamical restriction of network flows in signal transduction. *Syst Biol (Stevenage)*, 2(1):5–15, Mar 2005.

[39] J. R. Faeder, M. L. Blinov, B. Goldstein, and W.S. Hlavacek. Rule-based modeling of biochemical networks. *Complexity*, 10:22–41, 2005.

[40] James R Faeder, William S Hlavacek, Ilona Reischl, Michael L Blinov, Henry Metzger, Antonio Redondo, Carla Wofsy, and Byron Goldstein. Investigation of early events in FcϵRI-mediated signaling using a detailed mathematical model. *J Immunol*, 170(7):3769–3781, Apr 2003.

[41] Ying-Xin Fan, Lily Wong, and Gibbes R Johnson. EGFR kinase possesses a broad specificity for ErbB phosphorylation sites, and ligand increases catalytic-centre activity without affecting substrate binding affinity. *Biochem J*, 392(Pt 3):417–423, Dec 2005.

[42] R Faure, G Baquiran, JJ Bergeron, and BI Posner. The dephosphorylation of insulin and epidermal growth factor receptors. Role of endosome-associated phosphotyrosine phosphatase(s). *J Biol Chem*, 267(16):11215–21, Jun 1992.

[43] S. Felder, K. Miller, G. Moehren, A. Ullrich, J. Schlessinger, and C. R. Hopkins. Kinase activity controls the sorting of the epidermal growth factor receptor within the multivesicular body. *Cell*, 61(4):623–634, May 1990.

[44] Kathryn M Ferguson, Mitchell B Berger, Jeannine M Mendrola, Hyun Soo Cho, Daniel J Leahy, and Mark A Lemmon. EGF activates its receptor by removing interactions that autoinhibit ectodomain dimerization. *Mol Cell*, 11(2):507–517, Feb 2003.

[45] A. Finney and M. Hucka. Systems biology markup language: Level 2 and beyond. *Biochem Soc Trans*, 31(Pt 6):1472–1473, Dec 2003.

[46] Thomas P J Garrett, Neil M McKern, Meizhen Lou, Thomas C Elleman, Timothy E Adams, George O Lovrecz, Hong-Jian Zhu, Francesca Walker, Morry J Frenkel, Peter A Hoyne, Robert N Jorissen, Edouard C Nice, Antony W Burgess, and Colin W Ward. Crystal structure of a truncated epidermal growth factor receptor extracellular domain bound to transforming growth factor alpha. *Cell*, 110(6):763–773, Sep 2002.

[47] R. Gherzi, G. Andraghetti, G. Versari, and R. Cordera. Effect of insulin receptor autophosphorylation on insulin receptor binding. *Mol Cell Endocrinol*, 45(2-3):247–252, May 1986.

[48] D. Gillespie. A general method for numerically simulating the stochastic time evolution of coupled chemical reactions. *J Comp Phys*, 22:403–434, 1976.

[49] D. Gillespie. A rigorous derivation of the chemical master equation. *Physica A*, 188:404–425, 1992.

[50] M. Ginkel, A. Kremling, T. Nutsch, R. Rehner, and E. D. Gilles. Modular modeling of cellular systems with ProMoT/Diva. *Bioinformatics*, 19(9):1169–1176, Jun 2003.

[51] P. M. Guy, J. V. Platko, L. C. Cantley, R. A. Cerione, and K. L. Carraway. Insect cell-expressed p180 ErbB3 possesses an impaired tyrosine kinase activity. *Proc Natl Acad Sci U S A*, 91(17):8132–8136, Aug 1994.

[52] Mariko Hatakeyama, Shuhei Kimura, Takashi Naka, Takuji Kawasaki, Noriko Yumoto, Mio Ichikawa, Jae-Hoon Kim, Kazuki Saito, Mihoro Saeki, Mikako Shirouzu, Shigeyuki Yokoyama, and Akihiko Konagaya. A computational model on the modulation of mitogen-activated protein kinase (MAPK) and Akt pathways in heregulin-induced ErbB signalling. *Biochem J*, 373(Pt 2):451–463, Jul 2003.

[53] J. M. Haugh, K. Schooler, A. Wells, H. S. Wiley, and D. A. Lauffenburger. Effect of epidermal growth factor receptor internalization on regulation of the phospholipase C-gamma1 signaling pathway. *J Biol Chem*, 274(13):8958–8965, Mar 1999.

[54] J. M. Haugh, A. Wells, and D. A. Lauffenburger. Mathematical modeling of epidermal growth factor receptor signaling through the phospholipase C pathway: mechanistic insights and predictions for molecular interventions. *Biotechnol Bioeng*, 70(2):225–238, Oct 2000.

[55] Reinhart Heinrich and Stefan Schuster. *The regulation of cellular systems*. Chapman & Hall, 1996.

[56] William S Hlavacek, James R Faeder, Michael L Blinov, Alan S Perelson, and Byron Goldstein. The complexity of complexes in signal transduction. *Biotechnol Bioeng*, 84(7):783–794, Dec 2003.

[57] William S Hlavacek, James R Faeder, Michael L Blinov, Richard G Posner, Michael Hucka, and Walter Fontana. Rules for modeling signal-transduction systems. *Sci STKE*, 2006(344):re6, Jul 2006.

[58] M. Holgado-Madruga, D. R. Emlet, D. K. Moscatello, A. K. Godwin, and A. J. Wong. A Grb2-associated docking protein in EGF- and insulin-receptor signalling. *Nature*, 379(6565):560–564, Feb 1996.

[59] Stefan Hoops, Sven Sahle, Ralph Gauges, Christine Lee, Jürgen Pahle, Natalia Simus, Mudita Singhal, Liang Xu, Pedro Mendes, and Ursula Kummer. COPASI–a COmplex PAthway SImulator. *Bioinformatics*, 22(24):3067–3074, Dec 2006.

[60] Andreas Hoppe, Sabrina Hoffmann, and Hermann-Georg Holzhütter. Including metabolite concentrations into flux balance analysis: thermodynamic realizability as a constraint on flux distributions in metabolic networks. *BMC Syst Biol*, 1:23, 2007.

[61] F Hoppensteadt. Stability in systems with parameters. *J Math Anal Appl*, 18:129–134, 1967.

[62] F Hoppensteadt. Properties of solutions of ordinary differential equations with small parameters. *Comm Pure Appl Math*, 34:510–521, 1971.

[63] M. Hucka, A. Finney, H. M. Sauro, H. Bolouri, J. C. Doyle, H. Kitano, A. P. Arkin, B. J. Bornstein, D. Bray, A. Cornish-Bowden, A. A. Cuellar, S. Dronov, E. D. Gilles, M. Ginkel, V. Gor, I. I. Goryanin, W. J. Hedley, T. C. Hodgman, J-H. Hofmeyr, P. J. Hunter, N. S. Juty, J. L. Kasberger, A. Kremling, U. Kummer, N. Le Novre, L. M. Loew, D. Lucio, P. Mendes, E. Minch, E. D. Mjolsness, Y. Nakayama, M. R. Nelson, P. F. Nielsen, T. Sakurada, J. C. Schaff, B. E. Shapiro, T. S. Shimizu, H. D. Spence, J. Stelling, K. Takahashi, M. Tomita, J. Wagner, J. Wang, and S. B. M. L. Forum. The systems biology markup language (SBML): a medium for representation and exchange of biochemical network models. *Bioinformatics*, 19(4):524–531, Mar 2003.

[64] Nancy E Hynes and Heidi A Lane. ErbB receptors and cancer: the complexity of targeted inhibitors. *Nat Rev Cancer*, 5(5):341–354, May 2005.

[65] A Isidori. *Nonlinear Control Systems*. Springer, 2002.

[66] G. Jiang and T. Hunter. Receptor signaling: when dimerization is not enough. *Curr Biol*, 9(15):R568–R571, 1999.

[67] Xuejun Jiang, Fangtian Huang, Andriy Marusyk, and Alexander Sorkin. Grb2 regulates internalization of EGF receptors through clathrin-coated pits. *Mol Biol Cell*, 14(3):858–870, Mar 2003.

[68] Robert N Jorissen, Francesca Walker, Normand Pouliot, Thomas P J Garrett, Colin W Ward, and Antony W Burgess. Epidermal growth factor receptor: mechanisms of activation and signalling. *Exp Cell Res*, 284(1):31–53, Mar 2003.

[69] K. S. Kelly-Spratt, L. J. Klesse, J. Merenmies, and L. F. Parada. A TrkB/insulin receptor-related receptor chimeric receptor induces PC12 cell differentiation and exhibits prolonged activation of mitogen-activated protein kinase. *Cell Growth Differ*, 10(12):805–812, Dec 1999.

[70] H. K. Khalil. *Nonlinear Systems*. Prentice-Hall, 2002.

[71] A. H. Khan and J. E. Pessin. Insulin regulation of glucose uptake: a complex interplay of intracellular signalling pathways. *Diabetologia*, 45(11):1475–1483, Nov 2002.

[72] B. N. Kholodenko. Negative feedback and ultrasensitivity can bring about oscillations in the mitogen-activated protein kinase cascades. *Eur J Biochem*, 267(6):1583–1588, Mar 2000.

[73] B. N. Kholodenko, O. V. Demin, G. Moehren, and J. B. Hoek. Quantification of short term signaling by the epidermal growth factor receptor. *J Biol Chem*, 274(42):30169–30181, Oct 1999.

[74] Steffen Klamt, Julio Saez-Rodriguez, Jonathan A Lindquist, Luca Simeoni, and Ernst D Gilles. A methodology for the structural and functional analysis of signaling and regulatory networks. *BMC Bioinformatics*, 7:56, 2006.

[75] L. N. Klapper, S. Glathe, N. Vaisman, N. E. Hynes, G. C. Andrews, M. Sela, and Y. Yarden. The ErbB-2/HER2 oncoprotein of human carcinomas may function solely as a shared coreceptor for multiple stroma-derived growth factors. *Proc Natl Acad Sci U S A*, 96(9):4995–5000, Apr 1999.

[76] Peter Klein, Dawn Mattoon, Mark A Lemmon, and Joseph Schlessinger. A structure-based model for ligand binding and dimerization of EGF receptors. *Proc Natl Acad Sci U S A*, 101(4):929–934, Jan 2004.

[77] R. D. Kornberg. Eukaryotic transcriptional control. *Trends Cell Biol*, 9(12):M46–M49, Dec 1999.

[78] Markus Koschorreck, Holger Conzelmann, Sybille Ebert, Michael Ederer, and Ernst Dieter Gilles. Reduced modeling of signal transduction - A modular approach. *BMC Bioinformatics*, 8(1):336, Sep 2007.

[79] Markus Koschorreck and Ernst Dieter Gilles. ALC: automation of rule-based reduced modeling. *submitted*, 2008.

[80] Ursula Kummer, Borut Krajnc, Jürgen Pahle, Anne K Green, C. Jane Dixon, and Marko Marhl. Transition from stochastic to deterministic behavior in calcium oscillations. *Biophys J*, 89(3):1603–1611, Sep 2005.

[81] I. Lax, F. Bellot, R. Howk, A. Ullrich, D. Givol, and J. Schlessinger. Functional analysis of the ligand binding site of EGF-receptor utilizing chimeric chicken/human receptor molecules. *EMBO J*, 8(2):421–427, Feb 1989.

[82] M. A. Lemmon, Z. Bu, J. E. Ladbury, M. Zhou, D. Pinchasi, I. Lax, D. M. Engelman, and J. Schlessinger. Two EGF molecules contribute additively to stabilization of the EGFR dimer. *EMBO J*, 16(2):281–294, Jan 1997.

[83] M. A. Lemmon and J. Schlessinger. Regulation of signal transduction and signal diversity by receptor oligomerization. *Trends Biochem Sci*, 19(11):459–463, Nov 1994.

[84] A. E. Lenferink, R. Pinkas-Kramarski, M. L. van de Poll, M. J. van Vugt, L. N. Klapper, E. Tzahar, H. Waterman, M. Sela, E. J. van Zoelen, and Y. Yarden. Differential endocytic routing of homo- and hetero-dimeric ErbB tyrosine kinases confers signaling superiority to receptor heterodimers. *EMBO J*, 17(12):3385–3397, Jun 1998.

[85] Ying Leng, Hakan K R Karlsson, and Juleen R Zierath. Insulin signaling defects in type 2 diabetes. *Rev Endocr Metab Disord*, 5(2):111–7, May 2004.

[86] N. Li, A. Batzer, R. Daly, V. Yajnik, E. Skolnik, P. Chardin, D. Bar-Sagi, B. Margolis, and J. Schlessinger. Guanine-nucleotide-releasing factor Sos1 binds to Grb2 and links receptor tyrosine kinases to Ras signalling. *Nature*, 363(6424):85–88, May 1993.

[87] Jonathan A Lindquist, Luca Simeoni, and Burkhart Schraven. Transmembrane adapters: attractants for cytoplasmic effectors. *Immunol Rev*, 191:165–182, Feb 2003.

[88] Larry Lok and Roger Brent. Automatic generation of cellular reaction networks with Moleculizer 1.0. *Nat Biotechnol*, 23(1):131–136, Jan 2005.

[89] Johnny Ludvigsson. Why diabetes incidence increases–a unifying theory. *Ann N Y Acad Sci*, 1079:374–82, Oct 2006.

[90] R. Z. Luo, D. R. Beniac, A. Fernandes, C. C. Yip, and F. P. Ottensmeyer. Quaternary structure of the insulin-insulin receptor complex. *Science*, 285(5430):1077–1080, Aug 1999.

[91] Tadao Maeda, Yoshikazu Imanishi, and Krzysztof Palczewski. Rhodopsin phosphorylation: 30 years later. *Prog Retin Eye Res*, 22(4):417–434, Jul 2003.

[92] M. P. Mattson. Apoptosis in neurodegenerative disorders. *Nat Rev Mol Cell Biol*, 1(2):120–129, Nov 2000.

[93] Gisela Moehren, Nick Markevich, Oleg Demin, Anatoly Kiyatkin, Igor Goryanin, Jan B Hoek, and Boris N Kholodenko. Temperature dependence of the epidermal growth factor receptor signaling network can be accounted for by a kinetic model. *Biochemistry*, 41(1):306–320, Jan 2002.

[94] C. J. Morton-Firth and D. Bray. Predicting temporal fluctuations in an intracellular signalling pathway. *J Theor Biol*, 192(1):117–128, May 1998.

[95] D. K. Moscatello, M. Holgado-Madruga, A. K. Godwin, G. Ramirez, G. Gunn, P. W. Zoltick, J. A. Biegel, R. L. Hayes, and A. J. Wong. Frequent expression of a mutant epidermal growth factor receptor in multiple human tumors. *Cancer Res*, 55(23):5536–5539, Dec 1995.

[96] Catherine Mounier and Barry I Posner. Transcriptional regulation by insulin: from the receptor to the gene. *Can J Physiol Pharmacol*, 84(7):713–24, Jul 2006.

[97] Sanchita Mukherjee, Mathewos Tessema, and Angela Wandinger-Ness. Vesicular trafficking of tyrosine kinase receptors and associated proteins in the regulation of signaling and vascular function. *Circ Res*, 98(6):743–756, Mar 2006.

[98] Serge Nef, Sunita Verma-Kurvari, Jussi Merenmies, Jean-Dominique Vassalli, Argiris Efstratiadis, Domenico Accili, and Luis F Parada. Testis determination requires insulin receptor family function in mice. *Nature*, 426(6964):291–295, Nov 2003.

[99] M. Odaka, D. Kohda, I. Lax, J. Schlessinger, and F. Inagaki. Ligand-binding enhances the affinity of dimerization of the extracellular domain of the epidermal growth factor receptor. *J Biochem (Tokyo)*, 122(1):116–121, Jul 1997.

[100] Hideo Ogiso, Ryuichiro Ishitani, Osamu Nureki, Shuya Fukai, Mari Yamanaka, Jae-Hoon Kim, Kazuki Saito, Ayako Sakamoto, Mio Inoue, Mikako Shirouzu, and Shigeyuki Yokoyama. Crystal structure of the complex of human epidermal growth factor and receptor extracellular domains. *Cell*, 110(6):775–787, Sep 2002.

[101] L Onsager. Reciprocal relations in irreversible processes I. *Phys Rev*, 37:405–426, 1931.

[102] L Onsager. Reciprocal relations in irreversible processes II. *Phys Rev*, 38:2265–2279, 1931.

[103] F. P. Ottensmeyer, D. R. Beniac, R. Z. Luo, and C. C. Yip. Mechanism of transmembrane signaling: insulin binding and the insulin receptor. *Biochemistry*, 39(40):12103–12112, Oct 2000.

[104] Ferruh Ozcan, Peter Klein, Mark A Lemmon, Irit Lax, and Joseph Schlessinger. On the nature of low- and high-affinity EGF receptors on living cells. *Proc Natl Acad Sci U S A*, 103(15):5735–5740, Apr 2006.

[105] T. Pawson and J. D. Scott. Signaling through scaffold, anchoring, and adaptor proteins. *Science*, 278(5346):2075–2080, Dec 1997.

[106] Tony Pawson and Piers Nash. Assembly of cell regulatory systems through protein interaction domains. *Science*, 300(5618):445–452, Apr 2003.

[107] G. Pelicci, L. Lanfrancone, F. Grignani, J. McGlade, F. Cavallo, G. Forni, I. Nicoletti, F. Grignani, T. Pawson, and P. G. Pelicci. A novel transforming protein (SHC) with an SH2 domain is implicated in mitogenic signal transduction. *Cell*, 70(1):93–104, Jul 1992.

[108] R. Pinkas-Kramarski, I. Alroy, and Y. Yarden. ErbB receptors and EGF-like ligands: cell lineage determination and oncogenesis through combinatorial signaling. *J Mammary Gland Biol Neoplasia*, 2(2):97–107, Apr 1997.

[109] R. Pinkas-Kramarski, L. Soussan, H. Waterman, G. Levkowitz, I. Alroy, L. Klapper, S. Lavi, R. Seger, B. J. Ratzkin, M. Sela, and Y. Yarden. Diversification of Neu differentiation factor and epidermal growth factor signaling by combinatorial receptor interactions. *EMBO J*, 15(10):2452–2467, May 1996.

[110] Leona Plum, Bengt F Belgardt, and Jens C Brüning. Central insulin action in energy and glucose homeostasis. *J Clin Invest*, 116(7):1761–6, Jul 2006.

[111] Nathan D Price, Iman Famili, Daniel A Beard, and Bernhard Palsson. Extreme pathways and Kirchhoff's second law. *Biophys J*, 83(5):2879–2882, Nov 2002.

[112] Hong Qian and Daniel A Beard. Thermodynamics of stoichiometric biochemical networks in living systems far from equilibrium. *Biophys Chem*, 114(2-3):213–220, Apr 2005.

[113] Hong Qian, Daniel A Beard, and Shou dan Liang. Stoichiometric network theory for nonequilibrium biochemical systems. *Eur J Biochem*, 270(3):415–421, Feb 2003.

[114] D. R. Robinson, Y. M. Wu, and S. F. Lin. The protein tyrosine kinase family of the human genome. *Oncogene*, 19(49):5548–5557, Nov 2000.

[115] K. Sakaguchi, Y. Okabayashi, Y. Kido, S. Kimura, Y. Matsumura, K. Inushima, and M. Kasuga. Shc phosphotyrosine-binding domain dominantly interacts with epidermal growth factor receptors and mediates Ras activation in intact cells. *Mol Endocrinol*, 12(4):536–543, Apr 1998.

[116] Alan R Saltiel and Jeffrey E Pessin. Insulin signaling pathways in time and space. *Trends Cell Biol*, 12(2):65–71, Feb 2002.

[117] AR Saltiel and CR Kahn. Insulin signalling and the regulation of glucose and lipid metabolism. *Nature*, 414(6865):799–806, Dec 2001.

[118] George Scatchard. The aggregation of proteins for small molecules and ions. *Annals of the New York Academy of Science*, pages 660–672, 1949.

[119] J Schaffner. *Zum Beobachterentwurf für nichtlineare Systeme mit mehreren Meßgrößen.* PhD thesis, University of Stuttgart, 1997.

[120] J. Schlessinger. Cell signaling by receptor tyrosine kinases. *Cell*, 103(2):211–225, Oct 2000.

[121] Mirko H H Schmidt, Frank B Furnari, Webster K Cavenee, and Oliver Bögler. Epidermal growth factor receptor signaling intensity determines intracellular protein interactions, ubiquitination, and internalization. *Proc Natl Acad Sci U S A*, 100(11):6505–6510, May 2003.

[122] Birgit Schoeberl, Claudia Eichler-Jonsson, Ernst Dieter Gilles, and Gertraud Müller. Computational modeling of the dynamics of the MAP kinase cascade activated by surface and internalized EGF receptors. *Nat Biotechnol*, 20(4):370–375, Apr 2002.

[123] Waltraud X Schulze, Lei Deng, and Matthias Mann. Phosphotyrosine interactome of the ErbB-receptor kinase family. *Mol Syst Biol*, 1:2005.0008, 2005.

[124] Ahmad R Sedaghat, Arthur Sherman, and Michael J Quon. A mathematical model of metabolic insulin signaling pathways. *Am J Physiol Endocrinol Metab*, 283(5):E1084–E1101, Nov 2002.

[125] T. S. Shimizu, N. Le Novre, M. D. Levin, A. J. Beavil, B. J. Sutton, and D. Bray. Molecular model of a lattice of signalling proteins involved in bacterial chemotaxis. *Nat Cell Biol*, 2(11):792–796, Nov 2000.

[126] Rita Slaaby, Lauge Schäffer, Inger Lautrup-Larsen, Asser Sloth Andersen, Allan Christian Shaw, Ida Stenfeldt Mathiasen, and Jakob Brandt. Hybrid receptors formed by insulin receptor (IR) and insulin-like growth factor I receptor (IGF-IR) have low insulin and high IGF-1 affinity irrespective of the IR splice variant. *J Biol Chem*, 281(36):25869–25874, Sep 2006.

[127] Jörg Stelling and Ernst Dieter Gilles. Mathematical modeling of complex regulatory networks. *IEEE Trans Nanobioscience*, 3(3):172–179, Sep 2004.

[128] Jörg Stelling, Ernst Dieter Gilles, and Francis J Doyle. Robustness properties of circadian clock architectures. *Proc Natl Acad Sci U S A*, 101(36):13210–13215, Sep 2004.

[129] Cullen M Taniguchi, Brice Emanuelli, and C. Ronald Kahn. Critical nodes in signalling pathways: insights into insulin action. *Nat Rev Mol Cell Biol*, 7(2):85–96, Feb 2006.

[130] A. Tikhonov. On the dependence of solutions of differential equations on a small parameter. *Math. Sb.*, 22:193–204, 1948.

[131] A. Tikhonov. Systems of differential equations containing small parameters in the derivatives. *Math. Sb.*, 31:575–586, 1952.

[132] Mauro Togni, Jon Lindquist, Annegret Gerber, Uwe Kölsch, Andrea Hamm-Baarke, Stefanie Kliche, and Burkhart Schraven. The role of adaptor proteins in lymphocyte activation. *Mol Immunol*, 41(6-7):615–630, Jul 2004.

[133] A B Vasileva. Asymptotic behavior of solutions to certain problems involving nonlinear differential equations containing a small parameter multiplying the highest derivatives. *Russian Math Surveys*, 18:13–81, 1963.

[134] S Wanant and MJ Quon. Insulin receptor binding kinetics: modeling and simulation studies. *J Theor Biol*, 205(3):355–64, Aug 2000.

[135] Qian Wang, Greg Villeneuve, and Zhixiang Wang. Control of epidermal growth factor receptor endocytosis by receptor dimerization, rather than receptor kinase activation. *EMBO Rep*, 6(10):942–948, Oct 2005.

[136] Colin W Ward, Michael C Lawrence, Victor A Streltsov, Timothy E Adams, and Neil M McKern. The insulin and EGF receptor structures: new insights into ligand-induced receptor activation. *Trends Biochem Sci*, 32(3):129–137, Mar 2007.

[137] S. B. Waters, D. Chen, A. W. Kao, S. Okada, K. H. Holt, and J. E. Pessin. Insulin and epidermal growth factor receptors regulate distinct pools of Grb2-SOS in the control of ras activation. *J Biol Chem*, 271(30):18224–18230, Jul 1996.

[138] R Wegscheider. Ueber simultane Gleichgewichte und die Beziehungen zwischen Thermodynamik und Reaktionskinetik homogener Systeme. *Z Phys Chem*, 39:257–303, 1902.

[139] L Weiss and RE Kalman. Contributions to linear systems theory. *Int. J. Eng. Sc.*, 3:141–171, 1965.

[140] M. F. White. The IRS-signalling system: a network of docking proteins that mediate insulin action. *Mol Cell Biochem*, 182(1-2):3–11, May 1998.

[141] Dineli Wickramasinghe and Monica Kong-Beltran. Met activation and receptor dimerization in cancer: a role for the Sema domain. *Cell Cycle*, 4(5):683–685, May 2005.

[142] A. Wilde, E. C. Beattie, L. Lem, D. A. Riethof, S. H. Liu, W. C. Mobley, P. Soriano, and F. M. Brodsky. EGF receptor signaling stimulates SRC kinase phosphorylation of clathrin, influencing clathrin redistribution and EGF uptake. *Cell*, 96(5):677–687, Mar 1999.

[143] R. Worthylake and H. S. Wiley. Structural aspects of the epidermal growth factor receptor required for transmodulation of ErbB-2/Neu. *J Biol Chem*, 272(13):8594–8601, Mar 1997.

[144] Feng Yang, Hong Qian, and Daniel A Beard. Ab initio prediction of thermodynamically feasible reaction directions from biochemical network stoichiometry. *Metab Eng*, 7(4):251–259, Jul 2005.

[145] Jin Yang, William J Bruno, William S Hlavacek, and John E Pearson. On imposing detailed balance in complex reaction mechanisms. *Biophys J*, 91(3):1136–1141, Aug 2006.

[146] Y. Yarden. The EGFR family and its ligands in human cancer. signalling mechanisms and therapeutic opportunities. *Eur J Cancer*, 37 Suppl 4:S3–S8, Sep 2001.

[147] Y. Yarden and M. X. Sliwkowski. Untangling the ErbB signalling network. *Nat Rev Mol Cell Biol*, 2(2):127–137, Feb 2001.

[148] Gongyi Zhang. Tumor necrosis factor family ligand-receptor binding. *Curr Opin Struct Biol*, 14(2):154–160, Apr 2004.

[149] Minghua Zhu, Erin Janssen, and Weiguo Zhang. Minimal requirement of tyrosine residues of linker for activation of T cells in TCR signaling and thymocyte development. *J Immunol*, 170(1):325–333, Jan 2003.